METHANE DESTRUCTION IN AN ALTERNATING CURRENT PLASMA REACTOR

By

MICHAEL ALAN PIATT

Bachelor of Science in Chemical Engineering

Oklahoma State University

Stillwater, Oklahoma

1981

Submitted to the Faculty of the
Graduate College of the
Oklahoma State University
in partial fulfillment of
the requirements for
the Degree of
MASTER OF SCIENCE
May, 1988

METHANE DESTRUCTION IN AN ALTERNATING

CURRENT PLASMA REACTOR

Thesis Approved:

Arland H. Johannes
Thesis Adviser

Robert N. Will
Thesis Co-Adviser

Marvin M. Johnson

Robert S. Robinson Jr.

Norman N. Durham
Dean of the Graduate College

ACKNOWLEDGEMENTS

I wish to express sincere appreciation to my co-advisers, Dr. Robert A. Wills and Dr. Arland H. Johannes, for their support and advice throughout my graduate studies.

Also, I would like to thank Dr. R. L. Robinson Jr. and the members of the School of Chemical Engineering for their support and advice. Special thanks to Dr. R. S. Sheinson at the Naval Research Laboratories in Washington, D.C. for information, advice and some of the equipment used in my research.

In addition, I would especially like to thank my wife, Kathy, and my parents for their support and encouragement during this research.

Finally, the financial assistance received from the Phillips Petroleum Company is gratefully acknowledged.

TABLE OF CONTENTS

LIST OF TABLES

LIST OF FIGURES

NOMENCLATURE

A	area for flow
C_a	molor concentration of methane
C_a°	initial molar concentration
cc	cubic centimeter
cm	centimeter
D	diameter
D_{eff}	effective diameter
exp	exponential
GC	gas chromatograph
gm	gram
Hz	hertz
K	Boltzman constant
kw	kilowatts
l	liter
L	length of reactor
ln	natural log
log	log base 10
m	mass
mA	milliampere
min	minutes
mm	millimeter
MW	molecular weight
$\dot{n}_a$	molar flow rate of methane
P	power
p	pressure
ρ	mass density
ppm	parts per million
psi	pounds per square inch
Q	volumetric flow rate
R	gas constant

Re	Reynold's number
rms	root mean square
S	seconds
T	temperature
t	time
T_e	electron temperature
τ	residence time
μ	viscosity
μg	micrograms
Vel	gas velocity
V^t	reactor volume
V_r	random velocity
y_a°	initial mole fraction of methane
Z	length down the reactor

CHAPTER I

INTRODUCTION

Treatment of hazardous substances is an ever increasing concern and problem in our society [1]. While generators face increasing disposal and liability costs, the construction of new disposal facilities has been hampered by increased regulatory requirements and increased concern from local populations [2]. The sheer number of hazardous substances and forms suggests that a variety of treatment methods will be needed to solve this complex problem.

Current methods of treatment are adequate for many wastes; however, they have limitations. Some present methods, such as landfills, will become less available--possibly phased out entirely. Incinerators cannot easily handle dilute aqueous streams, polychlorinated biphenyls (PCB's), or waste gases. In both disposal methods, the generator gives up control of his wastes to a third party for transportation and disposal, which exposes the generator to increased liability. On-site treatment methods are needed to give the generator more control and verification of the disposal process [3].

In recent years, a number of new technologies have emerged as potential methods for treating hazardous wastes. One of these, the alternating current plasma reactor (ACPR), is the focus of the research presented in this thesis.

Process Description and History

The ACPR (also known as alternating current corona reactor, glow discharge reactor, or alternating current silent discharge plasma reactor) is a type of chemical reactor that utilizes electrical energy to create a low temperature plasma (electric discharge) in a reactor cavity. When organic materials are flowing in the plasma, their chemical bonds are broken by absorbing the electrical energy of the plasma. Elemental atoms result, which then recombine to form the reaction products.

To date, the ACPR has been studied as a method to remove toxic contaminants from air streams. Air is used to generate the plasma, and the entire reaction is carried out in the gas phase. Thus, this is a potential method of treating waste gases, one of the waste types previously mentioned as difficult to treat using current disposal methods.

Research on electrical discharge reactors as a method to treat toxic gases began in 1975. Early work used discharge tubes powered by microwave power sources. From this early research, the U.S. military developed the ACPR. Military uses would be on ships, tanks, and personnel carriers. An ACPR would purify air contaminated with toxic compounds from fire or chemical warfare agents. However, beyond the initial military uses, the ACPR has potential industrial applications such as:

1. Purification of stack gases from factories;

2. Emergency air purification in buildings and hazardous materials storage areas during fire; and

3. Destruction of hazardous waste gases.

So far, most of the research on the ACPR has been at the Naval Research Center (NRL) and the U.S. Army Chemical Research, Development and Engineering Center. Research at Oklahoma State University began as a joint effort with NRL. By mutual agreement, NRL will pursue research in scientific areas such as reaction mechanisms, while OSU will concentrate on engineering aspects such as kinetic modeling and scale up. Work presented in this thesis provides the first results from OSU.

The Plasma Environment

As mentioned before, the research presented in this thesis will concentrate mainly on engineering concerns pertinent to the ACPR; however, some background information on the plasma environment is given here.

In general, plasmas can be thought to be an ionized gas consisting of positive and negative charge carriers [4]. While individual particles may have an electric charge, the plasma must maintain overall electrical neutrality. Under this broad definition of plasmas, no restrictions are made as to the charged particle density, the presence of neutral species, the emission or absorption of electromagnetic radiations, or the motion of the particles. Plasmas may also exist in the solid and liquid phases; however, in this study only gas phase plasmas are generated in the ACPR.

In addition to the above requirements, a third criteria exists for plasmas. The motion of the particles must be controlled by electromagnetic forces instead of hydrodynamic forces [5]. An example would be the exhaust gases from a jet engine. These gases are weakly ionized; however, most collisions are with neutral particles. Under this condition, particle motion is controlled by hydrodynamic forces, and the gas is not considered a plasma.

There are both man-made and naturally occurring plasmas. In man-made plasmas, usually an electric current supplies the necessary energy to cause ionization. An everyday example of this is a neon light where the plasma emits electromagnetic radiation. Ionization in natural plasmas is induced by thermal energy. The primary example of this is stars, which are almost completely ionized due to their high temperatures. This implies that the majority of known matter in the universe exists as a thermal plasma.

An important difference exists between these two types of plasmas. Thermally induced plasmas are in thermal equilibrium, and the temperature of the neutral and charged species is equal. However, in electrically induced plasmas, the temperatures of the charged and neutral species can be quite different. This is the case for the ACPR.

Boenig [4] states that there are no available techniques for directly measuring temperatures of various species in a plasma. However, some methods exist for measuring velocities of atoms and molecules. For a simple system, such as inert-gas plasmas induced by direct current, a Maxwellian distribution can be shown to exist such that:

$$3/2\ K\ T_e = 1/2\ m\ (V_r)^2 \tag{1.1}$$

where K is the Boltzman constant, T_e is the electron temperature, and V_r is the random velocity. In glow discharges, induced by direct current, the ions and molecules are roughly at ambient temperatures, while the electron temperature is some two orders of magnitude greater.

It is important to emphasize that reactions in plasmas are fundamentally different than normal combustion reactions. In plasmas the initial step is believed to be rupture of the chemical bonds by the plasma energy. According to standard kinetic models, the initial step in combustion reactions involves collision of the reactant molecules. More detail on reaction mechanisms is given in Chapter III.

Background on Electrical Discharge Reactors

The use of electrical discharge reactor devices to study chemical reactions is certainly not new. One can find many different electrical discharge reactor types in the literature used to study a wide range of phenomena. The earliest work began around 1927 and concentrated on direct current reactors. It is the purpose of this section to give general background information of electrical discharge reactors, describe how the ACPR fits into the overall picture, and give advantages of the ACPR.

Due to the large number of investigators that have studied electrical discharges, a great deal of confusion in terminology has developed in the literature. Flinn and Goldberger [6] have classified electrical discharge devices based on three criteria (Figure 1) common to all such devices: power source, coupling mechanism (reactor design), and plasma environment (operating variables). Resistive reactors have their electrodes directly in the gas stream, and use a direct current power source. Figure 2 shows typical capacitive and inductive devices

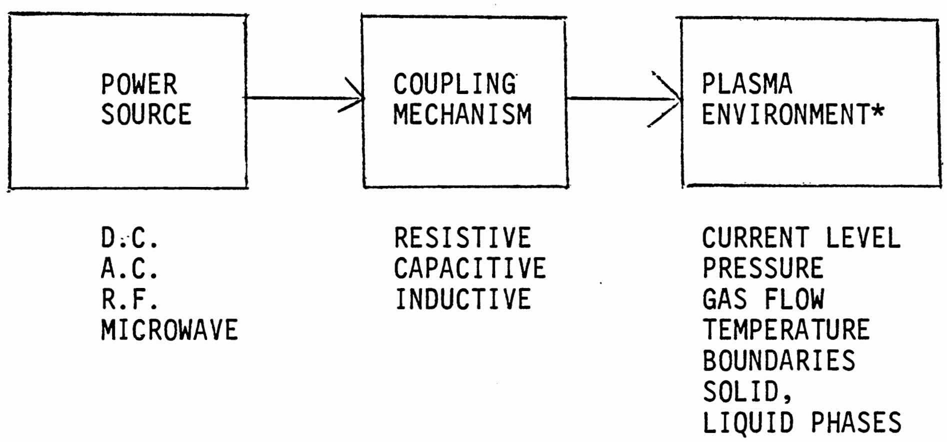

Source: Flinn, J. E. and W. M. Goldberger. " Viewpoint on Electrical Discharge Devices and their Application as Chemical Reactors," Advances in Chemistry Series, 80, 441-451 (1969).

Figure 1. Classification of Electrical Discharge Devices

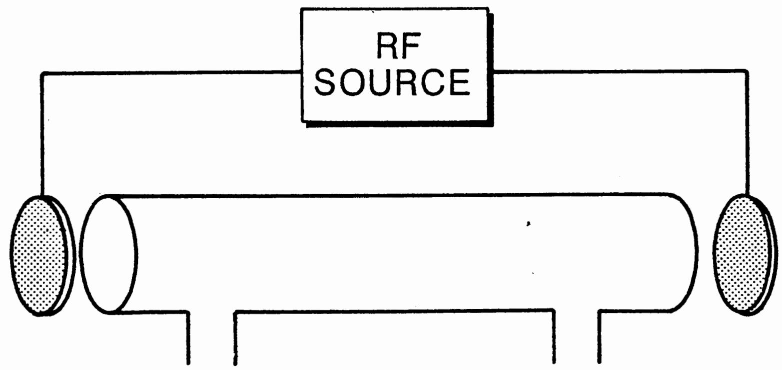

TYPICAL CAPACITIVE REACTOR

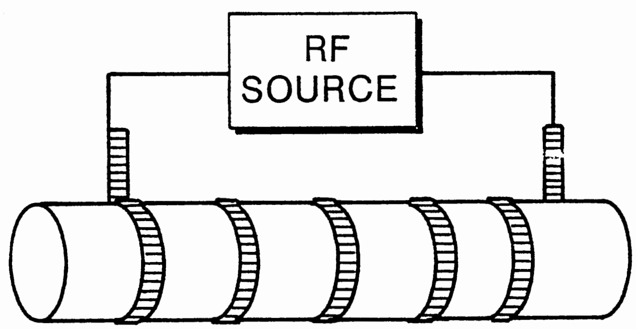

TYPICAL INDUCTIVE REACTOR

From: Boenig H. V., Plasma Science and Technology, Cornell University Press, 1982, p. 30

Figure 2. Typical Electrical Discharge Reactors

that have been used by past researchers. Radio or microwave frequencies are needed to generate plasmas in these reactors.

The ACPR is basically a combination of a capacitive and inductive device. It consists of two concentric glass cylinders which form an annulus for gas flow. An inductive coil is wrapped around the outer glass cylinder. In addition, a second electrode is positioned inside the inner cylinder. When an electric potential is applied across these electrodes, the glass walls serve as a dielectric causing the current to diffuse into a plasma or "glow" in the annulus. Figure 3 shows a typical ACPR. Using this reactor design, plasmas can be generated at atmospheric pressures using frequencies below 1000 Hz. More detail of the reactor design is given in Chapter IV.

Fraser and Sheinson [7] compared different reactor types and concluded that the ACPR was best suited for further study by the military for the following reasons:

1. Direct current devices have the electrodes exposed directly in the gas stream causing unacceptable levels of electrode corrosion;

2. Radio and microwave reactors require higher power levels and thus more expensive power equipment;

3. The ACPR can operate at atmospheric pressure, while most high frequency devices operate at below atmospheric pressures; and

4. The ACPR can be constructed out of standard materials and can easily be designed for continuous flow.

Overall Research Objective

Engineering research on the ACPR is in its early stages. Almost no work has been done on variables which could affect scale up to com-

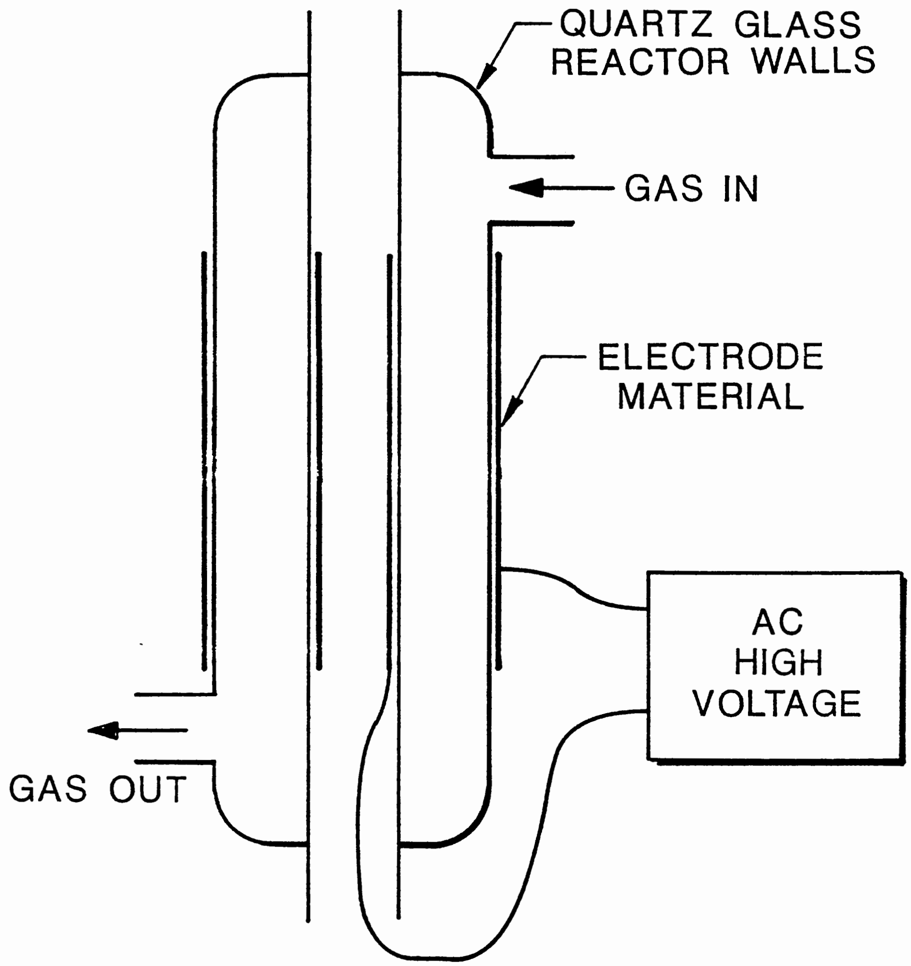

Figure 3. Typical Alternating Current Plasma Reactor

mercial units or on the overall kinetic model in such a reactor. While research on the basic science of the plasma itself is important and should continue, engineering concerns will ultimately determine if the ACPR is an economically viable process for the military and industry.

With this in mind, the primary focus of this research must be exploratory--to identify and recommend which variables are most critical for future engineering research. Specific research objectives are given in Chapter II.

CHAPTER II

OBJECTIVES

Objectives of the work presented in this thesis are summarized in this chapter. Since research, particularly engineering research, on the ACPR is in its infancy, the nature of this work is primarily exploratory and introductory. However, despite its preliminary nature, this work will build and expand upon previous research on the ACPR and lay the foundation for future research in this emerging technology.

The first objective is to build the experimental apparatus and have it operate properly. Ideally, all units of the apparatus will be off-the-shelf or easily obtained items. This requirement is to minimize costs and to show the potential of the technology as an economic air purification method.

The second objective is to conduct a series of non-destructive tests using inert gases under a variety of conditions. The purpose being to study the physical and electrical characteristics of the system. An optimum frequency corresponding to maximum power input should exist for a given set of conditions. Non-destructive testing will provide a way to show how the optimum condition varies with primary voltage, flow rate, gas type, reactor size, electrode type, and humidity.

The third objective is to propose a kinetic model for methane conversion. While previous work on ACPR's has concentrated on determining the reaction mechanism, this model will attempt to describe the macroscopic reaction kinetics from an engineering viewpoint. Initially, a plug flow type model will be assumed and tested.

The fourth objective is to run destructive tests in the reactor to test the proposed model and the destructive potential of the system. Methane will be the test compond and will be run in two bulk gases: air and an oxygen/helium mixture. Two different concentrations of methane (one at 12 to 13% and one less than 2%) will be used. Destructive tests will be run in the three different reactors of differing volume and electrode configuration.

Methane was selected as a test species for three primary reasons:

1. It has been used in previous research at NRL. By using methane this research can build upon previous research on ACPR's.

2. It is the simplest organic molecule. This will allow identification of important design variables before more complex chemical compounds are studied.

3. It has a relatively high bond energy compared to larger organic molecules. Thus, if the ACPR can be shown to decompose methane effectively, larger molecules should be even easier to dissociate to other molecules.

Initially, flow rate will be held constant and frequency varied. Based on previous work, different frequencies give different levels of electrical power input and thus different levels of destruction. An optimum frequency should exist which gives maximum destruction. Then frequency will be held constant, at or near the optimum, and flow rate will be varied. Results from these experiments will be used to test the proposed model.

Destructive tests will also be conducted in reactors of varying size and electrode types, and with different inlet concentrations of methane. Also, different carrier gases will be used to test that variable on destruction efficiency. While some conclusions may be drawn from these experiments, their primary function is to identify important variables for future study.

The fifth objective is to identify and recommend new areas to investigate in future research, and to recommend improvements in the experimental apparatus and procedure. This will be necessary in exploratory research due to the large number of variables to be investigated and the uncertainty of what will be observed.

CHAPTER III

LITERATURE REVIEW

Chemical reactions in various electrical discharge reactors have been studied since 1927. However, the number and variety of electrical discharge reactors reported in the literature is beyond the scope of this review. Instead, the following literature survey concentrates on research concerning the reactor of interest--namely the ACPR described earlier and its advantages over more conventional electric discharge reactors.

To accomplish this task, the survey is divided into five sections. Section one briefly reviews direct current and microwave destruction of airborne contaminants. Section two reviews methane destruction in an ACPR. Section three reviews the destruction of other test gases. Section four reviews research of toxic by-product formation in ACPR's. Section five reviews current theories on the chemical reaction mechanism of methane in an ACPR.

Direct Current and Microwave Destruction of Airborne Pollutants

Balin, Sibert, Jonas and Bell [8] were the first to consider using an electrical discharge to process toxic gases. They used a microwave power source with a simple (capacitive) discharge tube. The destruction potential of this device was tested with two compounds:

dimethyl methylphosphonate (DMMP) and diisopropyl methylphosphonate (DIMP). Each test species was run in both air and helium atmospheres at concentrations of 0.09 to 0.31 gm/l. Destruction efficiencies ranged from 62% to 99%. Power levels used were 150 to 200 watts with residence times of 1.5 to 2.4 seconds. All experiments were conducted at pressures of 3 to 70 torr and at a constant frequency of 2450 MHz.

In further work, Balin, Hertzler and Oberacker [9] ran a variety of pesticides and industrial wastes in a packed microwave discharge. They obtained very high destruction efficiencies (Table I). Power input ranged from 4.2 to 4.7 kW, and pressures varied from 28 to 120 torr. Flow rates ranged from 300 to 960 l/h. Some of the wastes studied were in liquid or powder form.

While high destruction efficiencies can be obtained from microwave power discharge devices, there are several disadvantages of their use as air purification systems. First is a relatively high initial cost. Balin et al. [9] report capital cost for their device at $100,000 per unit in 1978 dollars. Second is the high power requirements needed for high destruction. Third is the subatmospheric pressures used while operating the device. Helfritch, Feldman, and Efthimion [10] reported on a microwave discharge reactor that operated at atmospheric pressure, but did not report any destruction efficiency tests.

Fraser and Sheinson [7] compared several direct current (DC) devices against the ACPR. This work was done for the U.S. Navy, which is interested in air purification aboard ships. The authors concluded that the ACPR was best suited for further study. Direct current devices have the electrodes directly exposed to the gas streams which

TABLE I

DESTRUCTION TESTS IN A MICROWAVE DISCHARGE

Conversion (%)	Pesticide/ Waste	Microwave Power (kW)	Pressure Range (Torr)	Reactor Packing
99.9988	Malathion "Cythion"	3.7	28 - 46	wool plug
99.9999	Malathion "Cythion"	4.7	28 - 30	wool plug
> 99	PCB Aroclor 1242	4.6	17 - 35	wool plug
> 99	PCB Aroclor 1242	4.2	17 - 35	wool plug
> 99	PCB Aroclor 1254	4.5	13 - 25	solid rings
99.99	PMA Troysan PMA-30	4.6	120-140	Raschid rings
99.99	PMA Troysan PMA-30	4.0	100-120	Raschid rings
99.99	PMA Troysan PMA 30	4.3	100-120	Raschid rings
> 99	Keopone 80/20 20% Methanol Solution	4.6	45 - 60	Raschid rings
> 99	Keopone 80/20 10% Solids Aqueous Slurry	4.2	35 - 50	Raschid rings
> 99	Keopone 80/20 2 to 3 gM solid disks	4.6	30 - 70	Raschid rings
> 99.999	Red Dye Mixture 15.5% Solids Aqueous Slurry	4.6	35 - 60	Raschid rings

Source: Balin, L. J., B. L. Hertzler, and D. A. Oberacker. "Development of Microwave Plasma Detoxification Process for Hazardous Wastes." Environmental Science and Technology, 12(6), 1978.

causes unacceptable corrosion and by-product build up on the electrodes.

Methane Destruction in an ACPR

The following section summarizes research on the ACPR using methane as a test species. Methane has been used as a test species because of the high bond energy (104 kcal/mol) of the C-H bond [11]. All of the research in this section was at atmospheric pressure and room temperature.

Research on the ACPR has mainly been done at the Naval Research Laboratory in Washington, D.C. and the U.S. Army Chemical Research, Development and Engineering Center in Aberdeen, MD. Anticipated military uses include air purification on land vehicles (i.e., tanks and personnel carriers) during chemical weapons attack and air purification on ships during emergencies such as fire.

Fraser, Fee and Sheinson [12] investigated the destruction of methane in pure nitrogen and air atmospheres. With nitrogen as the carrier stream, principal products were hydrogen and hydrogen cyanide with trace levels of methyl cyanide, ethane, ethyl cyanide and cyanogen present. In an air carrier, principal products were carbon dioxide and water, with trace amounts of cyanogen. Table II shows methane destruction in pure nitrogen, while Table III shows methane destruction in increasing oxygen concentration. Voltage, frequency and flow rate were held constant at 16 kV, 60Hz and 350 cc/min. respectively. Current varied from 1.0 to 1.2 mA. Reactor variables were not optimized in this work.

TABLE II

METHANE CONVERSION IN PURE NITROGEN
IN AN ACPR

Input Methane Concentration (ppm)	Methane Destruction Efficiency (%)
120	67
420	24
770	18
950	18

Source: Fraser, M. E., H. G. Eaton and R. S. Sheinson. "Decomposition of Methane in an AC Discharge." Plasma Chemistry and Plasma Processing, 5(2), 1985.

TABLE III

METHANE DESTRUCTION IN NITROGEN/OXYGEN
IN AN ACPR

Input Methane Concentration (ppm)	Input Oxygen Concentration (ppm)	Destruction Efficiency (%)
120	35	67
120	110	50
120	210	50
560	35	39
560	500	36
560	1100	36

Source: Fraser, M. E., H. G. Eaton and R. S. Sheinson. "Decomposition of Methane in an AC Discharge." Plasma Chemistry and Plasma Processing, 5(2), 1985.

Sheinson, Smyth, Piatt and Wills [13] investigated methane destruction as a function of voltage, frequency and gas composition. Methane destruction was shown to increase with increasing power input. At a fixed voltage, power reached a maximum at an optimum frequency. This optimum occurred at lower frequencies as voltage increased. In pure helium flow the optimum occurred at a lower frequency than for pure nitrogen flow. Pure helium showed a higher maximum power input at a given frequency.

Destructive efficiencies for 100 to 120 ppm methane in 3300 ppm of oxygen in helium were in excess of 99% at the optimum conditions. Flow rate was held constant at 100 cc/min giving a residence time of 6.5 seconds. This work implies that an ACPR can be "tuned" to changing conditions by simply varying the frequency. Further investigations into these results are presented in this thesis.

Other Destructive Studies of the ACPR

In addition to methane, the destructive potential of the ACPR on other test gases has been studied. Some of the gases are themselves toxic, while others served as models for large toxic molecules. The results summarized here concentrate on destruction efficiency, carrier gas, power levels and frequencies. Again, all tests were conducted at room temperature and atmospheric pressure.

Much of the research reported in this section is from earlier investigations of the ACPR before the existence of an optimum frequency was known. Thus, many of the experiments were carried out at fixed frequencies of 60 Hz which is generally much lower than optimum frequencies later observed. Even at these conditions, respectable levels of destruction were obtained for small test molecules (i.e., formaldehyde), and very high destruction efficiencies were observed for large organophosphorus molecules.

Fraser, Eaton and Sheinson [14] studied the destruction of dimethyl methylphosphonate (DMMP) and trimethyl phosphate (TMP). Power to the reactor was supplied by a 16 kV, 60 Hz transformer. Table IV lists destruction efficiencies for different flow rates and compositions. Major products formed were methane, ethane, carbon monoxide, carbon dioxide and water. DMMP and TMP were used to simulate organophosphorus warfare agents.

Clothiaux, Koropchak and Moore [15] investigated the decomposition of phosphonofluoridic acid methyl-1, 2, 2-trimethylpropyl ester (PFA). This compound was also used as a model to study the destruction of an organophosphorus material. PFA concentrations were 1900 gm/l in air, and flow rates varied from 100 to 800 cc/min. Destruction results are given in Table V. Frequency was held constant at 60 Hz. Voltage levels were not reported, but maximum possible voltage of the equipment was reported to be 18 kV.

Fraser and Sheinson [16, 17] investigated the destruction of hydrogen cyanide (HCN) and cyanogen (C_2N_2). In pure helium, both test species were removed with nearly 100% efficiency leaving a yellow solid deposit in the reactor walls (Table VI). This residue oxidized in the presence of oxygen to form carbon monoxide, carbon dioxide and nitrogen.

TABLE IV

DECOMPOSITION EFFICIENCIES OF
DMMP AND TMP IN AN ACPR

Test Species	Flow Rate (cc/min)	Concentration Test Species (ppm)	Concentration Oxygen (%)	Destruction Efficiency (%)
DMMP	300	580	> 5	52
DMMP	300	580	160	72
DMMP	300	580	500	79
DMMP	300	150	> 5	99
DMMP	300	150	160	100
DMMP	1000	150	> 5	53
DMMP	1000	150	160	86
TMP	300	150	> 5	100
TMP	300	150	160	100

Source: Fraser, M. E., H. G. Eaton and R. S. Sheinson. "Initial Decomposition Mechanisms and Products of Dimethyl Melhylphosphonate in an Alternating Current Discharge." Plasma Chemistry and Plasma Processing, 4(1), 1984.

TABLE V

DECOMPOSITION EFFICIENCY OF PFA IN AN ACPR

Flow Rate (cc/min.)	PFA Concentration (gm/l)	Decomposition Efficiency (%)
100	1900	> 99.6
200	1850	> 99.8
800	1950	81.5

Source: Clothiaux, E. J., J. A. Koropchak and R. P. Moore. "Decomposition of an Organophosphorus Material in a Silent Electric Discharge." Plasma Chemistry and Plasma Processing, 4(1), 1984.

TABLE VI

DESTRUCTION OF HCN IN AN ACPR

Flow Rate (cc/min.)	Oxygen Concentration (ppm)	Destruction Efficiency (%)
150	< 10	> 99.6
150	180	91.4
150	330	91.4
150	630	94.3
300	< 10	85.7
300	630	74.3

Source: Fraser, M. E. and R. S. Sheinson. "Electric Discharge Induced Oxidation of Hydrogen Cyanide." Plasma Chemistry and Plasma Processing, 6(1), 1986.

The authors felt this solid to be a $(CN)_x$ polymer. HCN and C_2N_2 were selected for their known toxicity and presence in product streams from hydrocarbon discharges.

Neely, Best, and Clothiaux [18] studied formaldehyde destruction. The reactor frequency was held constant at 60 Hz and the voltage was varied. A mixture of 46 ppm of formaldehyde and pure oxygen was run at a flow rate of 400 cc/min in the reactor. At 12.6 kV a destruction efficiency of 40% was obtained. Formaldehyde is a well-known industrial pollutant.

Moore and Birmingham [19] studied the destruction of cyanogen chlorides. In this research, an adsorbant based packing in the reactor was used to increase residence time due to a chromatographic effect and allow for greater flow rates. Results are shown in Table VII. Major products were carbon dioxide and a white solid precipitate shown to be mostly ammonium chloride (>75%).

Davis and Tevault [20] investigated the destruction of dimethylsulfide (DMS) in three different atmospheres: $N_2/DMS = 200/1$, $N_2/DMS/O_2 = 400/2/1$, $N_2/DMS/O_2 = 200/1/10$. These figures represent mole ratios. In all cases, destruction efficiencies of nearly 100% were reported. Major products formed in the absence of oxygen were HCN and CS_2. As oxygen concentration increased, HCN was replaced by oxygen and SO_2. At low oxygen concentrations formaldehyde was detected, but disappeared as oxygen levels changed in either direction. The authors felt that formaldehyde was formed in the initial reaction but was subject to further oxidation in a plasma environment. Power levels and frequencies used were not reported.

TABLE VII

DECOMPOSITION OF CYANOGÉN CHLORIDE
IN A PACKED ACPR REACTOR

Flow Rate (ft^3/min)	Power Applied (kW)	Effective Residence (sec)	Destruction Efficiency (%)
1.0	1.0	10.6	> 99.6
2.59	1.0	7.3	> 99.6
5.00	1.3	2.3	98.8

Note: Composition was 4000 ug per liter of air

Source: Moore, R. R. and J. G. Birmingham. "The Decomposition of Toxic Chemicals in a Low Temperature Plasma Device." In Proceedings of the International Congress on Hazardous Materials Management, Chàtanooga, Tennessee (June 8-12, 1987).

Research on Toxic By-Products

In a commercial application, air will most likely be the carrier stream due to its availability. Formation of harmful gases are a concern with the ACPR under these conditions. The following section concentrates on research in this area.

The predominant toxic products formed with an air carrier are ozone, carbon monoxide and NO_x. Gilman, Birmingham, and Moore [21] showed that ozone was predominant at low destruction efficiencies. In contrast, at high destruction efficiencies, NO_x was the principal toxic by-product. The work of Sheinson, Smyth, Piatt, and Wills [13] showed that carbon dioxide is favored over carbon monoxide at high destruction efficiencies of hydrocarbons. Since high levels of destruction are desired in a working ACPR, further work concentrated on minimizing NO_x production.

Tevault, Chester, Simmons, and Birmingham [22] studied NO_x production as a function of frequency, power and humidity. Air was used at a flow rate of 1 l/min. At low relative humidities, NO_x levels were high--sometimes exceeding 100 ppm. However, when the inlet air was humidified to 100%, NO_x levels fell below detection limits. Thus, under these conditions, a way to handle the NO_x problem was found.

The above paper was the first to notice a resonant or optimum frequency for the ACPR. This was observed during the low humidity tests. At a fixed voltage, NO_x levels went through a maximum as frequency increased. The optimum frequency digressed at higher voltages. These results agree well with the extensive power input, frequency research covered in this thesis.

Moore, Birmingham, and Koropchak [23] showed that processing high humidity streams did not affect decomposition efficiencies. In their work, methyl cyanide was the test species. At optimum conditions, destruction levels of methyl cyanide were unchanged by humidifying the air streams.

In further work, Birmingham and Moore [24] studied high flow rate (2.0 ft^3/min.), high humidity air in a packed ACPR. Packing consisted of a catalyst with several metals impregnated on porous alumina spheres. At 90% relative humidity, NO_x concentrations remained at background levels up to 900 watts of applied power. Even at high power levels, NO_x levels never exceeded 20 ppm.

Methane Reaction Mechanisms in an ACPR

Reaction mechanisms in electrical discharges for a number of chemical species have been investigated. The following section concentrates on investigations into methane reaction mechanisms, since methane is the test species studied in this thesis.

Fraser, Fee, and Sheinson [12] studied the reaction mechanism of CH_4 in pure nitrogen and in nitrogen/oxygen mixtures. In pure nitrogen the authors believed the relevant reactions to be those shown below

$$H + CH_4 \rightarrow CH_3 + H_2 \tag{3.1}$$

$$CH_3 + N \rightarrow HCN + H_2 \text{ (or 2H)} \tag{3.2}$$

Also, possible as an initial step, is the following reactions.

$$CH_4 + N \rightarrow HCN + H_2 + H \tag{3.3}$$

The authors admit that the reaction of methane with discharged nitrogen is poorly understood. In the presence of oxygen, hydrogen cyanide breaks down to form carbon monoxide, carbon dioxide and water.

Tevault [25] used spectroscopy techniques to study methane reactions in nitrogen and nitrogen/oxygen mixtures. He concluded that the initial step appears to be hydrogen atom stripping from CH_4. This is followed by the formation of HCN and NH_3. When small amounts of oxygen are added, the product stream contains CO and H_2O. As oxygen content increases, CO and H_2O increase first then N_2O, NO_2 and O_3 levels rise. As oxygen content rises further, HONO and HNO_3 appear.

Boenig [4] also reported that the initial step of hydrocarbon decomposition in the absence of oxygen is hydrogen stripping as shown.

$$e + RH \rightarrow R + H + 2e \tag{3.4}$$

where R stands for a hydrocarbon.

Boenig also states that methane can react with nitrogen and oxygen as follows.

$$O + CH_4 \rightarrow OH + CH_3 \tag{3.5}$$

$$CH_4 + N \rightarrow HCN + 3/2\ H_2 \tag{3.6}$$

Sheinson [26] showed that methane destruction efficiency is not enhanced by addition of excess oxygen. Instead, the oxygen molecule can compete for the electrical energy of the plasma. The end result is that a significant portion of the electrical energy is used to oxidize by-products instead of decomposing the test species. This was seen in decomposition tests of DMMP. At high oxygen levels, destruction efficiency actually fell.

One of the objectives of this research is to develop a kinetic model for methane conversion. Mach and Drost [27] determined that methane conversion fit a first order reaction model in a direct current closed (batch) discharge tube. Operating pressures were 1 to 2 torr for the reactor. The first order model held at all residence times studied.

Tezuka and Miller [28] studied the reaction of anisole in a radio frequency, inductively coupled discharge reactor. They observed that the conversion of anisole obeyed the following relationship

$$- \log(C/C^{o}) = 0.021(P/\dot{n}_a) + 0.05 \tag{3.7}$$

where C is molar concentration of anisole, C^{o} is initial molar concentration of anisole, P is power, and $\dot{n}_a$ is molar flow rate.

CHAPTER IV

EXPERIMENTAL APPARATUS, PROCEDURE AND ANALYSIS

This chapter covers the area of experimental techniques. Section one describes in detail the reactor cavities used in the experiments. Section two describes the other units in the experimental apparatus. Section three summarizes the method of sample preparation. Section four describes the experimental procedures and analysis of the gas streams.

Reactor Cavity

Diagrams of the three reactors used are shown in Figures 4, 5, and 6. The small reactor shown in Figure 4 is the same as used in research described earlier at the Naval Research Laboratories [13]. By using this reactor, research in this thesis can build upon previous work. The large reactors were included as an initial attempt to study scale-up. In the rest of this thesis, these three reactors will be referred to, respectively, as Reactor 1, Reactor 2, and Reactor 3.

The basic reactor design is a capacitive device consisting of two concentric glass cylinders. This forms an annular space for gas flow. Reactor 1 was custom made; however, Reactors 2 and 3 were constructed with a standard glass condensing tube. Two electrodes were used to create an electric discharge or plasma in the annulus. The inner

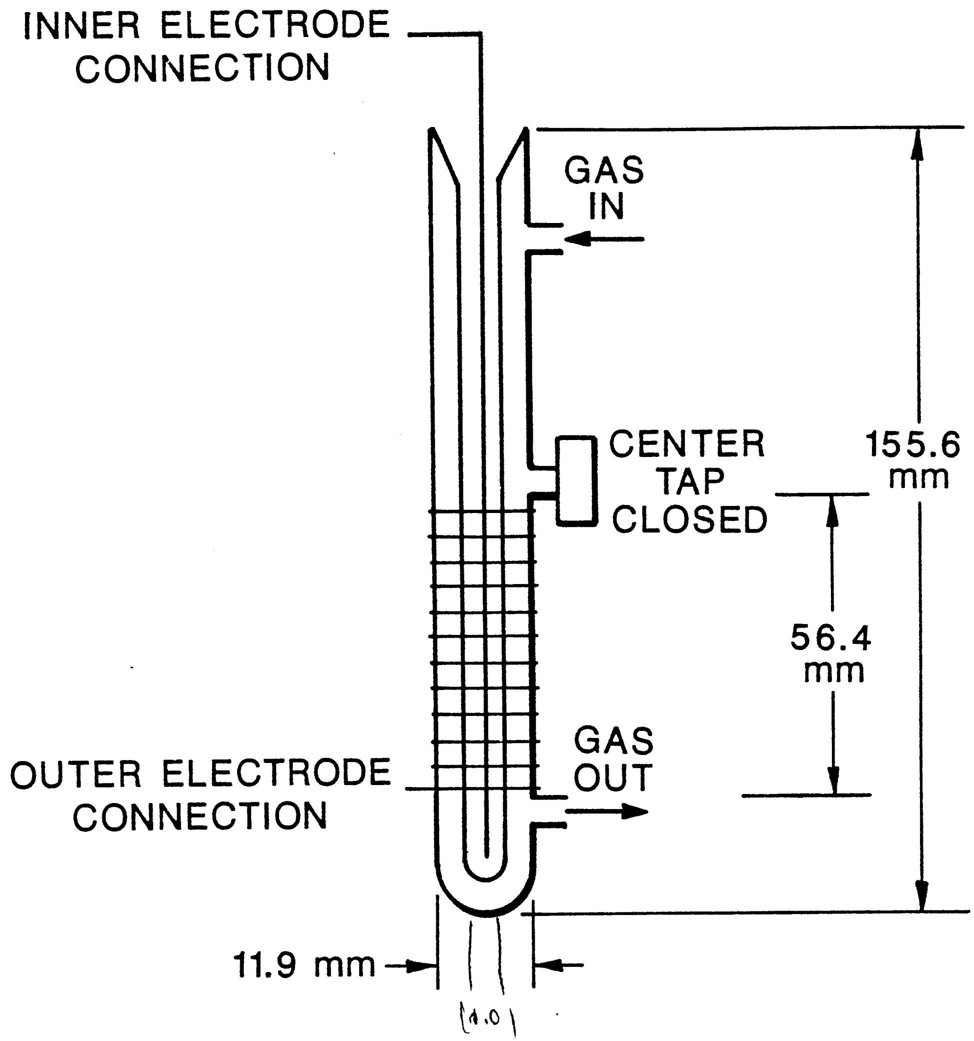

Figure 4. Reactor 1, Small Reactor with Copper Wire Inner Electrode, Volume = 10.8 cc

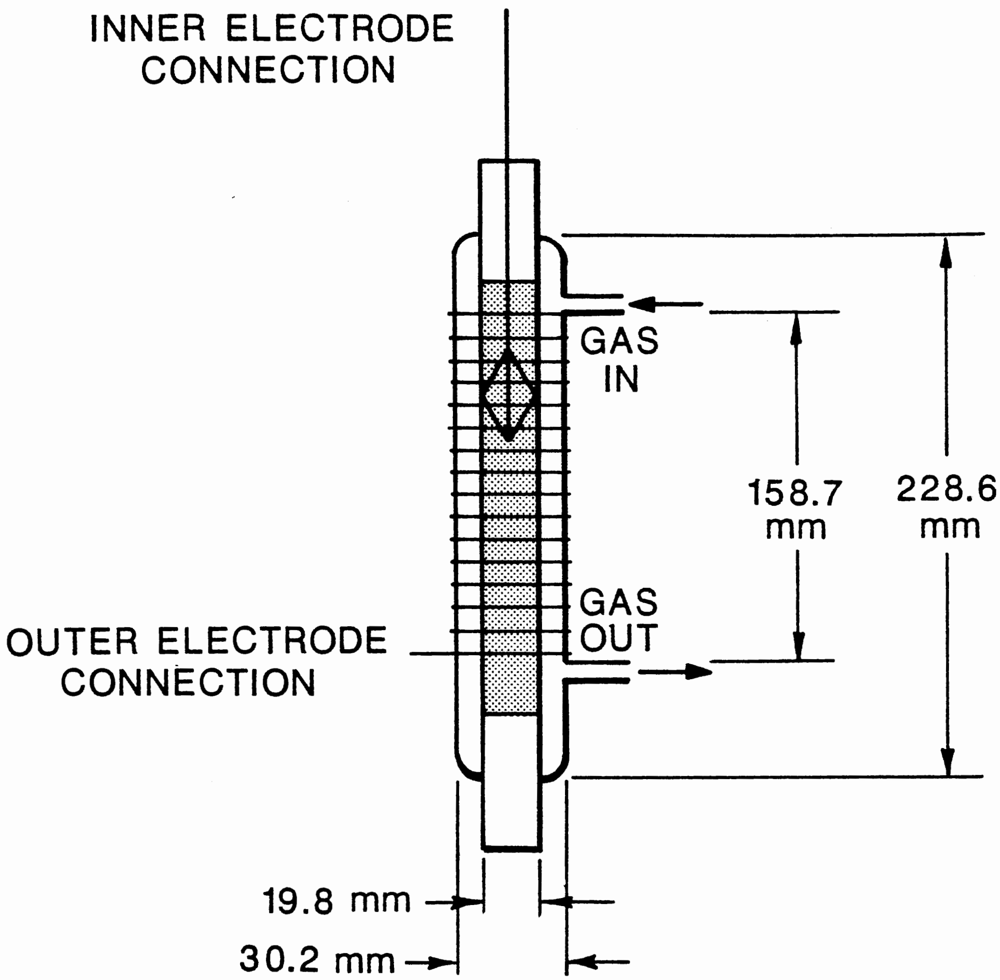

Figure 5. Reactor 2, Large Reactor with Copper Mesh Inner Electrode, Volume = 64.4 cc

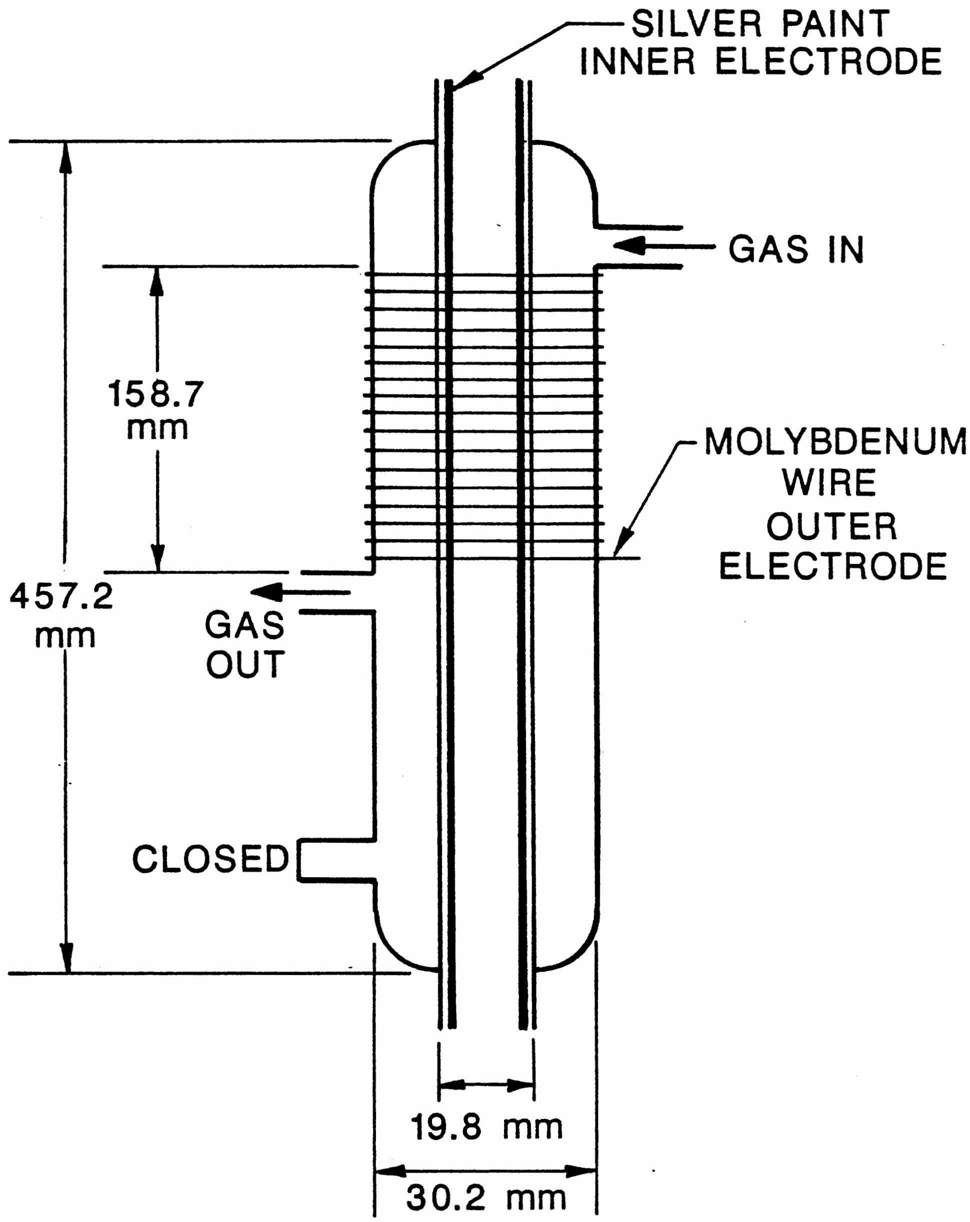

Figure 6. Reactor 3, Large Reactor with Silver Paint Inner Electrode, Volume = 64.4 cc

electrode was made of copper wire, copper mesh or silver paint, and was located inside the inner glass cylinder. The outer electrode consisted of a molybdenum wire (1 mm diameter) tightly wrapped on the outside of the outer glass cylinder. A wire wrap instead of a continuous coating was used to allow visual observation of the plasma.

When an electric potential is applied, the glass serves as a dielectric causing the current to diffuse into a continuous glow or plasma in the reactor annulus. The dielectric material is necessary to prevent arcing of the current between the electrodes and to separate the electrodes from the gas stream. Gases flowing in the annulus pass through the plasma where plasma energy causes breaking of chemical bonds and subsequent reactions. At no point in the reactor does the gas stream come in contact with the electrodes directly. This minimizes electrode corrosion and fouling from reaction by-products.

There are several differences among the reactors used in this study. Reactor 1, shown in Figure 4, has an annular volume of 10.8 cc, while Reactors 2 and 3 each have a volume of 64.3 cc. A 12 gauge copper wire served as the inner electrode for Reactor 1. For Reactor 2, the inner electrode consisted of a 40 mesh copper sheet wrapped into a cylinder and fitted into the inner glass cylinder. Reactor 3 was identical to Reactor 2 except the inner electrode consisted of silver paint coated on the inside of the inner glass cylinder. Contact with the electrical lead was provided by a 12 gauge wire which was spread apart to insure good contact with the copper mesh or paint. In all reactors the outer electrode was molybdenum wire. A constant 12 wraps of wire on the small reactor and 17 wraps on the large reactors were used in all experiments.

Experimental Apparatus

A schematic of the apparatus is shown in Figure 7. The gas mixture to be reacted was premixed and kept in a separate gas bomb. Flow rates to the reactor were measured by a calibrated rotameter. The gas stream flowed into the top port of the reactor and exited from the bottom port. After leaving the reactor, the gas stream could be directed either to the gas chromatograph or to the vent.

The three reactors were interchangeable in the apparatus. Nylon Swagelok connectors were used at the glass ports of the small reactor. The large reactors used ground glass connections held in place by plastic clamps which could be tightened to form a leak proof seal.

Power was supplied to the reactor by a California Instruments Model 161T oscillator. Instrument output range was from 0 to 120 volts rms and 40 to 5000 Hz. A step up in voltage from the power source to the reactor was provided by a Jefferson Electric luminous tube transformer having a primary voltage of 120 and secondary voltage of 7500. This type of transformer was used due to its similarity with the transformer used at the Naval Research Laboratories. Current to the reactor was measured by a Simpson Model 462 autoranging digital multimeter which was positioned on one of the leads between the transformer and reactor. Voltage across the reactor was measured by a Simpson AC high voltage test probe.

Several important safety features were included in the apparatus design. Due to the high voltages generated in the reactor, the apparatus was enclosed on all sides (except the bottom) by a non-conducting material which formed an auxiliary hood over the apparatus. Plastic shields and the room walls formed the sides, while the top was covered

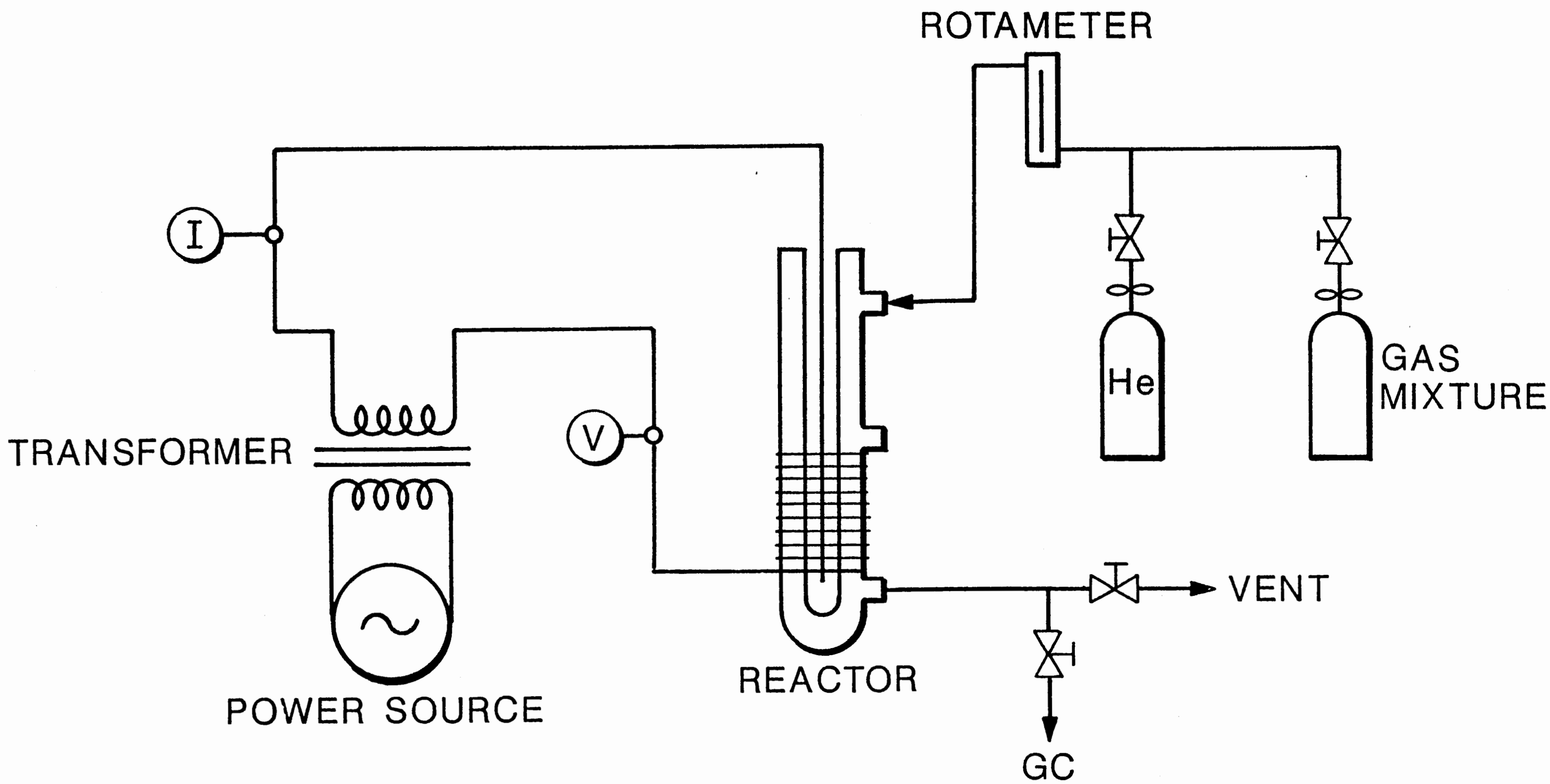

Figure 7. Experimental Apparatus

with wood. In addition, all components and measuring equipment except the power source were located on a table which was physically separate from and located inside the auxiliary hood. To prevent electric charges from traveling down the tubing, Norprene rubber tubing was used in place of copper tubing around the rotameter and reactor. During operation, the experimenter had access to the frequency and voltage controls, the gas cylinders and flow rate controlling valves, and the valves directing outlet gas flow.

In addition to high voltage, ozone formation around the reactor is a safety concern. The auxiliary hood serves to prevent any ozone formed from escaping to the room atmosphere. Ozone is removed from the auxiliary hood by means of a vent located directly above the reactor. A fan draws air from beneath the reactor up to the vent where it is then piped out to the main hood.

Sample Preparation

The inlet gas mixtures were prepared prior to the experimental runs using the apparatus shown in Figure 8. Premixing all three gases into a single bomb was used instead of flowing the gases from individual bombs into the inlet line as in previous work [13]. This was done to minimize variation of inlet concentrations between experimental runs.

The preparation of a typical sample was done as follows:

1. With the oxygen bottle attached and all gas cylinders closed, the lines were evacuated with a vacuum pump. This pump could draw the pressure down to about 1.5 torr.

2. The lines were flushed with methane and evacuated.

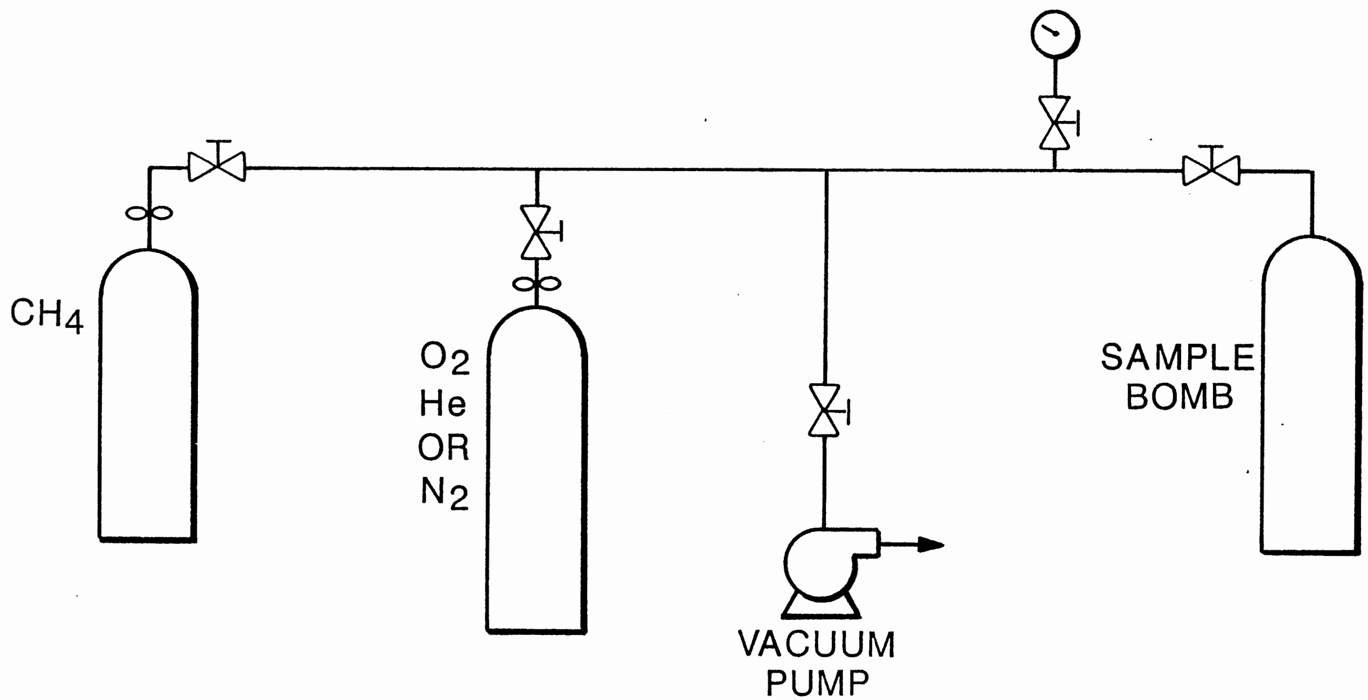

Figure 8. Sample Preparation Apparatus

3. The sample bomb was opened. The lines and the sample bomb were evacuated. Both were flushed several times with methane.

4. The valve leading to the vacuum pump was closed, and the sample bomb was filled with the desired amount of methane.

5. The methane bomb was closed. The sample bomb was then filled with the desired amount of oxygen.

6. The sample bomb was closed, and the oxygen cylinder was switched out for helium or nitrogen.

7. The lines were flushed several times with helium or nitrogen.

8. The sample bomb was opened and filled to the desired level with helium or nitrogen.

All connections were taped and checked periodically for leaks. Pressures could be measured by both a line gauge and the sample bomb regulator.

Experimental Procedure and Analysis

The following section is a brief description of the experimental procedures used in the non-destructive and destructive tests as well as the analysis of the gas streams.

For non-destructive tests, an inert gas such as helium, oxygen, air or nitrogen was used to study the physical and electrical characteristics of the reactor. The inert gas was first allowed to flow through the reactor for 3-5 minutes at the desired flow rate without the electrical power supply turned on. This was to purge any air remaining in the system and to establish a steady state flow regime. The power supply was then turned on, and the desired voltage for the particular run was set and held constant throughout the run.

Frequency was varied starting at 70 Hz and increasing to 1000 Hz. At each data point, current and voltage to the reactor were read and recorded. Sufficient time was allowed at each point for the current and voltage readings to stabilize. Power input to the reactor is given as the product of voltage and current. Near the optimum frequency, readings were taken every 10 Hz to insure that the optimum was located accurately. The number of data points taken per run varied but typically was between 20 and 30.

For the destructive tests, premixed gas samples of methane in air or a helium/oxygen mixture were used to study the destructive capabilities of the reactor. Initially, the sample flowed through the system with the power off, and inlet concentrations of methane were determined by a gas chromatograph. Power was then turned on at the desired primary voltage and frequency, and the effluent was routed to the gas chromatograph for analysis. In addition, current and voltage in the reactor were measured and recorded.

Except in one experiment where destruction versus frequency was tested, all destructive tests were run at or near the optimum frequency. This was determined by varying the frequency until the power input to the reactor was maximized. Analysis of the effluent was done after the system had stabilized.

After the last destruction sample was taken, the power was turned off, and the inlet sample allowed to flow through the system. Inlet methane concentration was then again measured. The number of data points per sample ranged from one to nine, depending upon flow rate and reactor volume used.

Analysis of the gas streams was done by a Perkin-Elmer Sigma 3B gas chromatograph using a flame ionization detector (FID). Helium was the carrier gas at 42 cc/min. Separation was accomplished with an Alltech CTR1 double column packed with porapak (inner column) and activated molecular sieve (outer column). This column is specifically designed to separate methane, oxygen, nitrogen, carbon dioxide and carbon monoxide. A gas sampling valve was employed to inject a 1 ml sample into the chromatograph. Also, the sample bomb regulator pressure was kept constant during a run. These last two items helped insure consistent results using the gas chromatograph.

Since a FID can only detect methane, only destruction of methane, based on area difference of inlet and effluent samples, could be determined directly from the chromatograms. A linear relationship between peak area and methane concentration was established. Before each run, a standard was made with methane at atmospheric pressure and an inert gas at some higher pressure. The mole fraction of methane of this standard was known by partial pressures (assuming ideal gas). This standard flowed through the system at the same regulator pressure (and same regulator) as the destructive tests to establish GC area per percent methane.

Inlet and outlet methane concentrations could then be determined by comparison with the standard. Inlet oxygen concentrations could be determined by partial pressures, but effluent oxygen concentrations could not be determined using this method. A more detailed list of the gas chromatograph operating conditions along with a sample chromatogram and sample calculations are given in Appendix A.

CHAPTER V

KINETIC MODEL

In this chapter, a kinetic model developed to describe the rate of disappearance of methane in an ACPR is described. The purpose of this model is to predict methane destruction in an ACPR as a function of inlet concentration and reactor variables. Assumptions used in developing this model are discussed, and initially a zero order reaction model is hypothesized. Experimental data presented in Chapter VII will test the proposed model. Any changes in the assumptions will be discussed there.

Assumptions

Assumptions used in developing this model are as follows:

1. Steady state conditions exist.
2. All chemical species (including water) are in the gas phase only.
3. The ideal gas law applies to the feed and product streams.
4. Pressure of the system is constant and taken to be 1 atmosphere.
5. Temperature of the feed and product streams is approximately equal and taken to be 25°C.
6. Chemical reaction occurs only in the reactor, not in the inlet and outlet lines.

7. The primary reaction is the following:

$$CH_4 + 2O_2 \rightarrow CO_2 + 2\ H_2O \tag{5.1}$$

Therefore, there is no net mole change.

8. Reaction is irreversible.

9. This is a plug flow reactor.

10. The rate of methane disappearance can be expressed as a zero order reaction or

$$dC_a/dt = \frac{k_1\ C_a}{1 + k_2\ C_a} \tag{5.2}$$

where C_a is the molar concentration of methane, t is time, k_1 and k_2 are rate constants.

At this point, the first eight assumptions are believed to be reasonable. Assumption 9, plug flow reactor, is questionable. Reynold's number calculations show laminar conditions for the flow rates studied (Appendix C). However, it is not clear that laminar flow actually existed in the reactor during operation. The highly energetic nature of the plasma could cause sufficient turbulence and mixing to make a plug flow assumption valid. Assumption 10 was hypothesized and is subject to change.

Derivation

A general material balance for methane can be written:

$$\text{Methane In} - \text{Methane Out} + \text{Methane Generation} = \text{Methane Accumulation} \tag{5.3}$$

For a differential element of the reactor, $A\Delta Z$, a shell balance can be written for each term.

$$\text{Methane In} = Q\, C_a\big|_Z \tag{5.4}$$

$$\text{Methane Out} = Q\, C_a\big|_{Z+\Delta Z} \tag{5.5}$$

$$\text{Methane Generation} = -\, r_a V^t = -\left(\frac{k_1 C_a}{1 + k_2 C_a}\right)(A\Delta Z) \tag{5.6}$$

$$\text{Methane Accumulation} = 0 \tag{5.7}$$

where Q is the volumetric flow rate, r_a is the rate of methane appearance, V^t is the volume of the element, A is the area for flow, and Z is the length down the reactor. Substituting eqs. 5.4-5.7 into 5.3 yields the following:

$$Q(C_a\big|_Z - C_a\big|_{Z+\Delta Z}) - \left(\frac{k_1 C_a}{1 + k_2 C_a}\right)(A\Delta Z) = 0 \tag{5.8}$$

Dividing by ΔZ and taking the limit as ΔZ approaches zero gives the following:

$$-Q\,\frac{dC_a}{dZ} - \left(\frac{k_1 C_a}{1 + k_2 C_a}\right) A = 0 \tag{5.9}$$

Rearranging eq. 5.9 yields

$$\left(\frac{1 + k_2 C_a}{C_a}\right) dC_a = -\,\frac{Ak_1}{Q}\, dZ \tag{5.10}$$

Integrating eq. 5.10 yields

$$\ln C_a + k_2 C_a = -\left(\frac{Ak_1}{Q}\right) Z + \text{Constant} \tag{5.11}$$

To evaluate the constant of integration, the initial condition that at

$Z = 0$, $C_a = C_a^\circ$ (where C_a° is the inlet methane concentration) is applied.

$$\text{Constant} = \ln C_a^\circ + k_2 C_a^\circ \tag{5.12}$$

Eq. 5.11 can be written as

$$\ln \frac{C_a^\circ}{C_a} + k_2(C_a^\circ - C_a) = k_1 \left(\frac{AZ}{Q}\right) \tag{5.13}$$

But AZ/Q is equal to the residence time τ. So, eq. 5.13 can be written as

$$\ln C_a^\circ/C_a + k_2(C_a^\circ - C_a) = k_1\tau \tag{5.14}$$

Discussion

Data presented in Chapter VII will be used to test the proposed model. Eq. 5.14 can be tested by rearranging its form.

$$\frac{\ln (C_a^\circ/C_a)}{C_a^\circ - C_a} = -k_2 + \frac{k_1\tau}{C_a^\circ - C_a} \tag{5.15}$$

The model is valid if a straight line results when

$$\frac{\ln (C_a^\circ/C_a)}{C_a^\circ - C_a}$$

is plotted against $\dfrac{\tau}{C_a^\circ - C_a}$.

This line will have a slope of k_1 and a y - intercept of - k_2. After evaluating the experimental data, a different expression for eq. 5.6 may be proposed.

CHAPTER VI

NON-DESTRUCTIVE TEST RESULTS

One of the objectives of this thesis was to use inert gases in the system to study the physical and electrical characteristics of an ACPR. By conducting these experiments, key variables could be identified for further study in the destructive tests.

To accomplish this objective, a wide variety of variables were tested using several inert gases: helium, nitrogen, oxygen, and air. Independent variables tested were frequency, primary voltage, gas composition, flow rate, humidity, reactor size, and electrode material. The dependent variable was power input to the reactor which is the product of measured secondary voltage and measured secondary current. Atmospheric pressure and room temperature were used in all experiments. Understanding the relationship between power input and these variables is believed to be important. Previous work [13] showed that methane destruction increased as power input increased. This same research also discovered that, for a given set of conditions, an optimum frequency existed which would give a maximum power input to the reactor. Research presented in this chapter shows how this optimum condition is affected under a variety of conditions.

The reason for this optimum condition occurring is believed to be a result of the secondary electrical circuit loading on the transformer. Transformers are basically inductive devices which convert current into voltage and consist of two sets of windings (primary and secondary) around a magnet. When a capacitance generating circuit is connected to the secondary side of a transformer, a frequency may exist where the capacitance of the circuit is equal to the inductance of the transformer. This condition is called resonance, and at this point, secondary voltage goes through a maximum [29]. Secondary current also reaches a maximum due to the basic relationship between current and voltage.

A detailed mathematical description of this phenomena for the system of interest is not one of the objectives of this research. Rather, a basic understanding of the effect of different operating variables on the optimum condition is desired at this time. From this information, future research can concentrate on critical variables affecting the ACPR. To accomplish this objective, results from non-destructive testing are presented in graphical form and discussed in the following sections. Experimental data with all fixed conditions is tabulated in Appendix D.

Power Input Dependence on Frequency, Primary Voltage and Gas Composition

Figure 9 shows the relationship between power input and frequency at different primary voltages. All tests were conducted with pure helium flowing at 13 cc/min in Reactor 1 (volume of 10.8 cc). Each curve represents a constant primary voltage to the transformer. As primary voltage increased, the value of maximum power input increased. Note that the optimum frequency decreases as primary voltage increases. This same phenomena was observed in previous work [13].

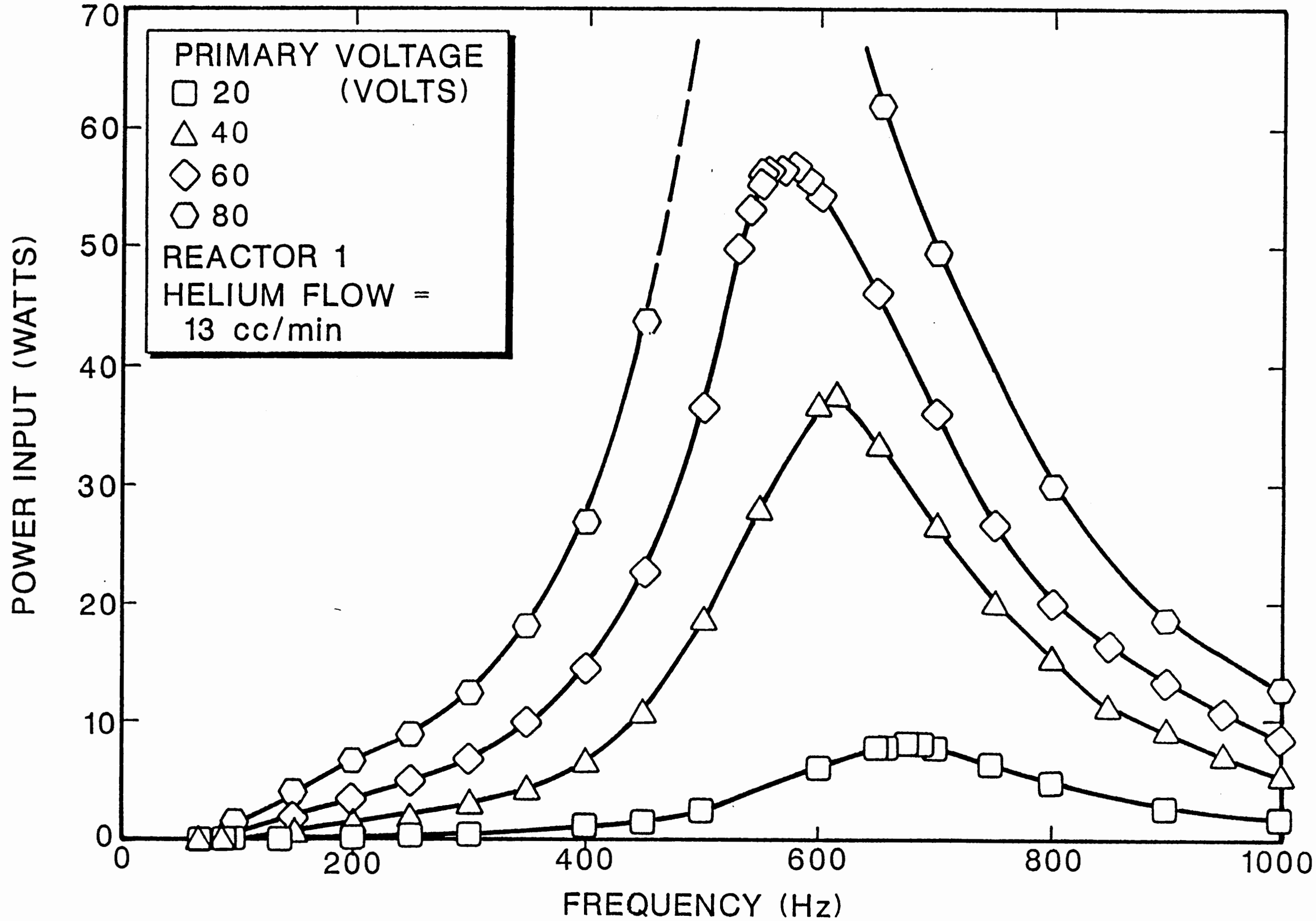

Figure 9. Power Input Dependence on Primary Voltage (Helium)

Values for power input near the maximum at a primary voltage of 80 could not be obtained. At these points, the secondary voltage would have exceeded the output voltage rating of the transformer. At high voltages, the glow can become unstable and arcing to a nearby metal surface can result. Care in insulating the circuit can minimize this phenomena.

Figure 10 reproduces the conditions in Figure 9 except that the gas was pure nitrogen flowing at 13 cc/min. Once again the same general phenomena were observed; however, the locations of the optimum frequencies were at higher values for each value of primary voltage. Also, the measured power input was greater for nitrogen than for helium at each primary voltage value. Thus, gas composition can have an important effect upon power input along with primary voltage and frequency.

To further study the dependence of power input on gas types, pure oxygen and air were also tested at a flow rate of 13 cc/min. Figure 11 shows the results of all four gas types run at the same flow rate, primary voltage and reactor volume. The results for nitrogen, oxygen and air are all relatively close to each other when compared to helium. By analyzing the experimental data, one can conclude that the major difference between helium and the other gases is in the secondary current generated, not the secondary voltage. In Figures 12 and 13, current and voltage (respectively) are plotted against frequency for the different gases. One explanation for this phenomena is that helium being a monotomic and smaller molecule cannot liberate as many electrons in the excited state and therefore cannot generate as much electric current.

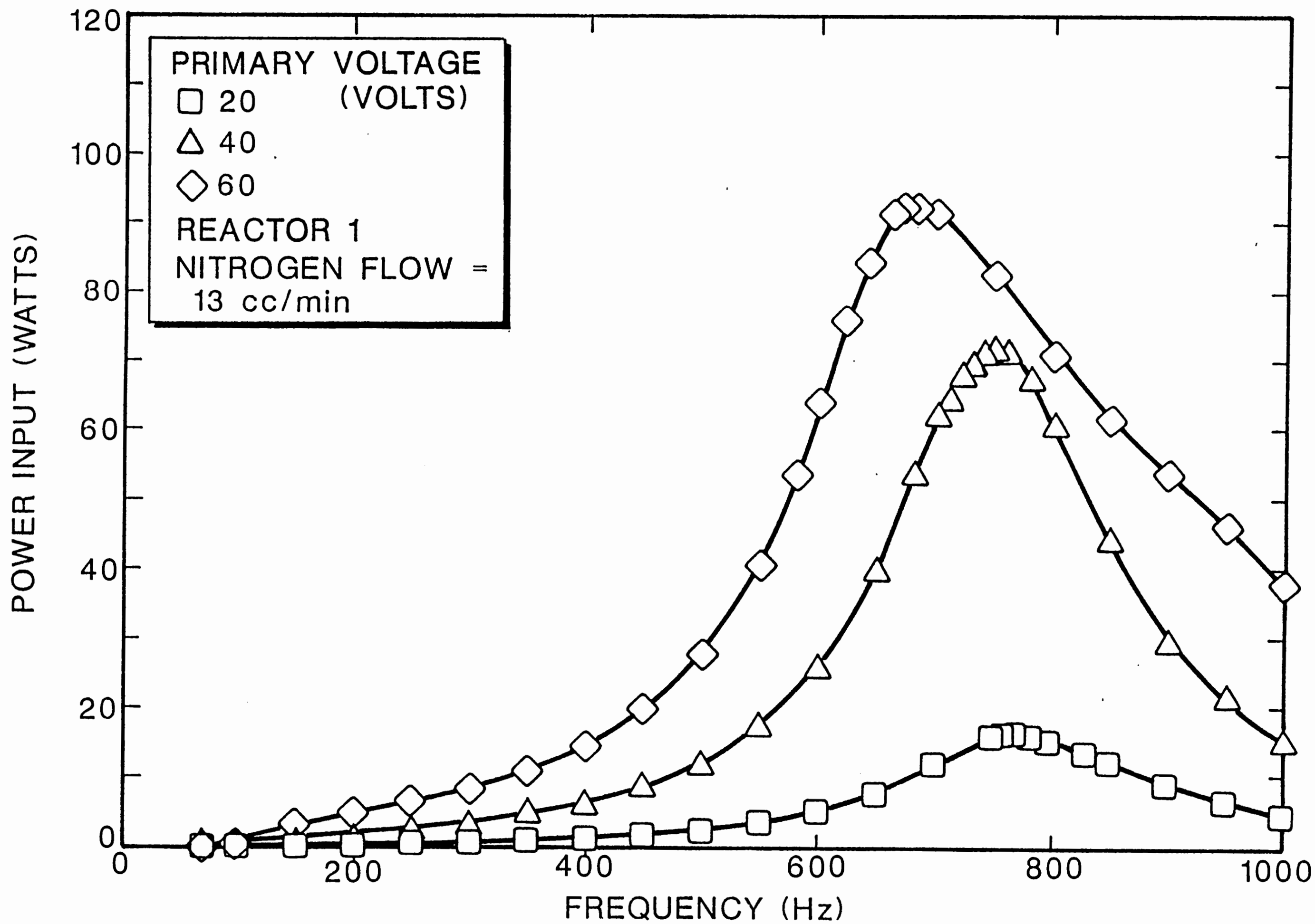

Figure 10. Power Input Dependence on Primary Voltage (Nitrogen)

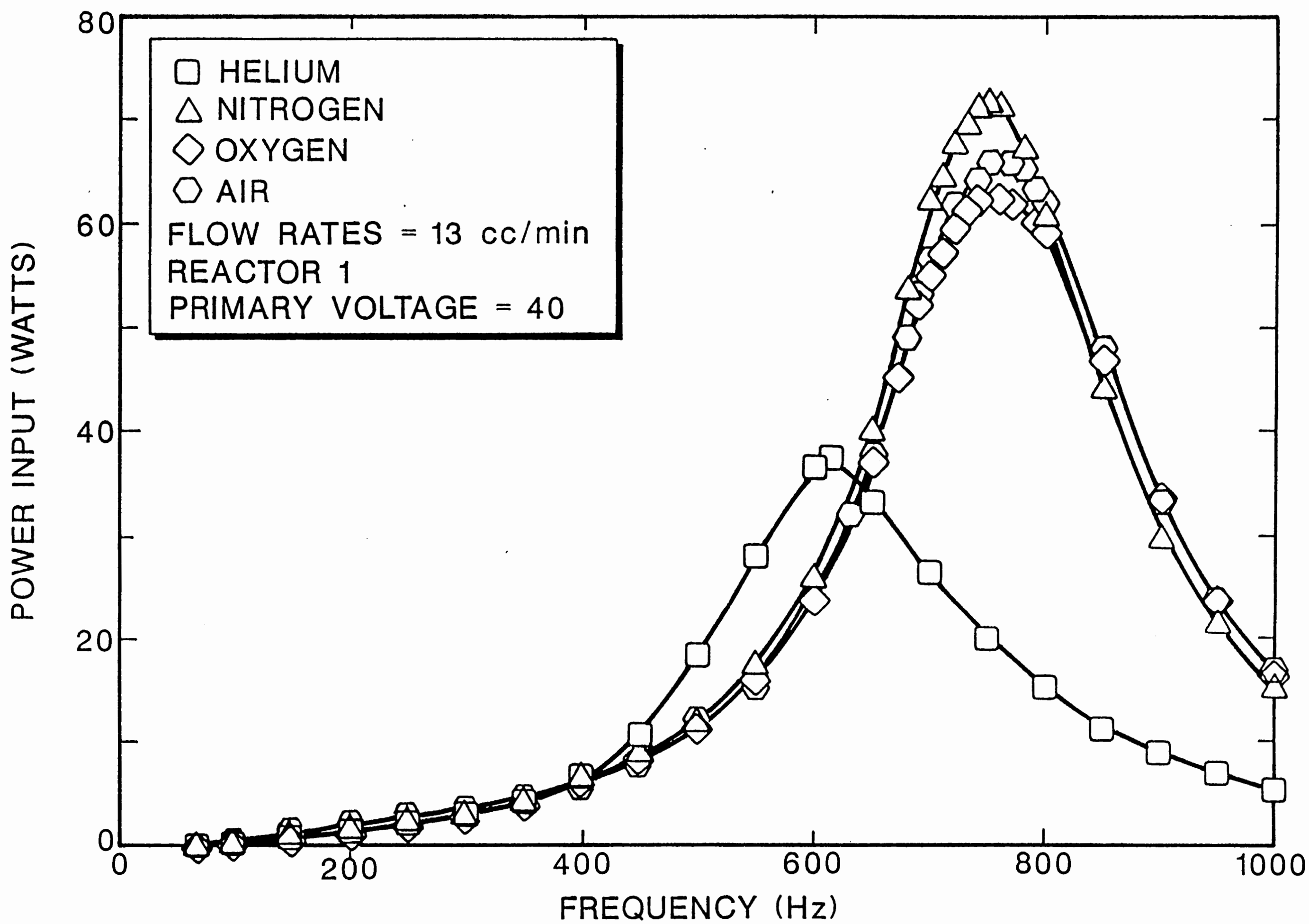

Figure 11. Power Input Dependence on Gas Type

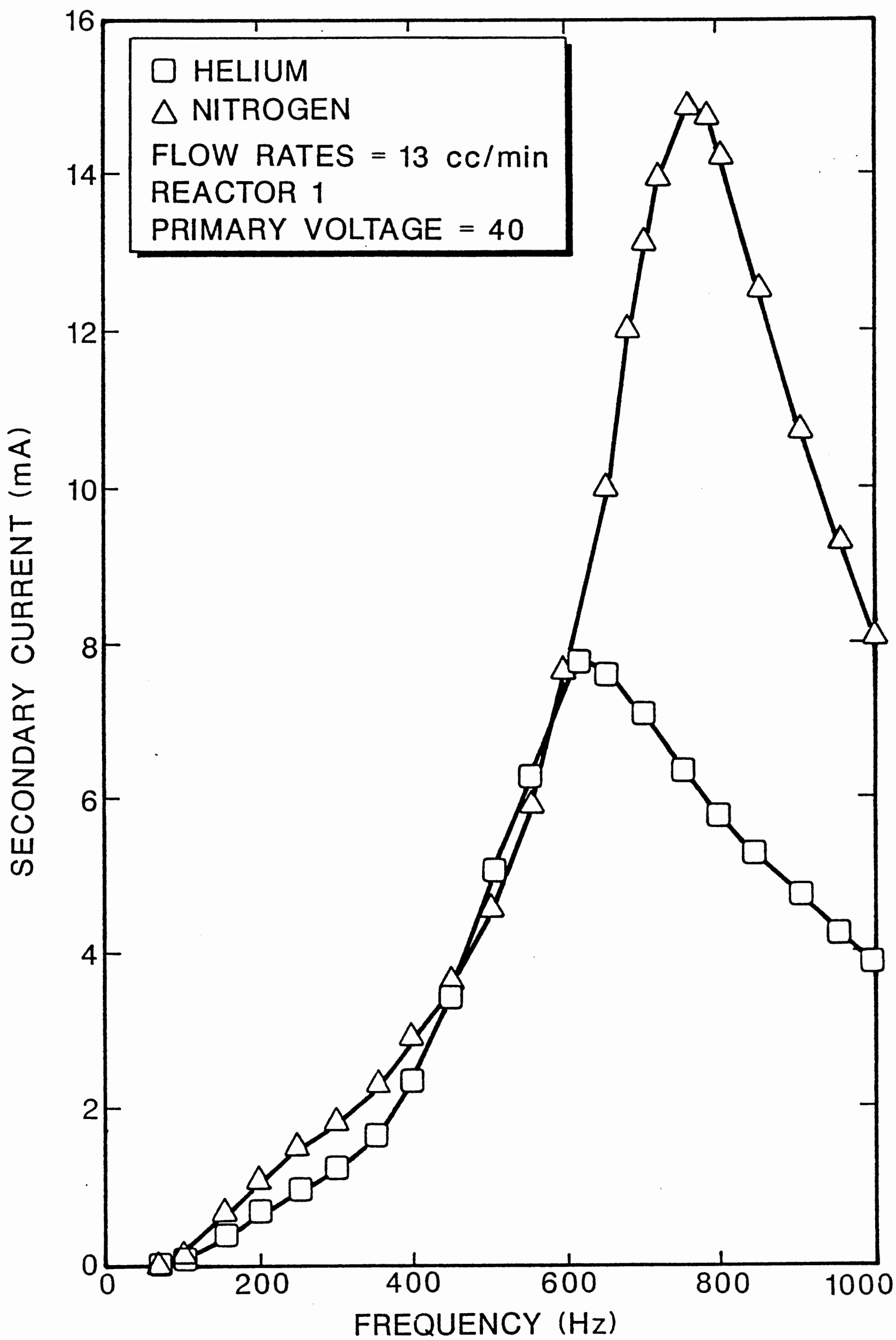

Figure 12. Secondary Current Dependence on Gas Type

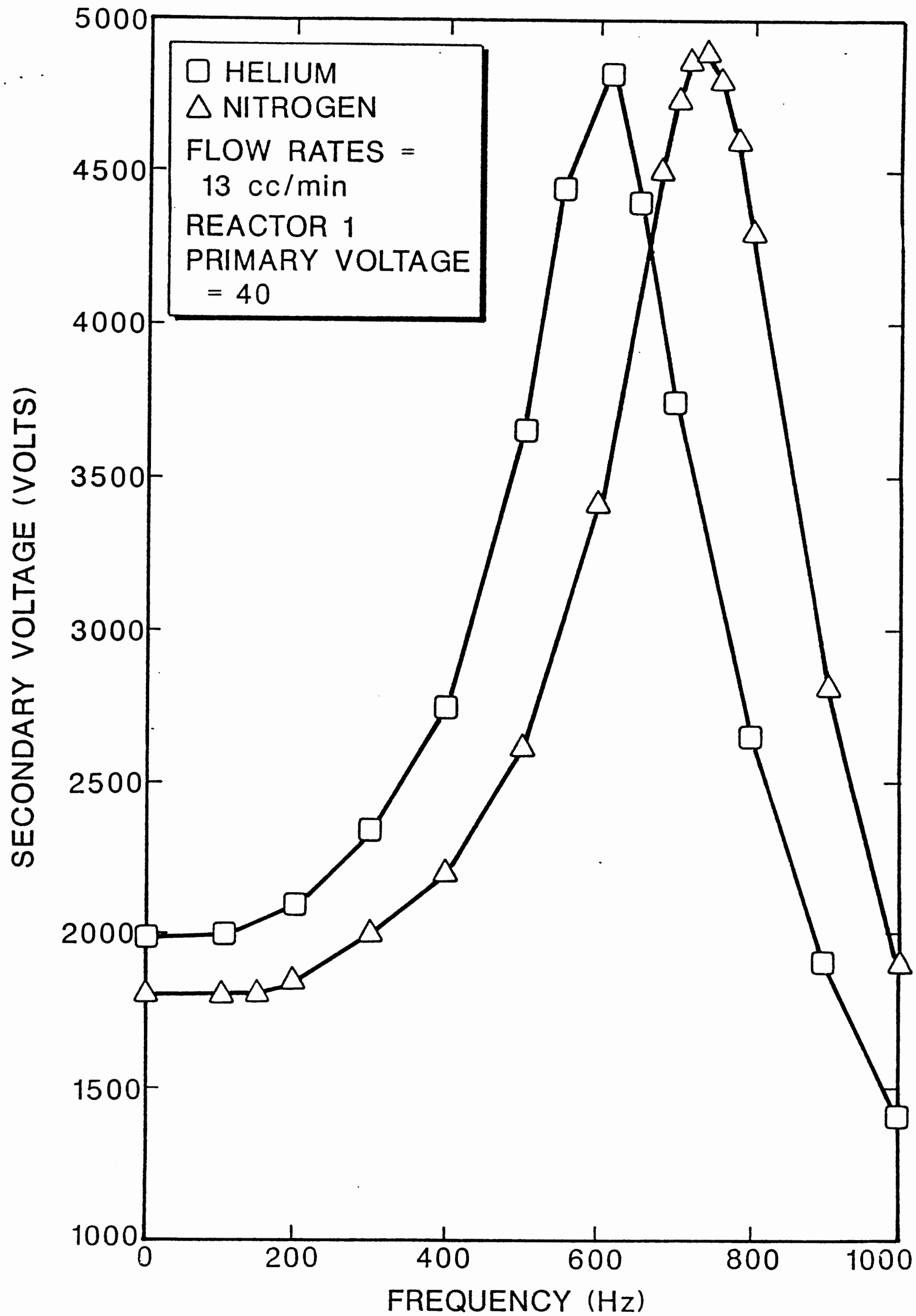

Figure 13. Secondary Voltage Dependence on Gas Type

Power Input Dependence on Flow Rate

Determination of power input dependence on gas flow rate was accomplished by flowing helium and nitrogen at two different rates, 13 cc/min and 528 cc/min, at different primary voltages. Figures 14 and 15 show the results of helium flow at primary voltages of 20 and 60, respectively. Power input does appear to be dependent on flow rate near the optimum frequency; however, it is not a strong dependency. At a primary voltage of 60, the power input fell 5% when flow rate was increased 41 times. This variation in power input was confirmed by holding frequency constant and varying flow rate. Figure 16 shows the same results of varying nitrogen flow rates. Once again, only a weak dependency is observed.

Two possible mechanisms can explain the lower power input at higher flow rates. One, the molecules' residence time in the reactor at high flow rates is less. Therefore, they have less chance to absorb plasma energy and release electrons. Two, gas flow is at right angles to electron movement between the electrodes. From these experiments, no determination could be made as to which mechanism was dominant.

From research presented in this section, it can be concluded that power input is only weakly dependent on flow rate for the conditions studied. However, both flow rates lie in the laminar flow regime when Reynold's numbers are calculated (Appendix C). Further investigations in turbulent flow are warranted.

Power Input Dependence on Reactor Size

As a first step to study scale-up, inert gases were run in two reactors, each having an annular volume of 64.4cc (now referred to as

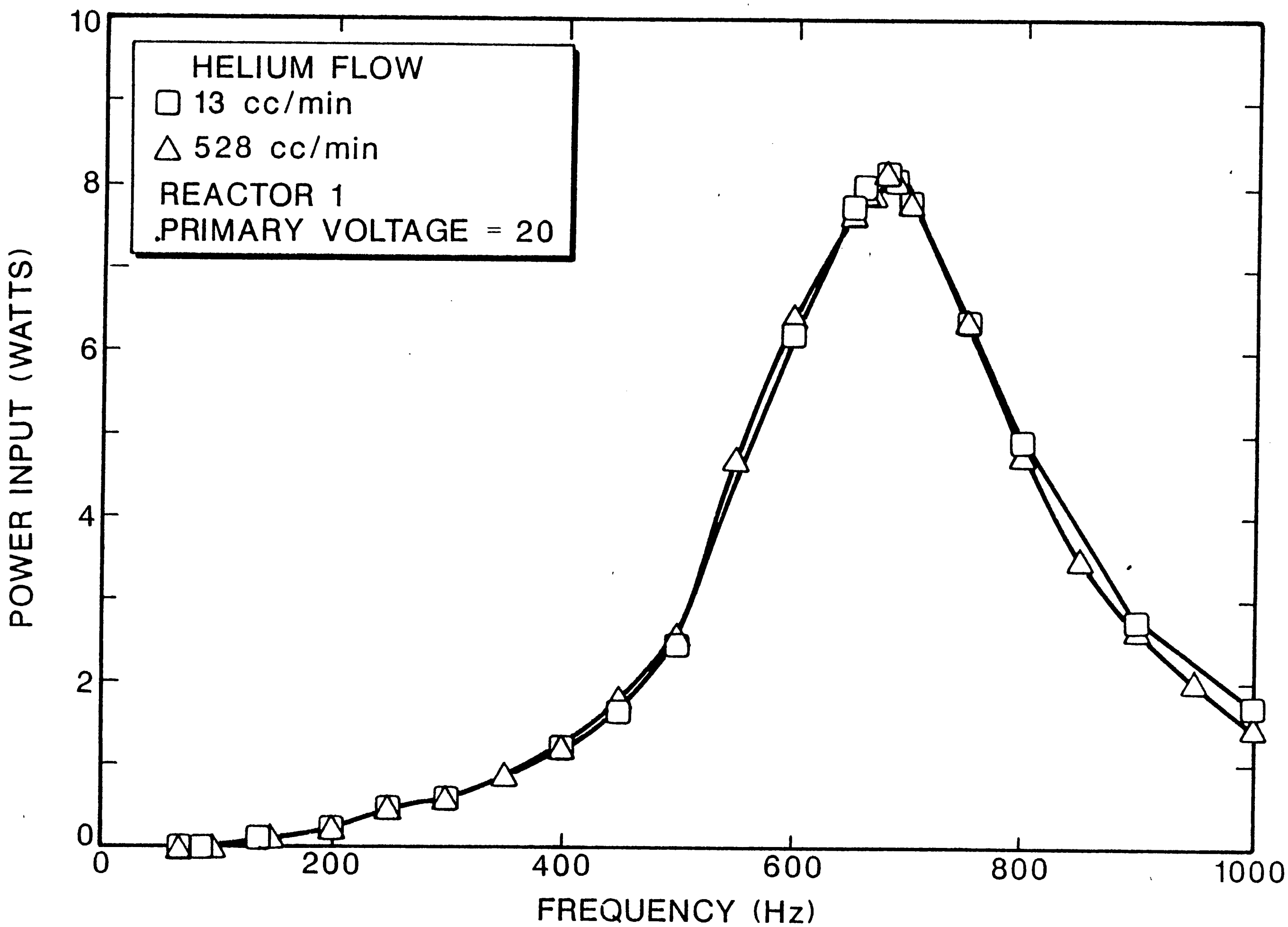

Figure 14. Power Input Dependence on Flow Rate (Helium)

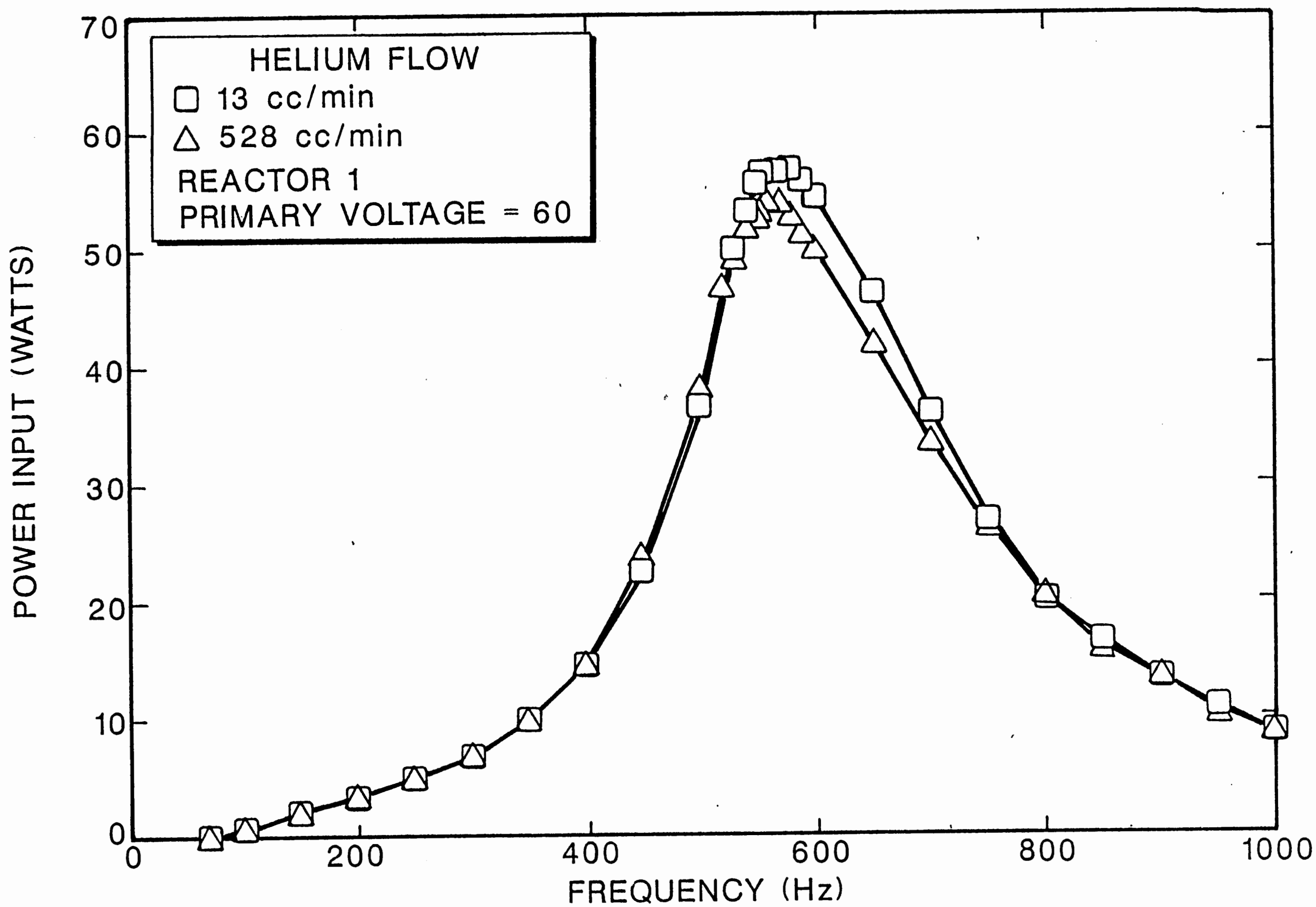

Figure 15. Power Input Dependence on Flow Rate (Helium)

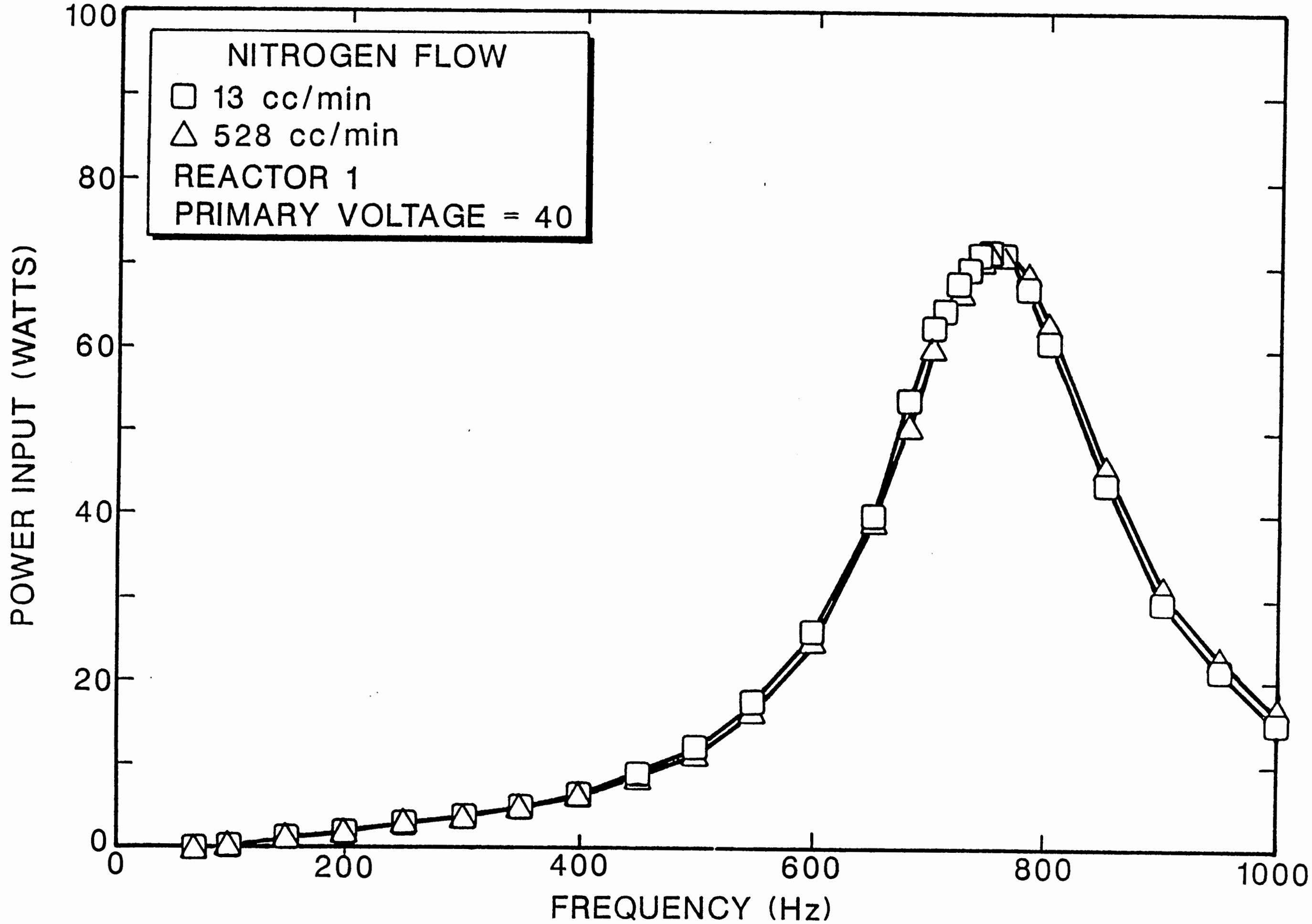

Figure 16. Power Input Dependence on Flow Rate (Nitrogen)

Reactors 2 and 3). Reactor 2 had an inner electrode made of copper mesh, while a silver paint served as the inner electrode for Reactor 3. More details of the reactors are given in Chapter IV.

Figures 17, 18 and 19 illustrate the results from flowing helium, nitrogen and oxygen in Reactor 1 and Reactor 2. All experiments were conducted with a primary voltage of 40 and a gas flow rate of 13 cc/min. For helium, the maximum power input in Reactor 2 is only 51% of the maximum power of Reactor 1. However, using nitrogen flow, power input of Reactor 2 is 93% of reactor 1, and for oxygen the maximum power input for Reactor 2 actually exceeds that for reactor 1 by 12%. For all gases tested, the optimum frequency for Reactor 2 was at a lower value than for Reactor 1.

Once again, the component of power most sensitive to gas composition is current. Using helium, the current generated in Reactor 2 is only 55% of the current generated in Reactor 1, while voltage in Reactor 2 was 88% of the voltage in Reactor 1. With nitrogen, current in Reactor 2 was 86% of the current in Reactor 1, and voltage in Reactor 2 was actually 7% higher than in Reactor 1. Again, it appears that helium is unable to produce as many electrons (and thus electric flow) as the larger molecules in the ionized state.

The reason for oxygen having a higher power input in Reactor 2 than Reactor 1 is not clear at this time. However, this observation is not believed to be caused by experimental error. Maximum power input values for air (which consists of nitrogen and oxygen) fell between oxygen and nitrogen in both reactors.

In future research, a great deal of work needs to be done in the area of reactor scale-up. Variables that should be tested are elec-

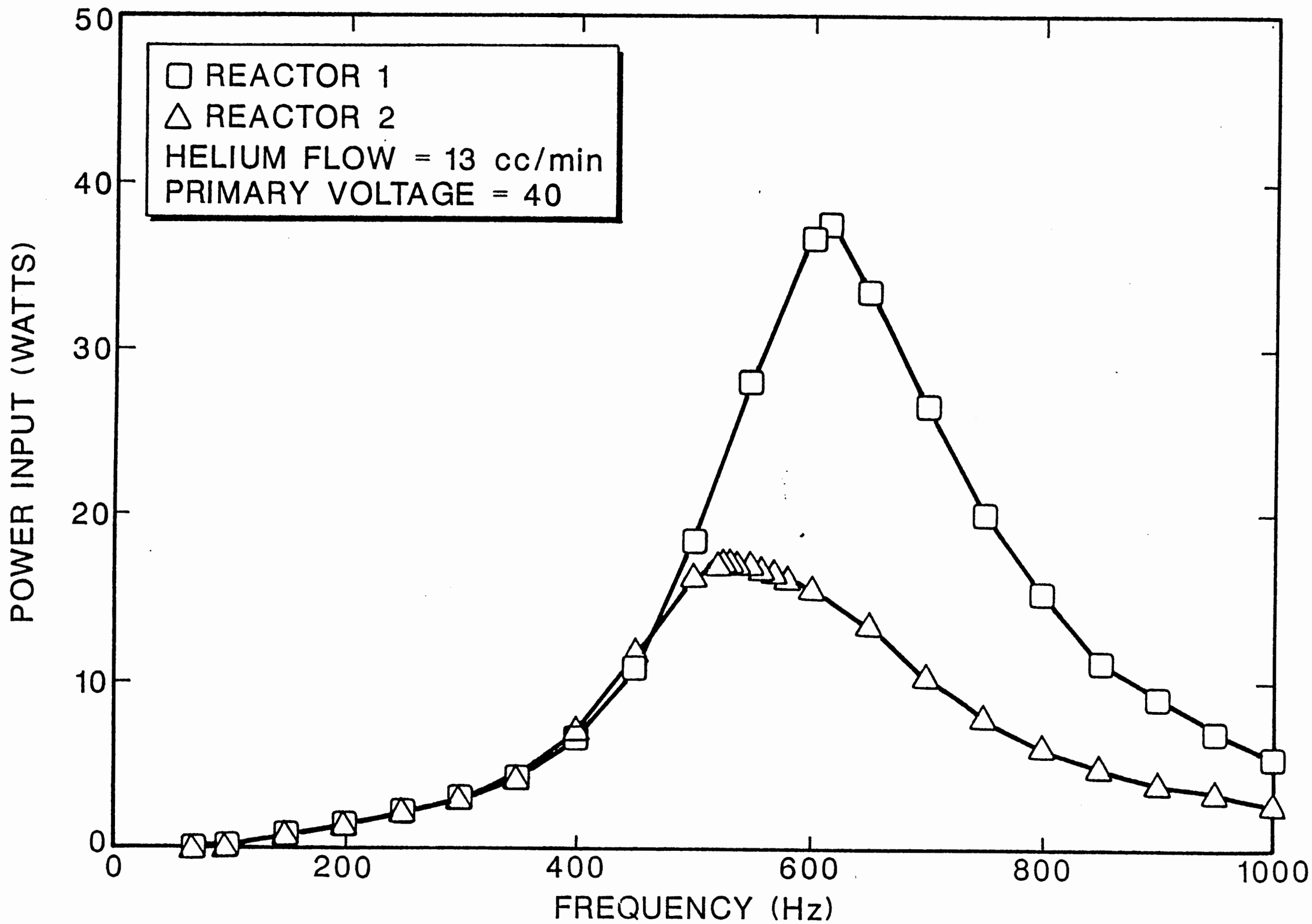

Figure 17. Power Input Dependence on Reactor Size (Helium)

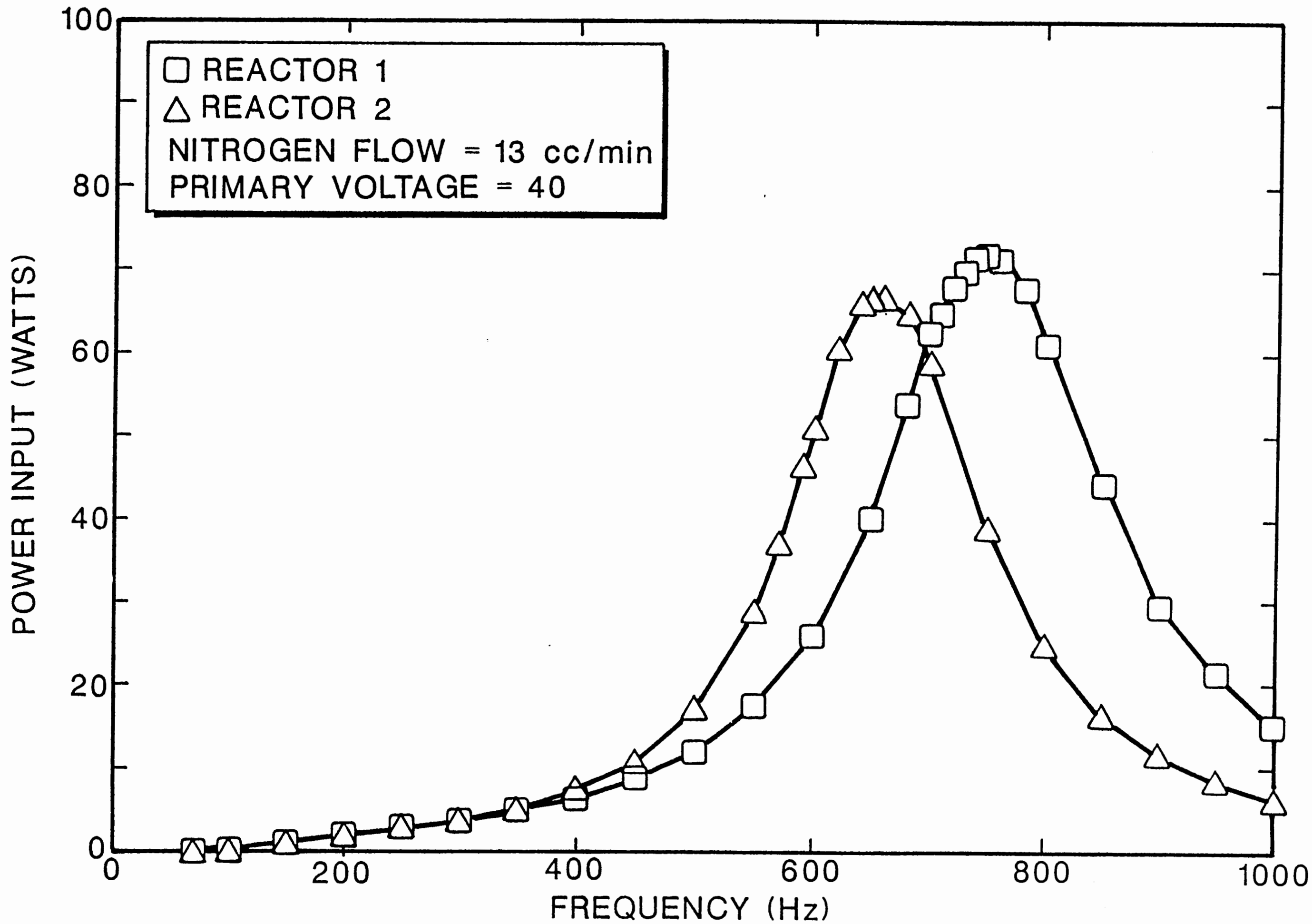

Figure 18. Power Input Dependence on Reactor Size (Nitrogen)

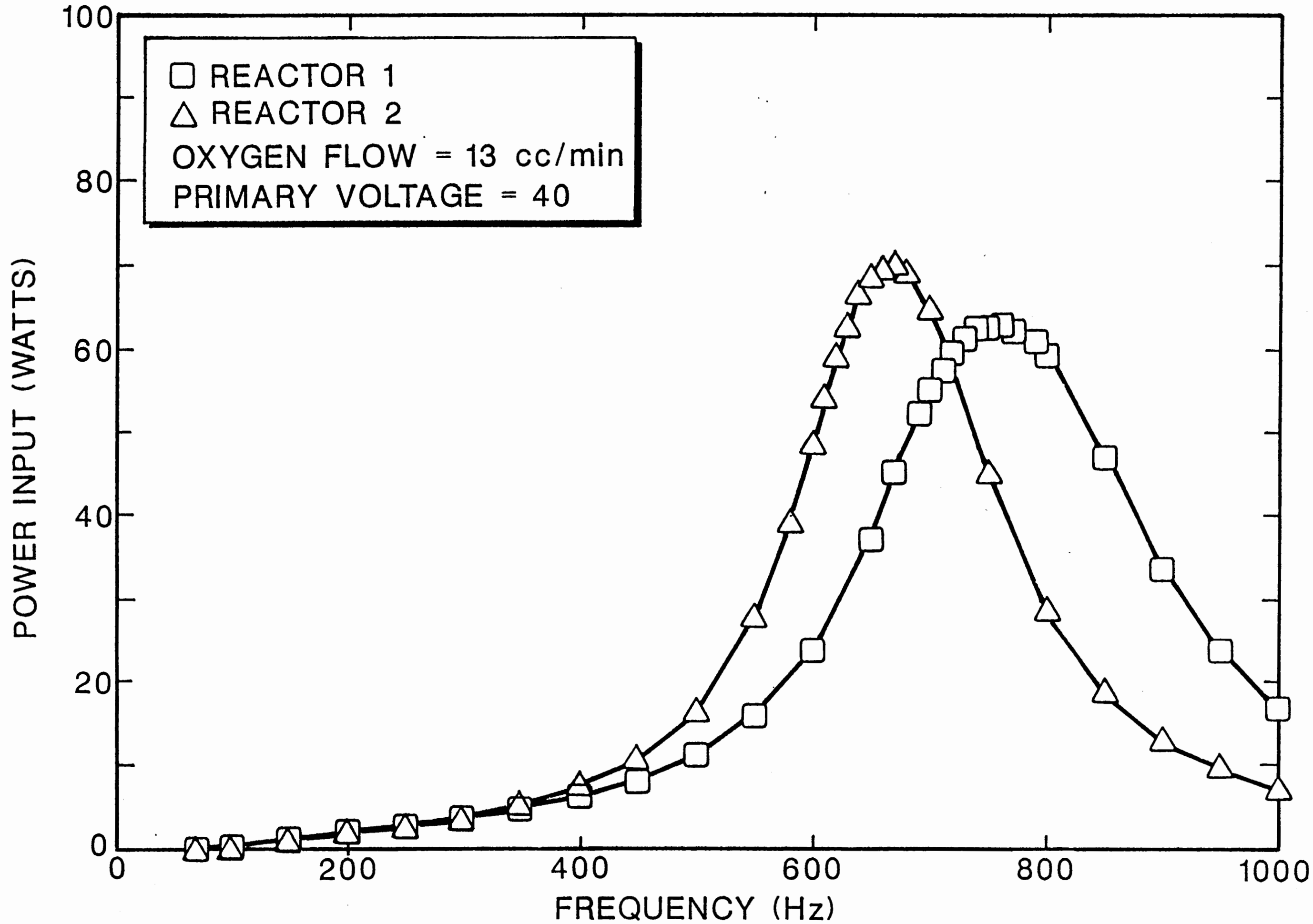

Figure 19. Power Input Dependence on Reactor Size (Oxygen)

trode gap width, reactor length and gas composition. The research presented here has shown that using inert gases in non-destructive tests is an effective and time efficient method for studying their variables and their affect upon maximum power input.

Power Input Dependence on Electrode Material and Humidity

Reactor 3 was used to test the effect of changing electrode material. It has the same annular volume (64.4 cc) as Reactor 2, but has an inner electrode made of silver paint as opposed to copper. Figure 20 shows the three power curves obtained from the three reactors using air flowing at 13 cc/min and a primary voltage of 40. Notice that Reactor 3 has its optimum occurring at the lowest frequency of the three reactors, but its maximum power input is less than Reactor 2 and only slightly greater than Reactor 1.

This result was unexpected. Before performing the experiments, Reactor 3 was expected to be able to deliver more current since silver is a better conductor of electricity that copper. Voltage was expected to be about the same in both Reactors 2 and 3 since the gap between electrodes, gas type and flow rate were identical. In fact, current in Reactor 3 was less than in Reactor 2; however, voltage in both reactors was about the same. At this time, there is not a good explanation for this phenomena, and further investigation into electrode material and configuration is certainly warranted.

The effect of humidity on power input is shown on Figure 21. At the maximum, power input for the humidified oxygen stream was basically the same as for the dry oxygen stream. Oxygen was humidified by bub-

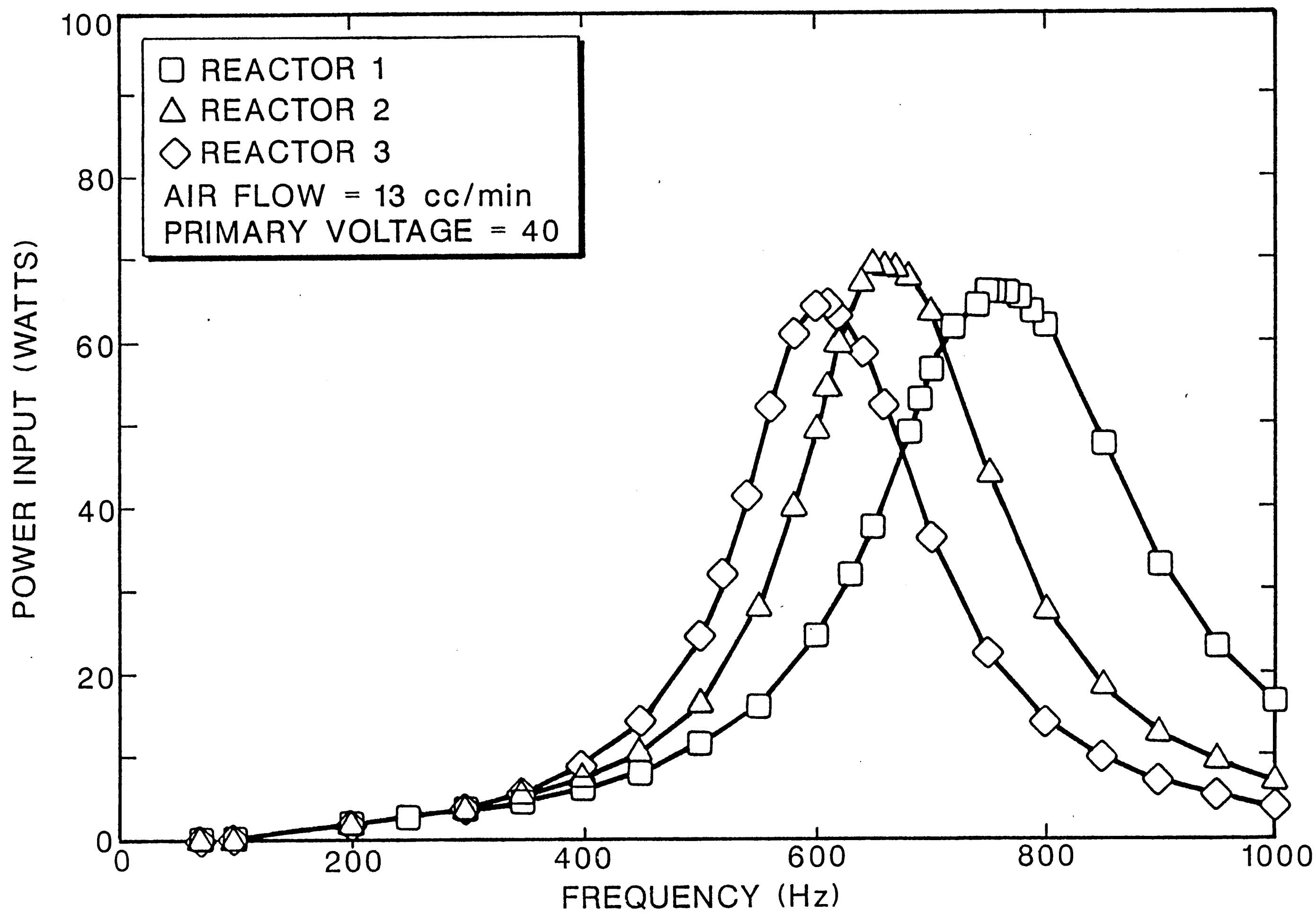

Figure 20. Power Input Dependence on Electrode Type

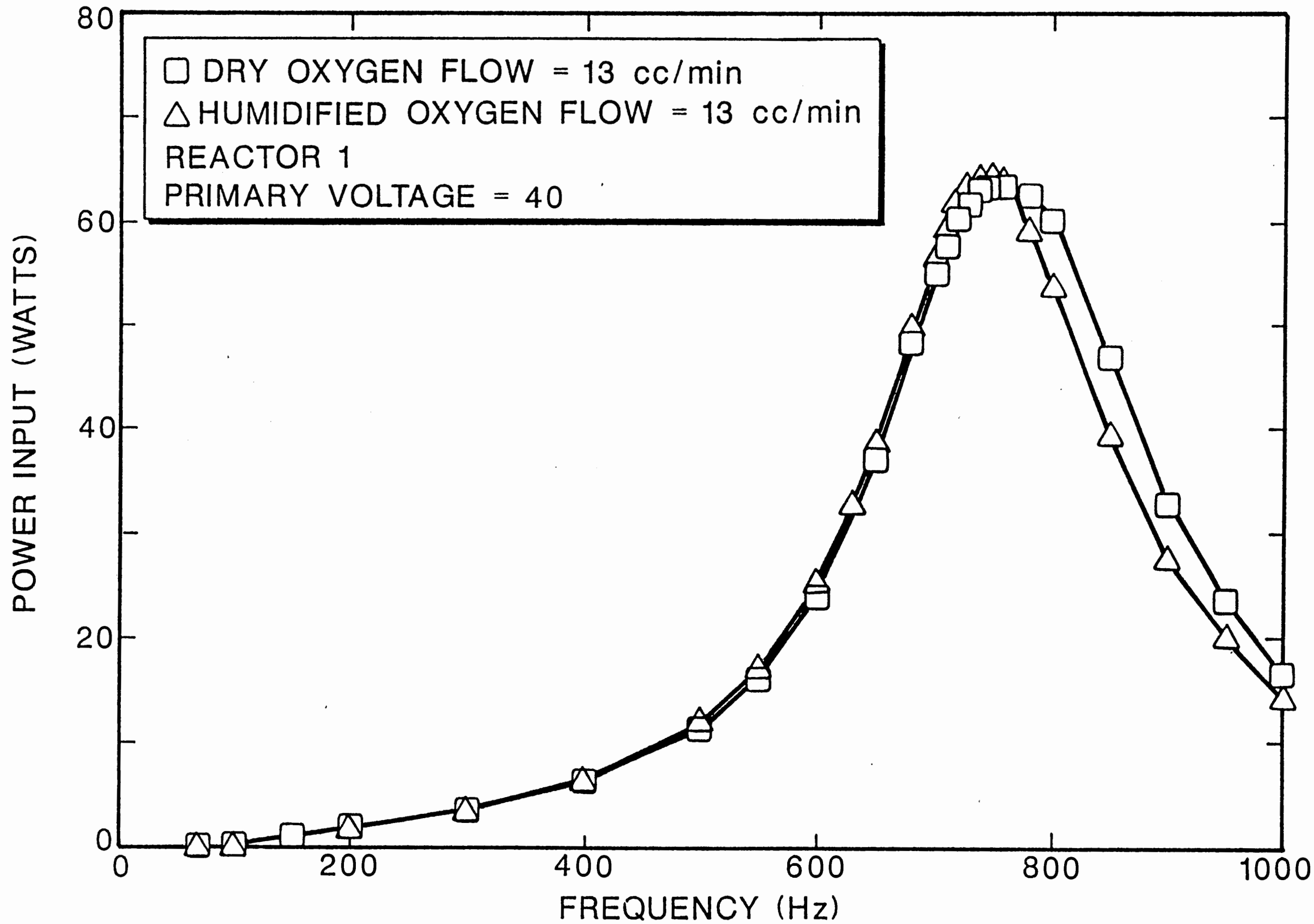

Figure 21. Power Input Dependence on Humidity

bling a dry oxygen flow through water before the stream entered the reactor. The actual relative humidity was not measured.

Humidity of the entering gas stream is a parameter studied by previous researchers. Tevault, Chester, Simmons and Birmingham [22] observed that NO_x production is suppressed when an air stream is first humidified. The previously described experiment was conducted to investigate if NO_x suppression is accompanied by decreased power levels. This work agrees with Moore, Birmingham and Koropchak [23] who observed unchanged destruction efficiencies of methyl cyanide when the air stream was humidified.

The basic conclusion of this particular experiment is that power levels are not seriously affected by increased humidity at the condition tested. Humidifying the incoming gas stream appears to be an effective and relatively simple way of suppressing formation of noxious NO_x by-products.

Error Analysis

Experimental error of the non-destructive tests was determined using duplicate and replicate data runs.

Duplication of data points was achieved two ways. After a non-destructive test run, several data points were retaken. Maximum deviation from the original reading was $\pm$ 0.2 mA and $\pm$ 50 volts giving a relative error of $\pm$ 0.02 watts (0.04 watts absolute error). Also, the humidified oxygen in Reactor 1 at a primary voltage of 40 was completely duplicated on the same day and with the same basic conditions (Appendix D, Tables XXV and XXVI). Error of the power input at the maximum was $\pm$ 2.2% ($\pm$ 1.4 watts), and optimum frequency error was $\pm$ 10

Hz. Maximum power input error for any point was ± 8% which occurred just before the maximum at 730 Hz.

Several runs were replicated on different days. Not only were ambient temperature and atmospheric pressure slightly different but the electrical system could have been slightly different due to changed lead connections caused by changing out different reactors. Oxygen flow in Reactor 1 with a primary voltage of 40 was replicated. Power input difference at the maximum was ± 6.2%. Interestingly, when the inner electrode was replaced by a new copper wire, no significant change in power levels was observed (Appendix D, Table XIX) desipite less corrosion on the new electrode. Further studies on the effect of electrode corrosion on power input is warrented.

Nitrogen flow in Reactor 1 with a primary voltage of 20 was also replicated. In this replication, the leads to the two electrodes were switched. Error of the maximum power input error ± 3.3%. Once again the optimum frequency varied by ± 10 Hz. However, power input error at high frequencies (900-1000 Hz) was relatively high at ± 20%. These relatively high error levels were caused by overall low power levels. Maximum difference in power did not exceed 2 watts. Data for this replicate run is listed in Appendix D, Table XXX.

CHAPTER VII

DESTRUCTIVE TEST RESULTS

In Chapter VII, results of the destructive tests are discussed. The purpose of these experiments was to determine how methane destruction is affected by frequency, inlet methane concentration, bulk gas type and reactor type. Also, this data will be used to test the validity of the kinetic model developed in Chapter V. Results of the destructive tests are summarized in Table VIII. More detailed information for each data run is given in Appendix E.

Destruction levels obtained in these experiments may appear to be rather low, particularly when compared to results obtained at NRL. A maximum destruction level of 75% was achieved, while at NRL, destruction efficiencies in excess of 99% were reported. There are two reasons for this difference. First, higher inlet methane concentrations were used. In these experiments, the lowest inlet concentration was 11,400 ppm (1.14%) which is greater than the 100 ppm used at NRL. Second, voltage levels were lower. Maximum secondary voltage obtainable was 7500 volts for the transformer used in this research. The transformer at NRL was capable of 15,000 volts secondary. One recommendation for future experiments is to purchase a custom wound transformer capable of delivering higher secondary voltages.

TABLE VIII

SUMMARY OF DESTRUCTIVE TEST RESULTS

Run #	Reactor	Inlet Methane (%)	Bulk Gas	Power Input (Watts)	Primary Voltage	Frequency (Hz)	Flow Rate (cc/min)	Destruction Efficiency (%)
1	Reactor 1	12.6	O_2/He	96.4	60	600	13	31.3
		12.6	O_2/He	37.1	60	800	13	19.0
		12.6	O_2/He	22.5	60	1000	13	0.0
		12.6	O_2/He	16.2	60	400	13	3.1
		12.6	O_2/He	37.7	60	500	13	10.8
		12.6	O_2/He	26.0	40	600	13	10.8
		12.6	O_2/He	94.6	60	600	35	16.6
2	Reactor 2	12.4	O_2/He	39.7	60	540	13	47.6
		12.4	O_2/He	38.8	60	540	35	28.8
		12.4	O_2/He	37.4	60	540	95	15.3
3	Reactor 2	12.9	O_2/N_2	110.9	60	608	13	14.2
4	Reactor 1	13.0	O_2/N_2	88.9	60	685	30	13.9
		13.0	O_2/N_2	90.2	60	685	10	17.9
		13.0	O_2/N_2	87.2	60	685	65	10.3
		13.0	O_2/N_2	95.8	60	685	95	5.4
5	Reactor 3	12.7	O_2/N_2	91.4	60	600	35	15.6
6	Reactor 3	1.3	O_2/N_2	83.2	60	615	35	56.5
7	Reactor 1	1.1	O_2/N_2	116.2	70	700	13	75.0
		1.1	O_2/N_2	87.0	60	700	35	39.3
8	Reactor 1	14.1	O_2/N_2	65.1	60	680	123	2.5
9	Reactor 1	11.4	O_2/N_2	68.2	60	685	30	12.8

From a research viewpoint, there are actually several advantages of lower methane conversion experiments. Primarily, those factors having the greatest impact on destruction can be readily observed. Also, methane conversion can be modeled over a wide range of destruction levels. Kinetic relationships are harder to ascertain if most (or all) of the data points are at > 99% conversion. Finally, by operating at mild voltage levels, arcing and short circuits can be avoided. Electrical shorts can cause unstable operating conditions, uncertainty in the experimental results, and erroneous power measurements.

Analysis of the inlet and product gas streams was accomplished using a gas chromatograph with a flame ionization detector (FID). Since a FID can only detect methane, product compositions of carbon dioxide, carbon monoxide, and oxygen could not be measured. Determining which factors affected methane destruction was the primary objective of these experiments. A detailed experimental procedure is given in Chapter IV.

Dependence of Methane Destruction on Frequency

In previous work at NRL [13], maximum destruction in an ACPR has been shown to occur at the optimum frequency--where power to the reactor is maximized. This experiment was replicated using a much higher inlet methane concentration (12.6% as opposed to 100 ppm).

Results are given in Table VIII, Run 1, and shown graphically in Figure 22. Methane destruction is clearly maximized at an optimum frequency. Fixed conditions were a flow rate of 13 cc/min in Reactor 1, an oxygen/helium atmosphere, and a primary voltage of 60.

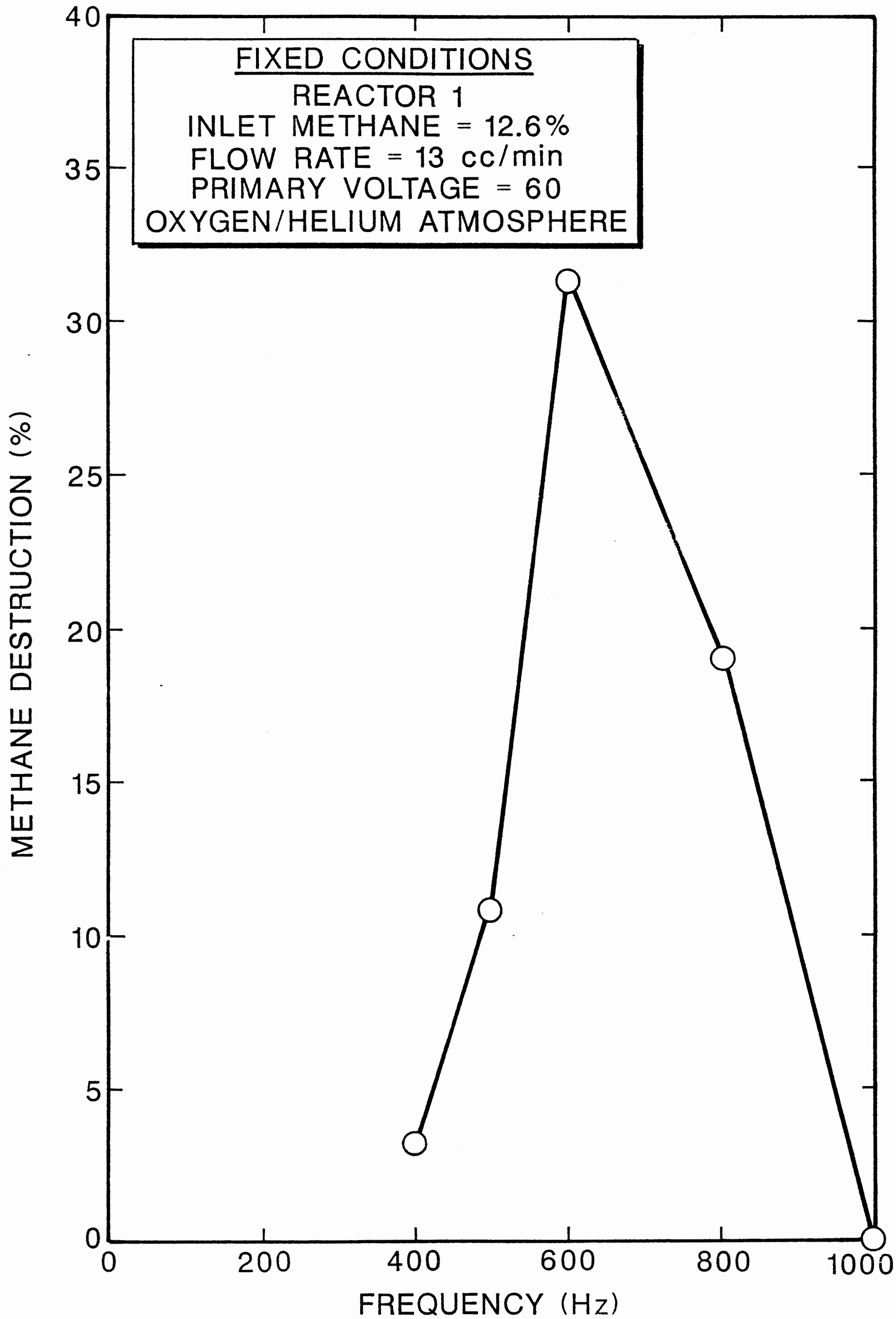

Figure 22. Methane Destruction versus Frequency

These results confirm the observations from NRL. All subsequent experiments reported in this thesis were conducted at the optimum frequency.

Dependence of Methane Destruction on Flow Rate, Reactor Type and Bulk Gas

Flow rate can have a very profound impact on methane destruction in an ACPR. By varying flow rate under constant conditions in Reactor 2, methane conversion fell from 47.6% at 13 cc/min to 15.3% at 95 cc/min, as illustrated in Figure 23 and Table VIII, Run 2. This experiment was conducted in an oxygen/helium atmosphere with an inlet methane concentration of 12.4%.

Using an oxygen/helium atmosphere, Reactor 2 gave better destruction than Reactor 1 at the same conditions. At 13 cc/min, Reactor 2 had 47.6% destruction versus 31.3% for Reactor 1, and at 35 cc/min, Reactor 2 had 28.8% destruction versus 16.6% for Reactor 1. Reactor 2 had these better destruction levels despite a power input of approximately 39 watts as opposed to approximately 95 watts in Reactor 1. This result can be explained by higher residence times in the larger volume Reactor 2.

When nitrogen was substituted for helium, several unexpected results occurred. In Reactor 2, conversion at 13 cc/min fell from 47.6% to 14.2% despite a higher power input (111 watts versus 39 watts). Methane destruction in Reactor 1 was lower for the nitrogen case; however, in an oxygen/nitrogen atmosphere, Reactor 1 had about the same or better destruction levels as Reactor 2 (Table VIII, Runs 3 and 4).

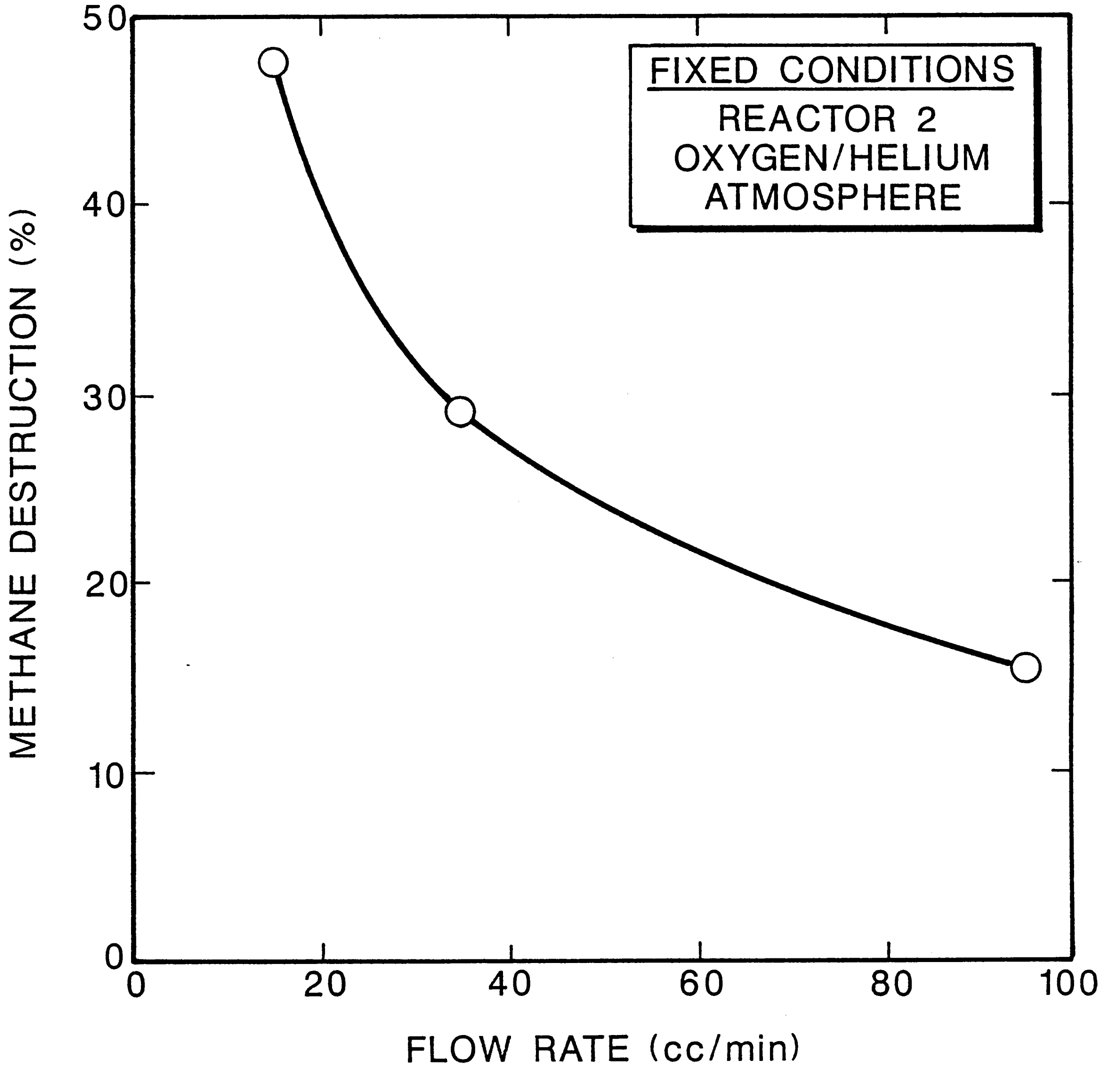

Figure 23. Methane Destruction versus Flow Rate

Two probable mechanisms exist to explain the above results. First, though nitrogen gives higher power input levels, the nitrogen molecule, being diatomic, competes for the plasma energy. This was also observed by Fraser, Eaton and Sheinson [14], who found that destruction efficiencies of DMMP in an ACPR fell at high oxygen levels. Second, it was subjectively observed that nitrogen gave a less intense "glow" than helium. In particular, this was true for Reactor 2 where the glow was fragmented and did not fill the entire reactor volume.

Run 5, using Reactor 3, confirmed this hypothesis. Using an inner electrode of silver paint instead of copper mesh yields a more continuous glow. The result is a higher destruction efficiency at a higher flow rate and a lower power level. Reactor 3 also yielded a slightly higher destruction level than Reactor 1--probably due to a longer residence time (Table VIII; Runs 3, 4 and 5).

Several important conclusions can be drawn from the previous discussion:

1. Besides power level and residence time, bulk gas type is an important factor affecting destruction efficiencies in an ACPR.

2. Air should be the bulk gas used in all future experiments with the ACPR to give realistic information on destruction levels and kinetic modeling.

3. Large reactors should be constructed so that the glow fills the entire volume. This problem can be corrected by using higher voltage transformers, silver paint for the inner electrode, and a higher density of wire wrap for the outer electrode.

Kinetic Model for Methane Destruction

From the previous observations, Reactor 1 using an oxygen/nitrogen atmosphere was selected to test the kinetic model. Glow in Reactor 1 was observed to be continuous and filling the entire reactor volume at the power levels studied. An oxygen/nitrogen bulk gas was selected so that the kinetic model would reflect a more realistic case. Data were taken for different inlet methane concentrations, flow rates and power levels. Results of these experiments are listed in Table VIII; Runs 4, 7, 8 and 9.

The test for a zero order reaction mechanism is shown on Figure 24. As developed in Chapter V, the test for zero order is to plot

$$\frac{\ln(C_a^\circ/C_a)}{C_a^\circ - C_a} \quad \text{versus} \quad \frac{\tau}{C_a^\circ - C_a} \tag{7.1}$$

If the zero order assumption is valid, a straight line will result. As can be seen from Figure 24, methane destruction does not follow a zero order assumption. Instead, as flow rate increases, the curve first advances from right to left, but then reverses--moving from left to right. The result is no intercept for the y-axis. Sample calculations for the data points are given in Appendix B.

After the above result, it was decided to test the data using a relationship similar to that found by Tezuka and Miller [28]. They observed that anisole decomposition in a radio frequency discharge can be expressed as

$$-\ln(C/C^{o}) = k_1 \ (P/\dot{n}_a) + k_2 \tag{7.2}$$

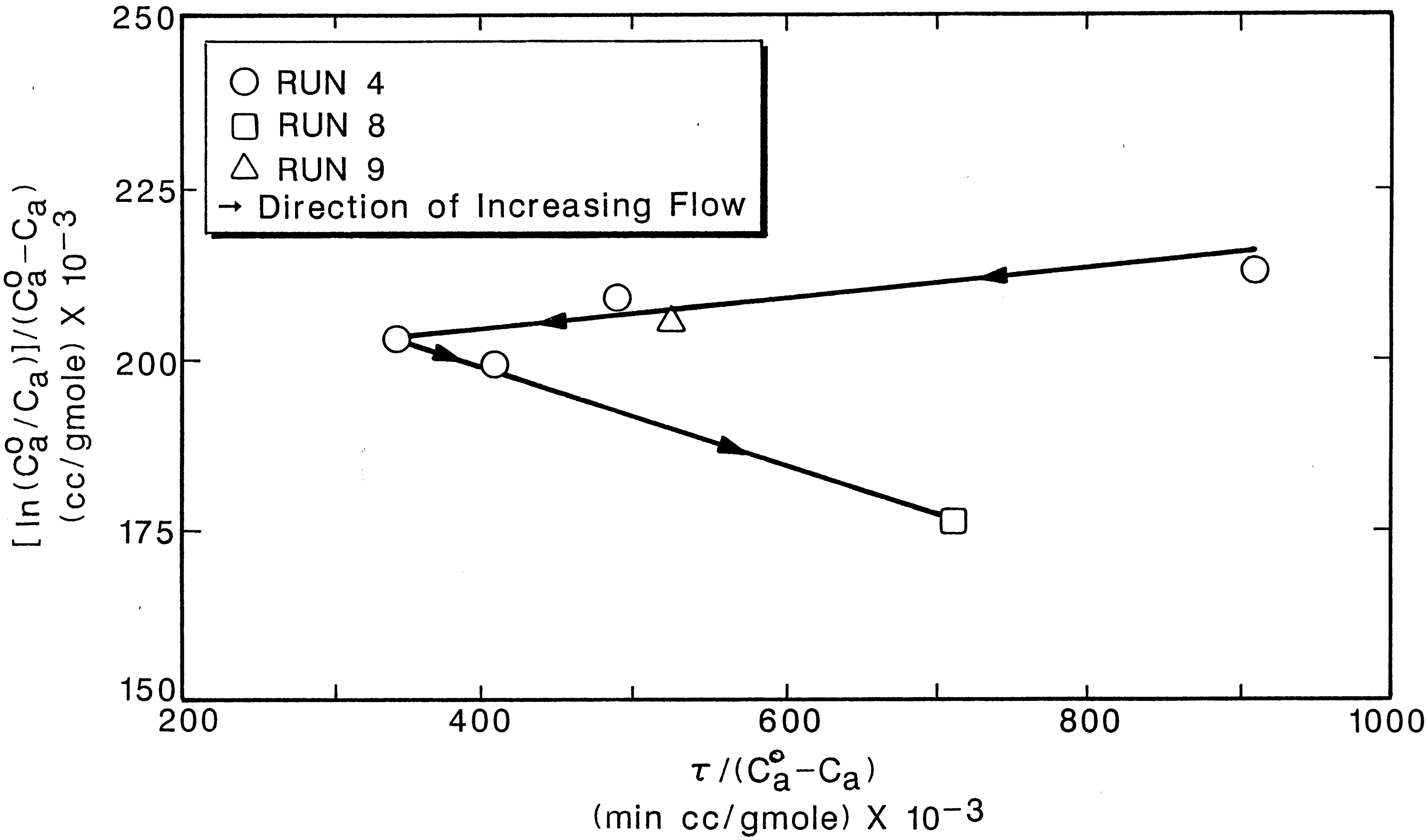

Figure 24. Zero Order Test for Methane Destruction

where P is power in watts, $\dot{n}_a$ is flow rate in moles/min, C is concentration in moles/cc, and k_1 and k_2 are constants. This equation is in the form of a straight line when $-\log(C/C^o)$ is plotted against $(P/\dot{n}_a)$ where k_1 is the slope and k_2 is the y-intercept.

Testing of eq. 7.2 for methane destruction in an ACPR is shown in Figures 25 and 26. Sample calculations are shown in Appendix B. A linear relationship is observed over most of the x-axis range. However, this line does not intersect the origin, which it should. The origin represents zero methane conversion at zero power (or infinite flow rate). Below a $P/\dot{n}_a$ value of 480,000 (which corresponds to a methane destruction of 14%), the linear relationship breaks down, and data taken in this low conversion range shows a curved relationship down to the origin. It should be noted that Tezuka and Miller's straight line relationship for anisole conversion also did not intersect the origin. Their y-intercept occurred at 0.05.

Rearrangement of eq. 7.2 yields

$$C_a = C_a^\circ \, k_2 \exp[-k_1(P/\dot{n}_a)] \tag{7.3}$$

In this expression $\dot{n}_a$ can be written in terms of reactor volume, residence time, and methane concentration.

$$C_a = C_a^\circ \, k_2 \exp[-k_1(P\tau/V^t C_a^\circ)] \tag{7.4}$$

For methane destruction in Reactor 1, the constants can be evaluated and the final expression written

$$C_a = 0.11 \, C_a^\circ \exp[(-6.94 \times 10^{-8})(P\tau/V^t C_a^\circ)] \tag{7.5}$$

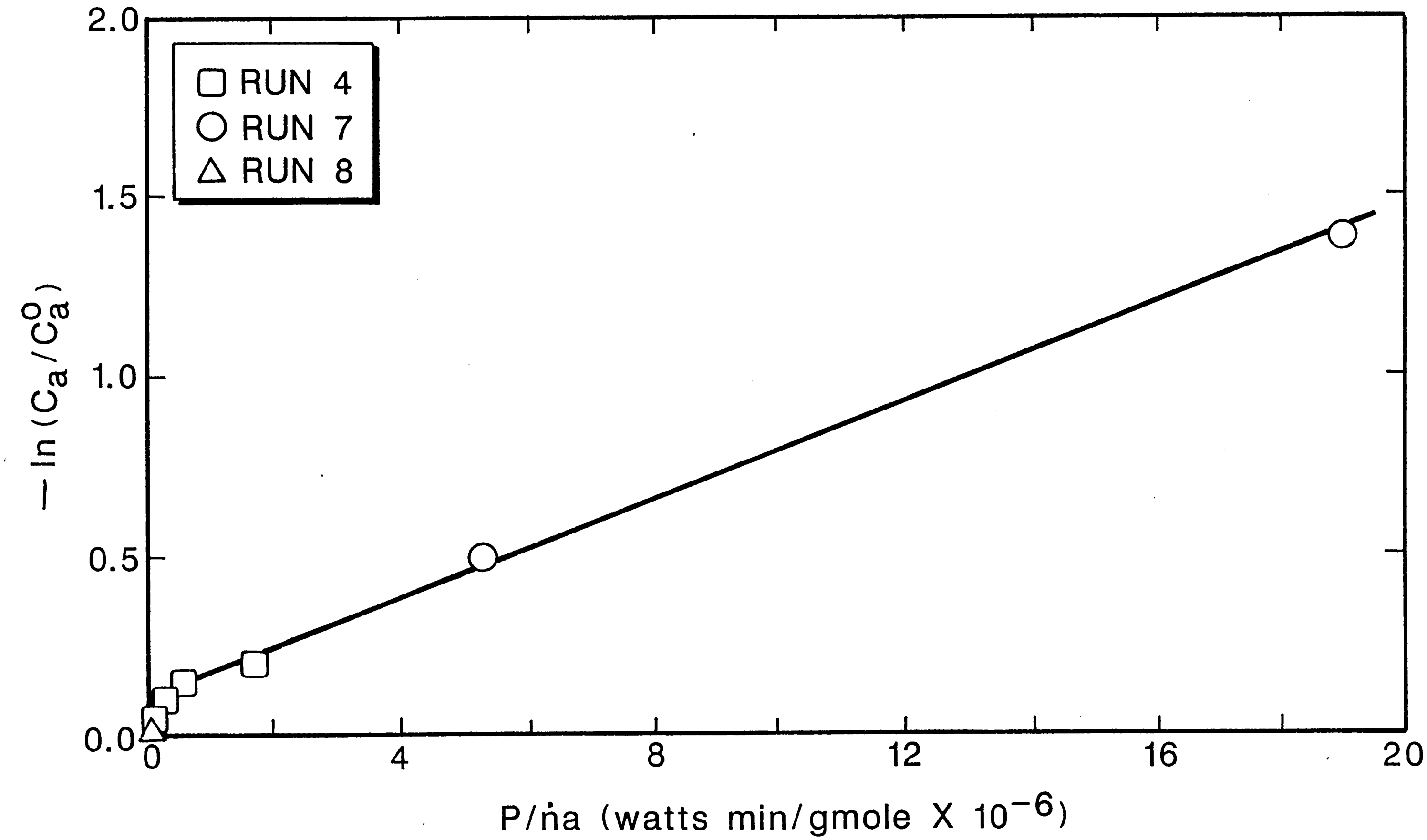

Figure 25. Test of Proposed Kinetic Model for Methane Destruction

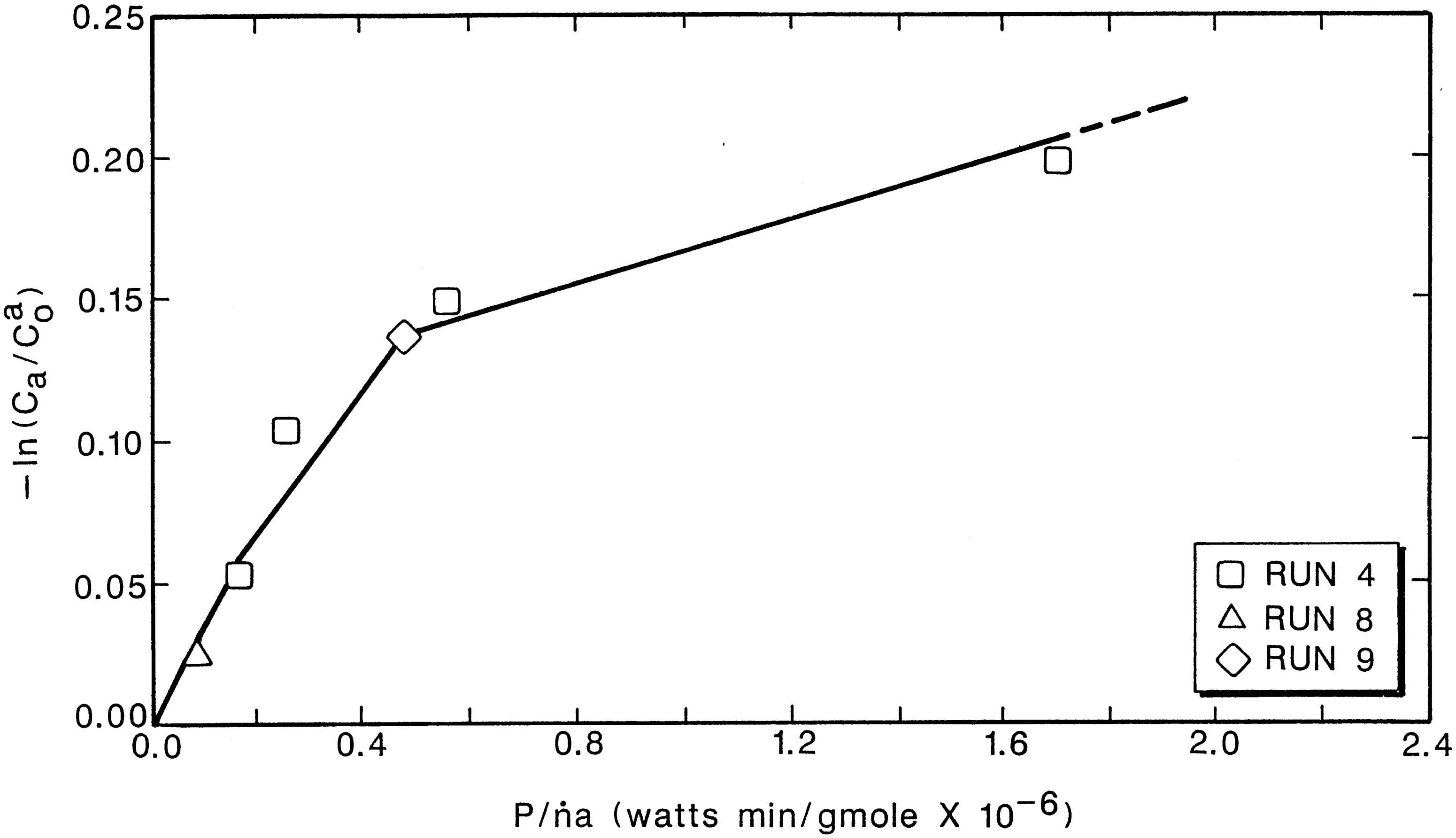

Figure 26. Enlargement of Figure 25

Eq. 7.5 is valid for methane destruction in Reactor 1 with an oxygen/nitrogen atmosphere for methane conversions above 14%. In the appropriate range, this expression is valid for varying power levels, flow rate and inlet methane concentrations. Data taken for Reactors 2 and 3 did not follow eq. 7.5. At this time it appears that each reactor has different constants for eq. 7.3. Future research should attempt to establish a relationship between different size reactors through the constants k_1 and k_2.

Solid Film Deposit

In addition to the previous discussion, an important observation was made during the destructive tests. After Run 4, a milky white solid was observed covering the reactor walls. This film was seen in all data runs with Reactor 1 in an oxygen/nitrogen atmosphere. Since this film was not detected when helium was used in place of nitrogen, it is assumed this film is a $(CN)_x$ polymer. Upon addition of water, the film dissolved readily and produced no visible gas.

Fraser and Sheinson [16] and [17] also observed a solid deposit on the walls of an ACPR during decomposition of hydrogen cyanide and cyanogen. This residue could be further oxidized to produce carbon monoxide, carbon dioxide and nitrogen, which led the authors to believe the solid to be a $(CN)_x$ polymer.

Although they describe the solid as yellow, it is possible that the solid is similar to the solid observed in this research. Upon decomposition in oxygen and nitrogen, methane may produce hydrogen cyanide which further decomposes to form the solid film observed. Evaluating and minimizing harmful by-products from an ACPR was not one of the objectives of this research, but definitely needs attention in future experiments.

Error Analysis

Determining experimental error was accomplished with duplicate data points and one attempted replicate data run.

Several data points were duplicated within an experimental run and are denoted in Appendix E. These points helped establish how repeatably the gas chromatograph behaved. Maximum percent differences for any duplicated point was 6.2%. All but three duplicated points were below 4.0% difference.

The gas streams to be analyzed flowed through copper tubing to the gas chromatograph (GC) and were injected into the GC by means of a 1 cc sample loop. Gas pressure in the sample loop was kept constant by maintaining the same regulator pressure throughout an experimental run. Inlet concentrations were obtained by flowing the inlet gas through the system with power to the reactor turned off.

Since the GC could detect only methane, an absolute calibration method was used to establish methane concentrations. A standard of known methane concentration was prepared using methane at 1 atmosphere pressure and an inert at some higher pressure. This standard flowed through the system at the same regulator pressure (and same regulator) as the experimental run. Previously, a linear relationship for methane concentration and GC area was established for this particular GC, so methane concentration for any sample could be determined by direct comparison of GC area with the standard's GC area. This method was employed to prevent bias and error caused by syringe injected standards. At least one standard was prepared for each experimental run. Details of GC operating conditions are given in Appendix A.

One data point was replicated, Run 9 (Table VIII) replicated Run 4, data point 1. A new inlet gas sample was prepared and reacted under the same conditions on a different day from the original data point. However, inlet methane concentration and power input were slightly less for the replicate point. The percent difference in methane destruction was 8.2%. Due to the slightly different conditions, however, the author believes that a maximum relative error of ± 10% is probably more realistic for the equipment and analysis methods used in these experiments.

CHAPTER VIII

SUMMARY AND CONCLUSIONS

Research was conducted to investigate the potential usefulness of an alternating current plasma reactor (ACPR) as an air purification device. Electrical power was used to create an electric discharge or plasma inside the reactor. Organic contaminates in air streams passing through this plasma are broken down by the plasma energy into atoms. These atoms then recombine to form the reaction products. This technology is currently being researched by the military as an air purification device for ships, tanks, and personnel carriers. In addition, there are potential industrial applications.

Previous research on the ACPR has concentrated on scientific concerns such as reaction mechanisms. Research presented in this thesis was an initial attempt to study the ACPR from an engineering viewpoint. This work was primarily exploratory--to identify critical variables affecting scale-up, to determine a kinetic model for methane destruction, and to recommend areas for further investigation.

To accomplish these objectives, an experimental apparatus was constructed out of standard or easily obtained items. However, future experiments may require some custom-made components such as higher voltage transformers. With this apparatus, a series of non-destructive (using inert gases) and destructive tests were conducted.

The results, conclusions and recommendations from these experiments are summarized in the following discussion.

An optimum frequency exists in an ACPR which yields a maximum power input to the reactor. This optimum is a function of primary voltage, gas composition, reactor size, electrode material and flow rate. These factors affecting the optimum condition are an expansion of previous work and are summarized below.

1. Higher primary voltages gave higher power inputs at all frequencies studied. The optimum frequency did not remain constant but shifted to lower frequencies as primary voltage increased.

2. Nitrogen, oxygen and air gave a much higher maximum power input than helium. The major difference being in current not voltage. For a given primary voltage, the optimum frequency occurred at a lower value for helium than for the other three gases.

3. The larger volume Reactor 2 had much less power input than Reactor 1 using helium; however, using nitrogen, power input in Reactor 2 was only slightly less than Reactor 1. Surprisingly, when oxygen was used, Reactor 2 yielded a slightly greater power input than Reactor 1. Currently, a satisfactory explanation for this behavior does not exist. Optimum frequencies were lower in Reactor 2 than Reactor 1 for all gases studied.

4. Reactor 3, which used silver instead of copper for the inner electrode, has a slightly lower maximum power input than Reactor 2 using air. However, the observed "glow" in Reactor 3 was more continuous in the reactor volume than Reactor 2.

5. Increasing flow rate did measurably decrease maximum power input, but the effect was not significant under the conditions studied.

6. Humidity of the gas stream was another variable tested, but it did not measurably affect maximum power input.

Methane was selected as a test compound to determine which variables affected destruction in an ACPR. A variety of experiments testing methane destruction were conducted, and the results are summarized below.

1. For a set of fixed conditions, methane destruction is maximized at the optimum frequency which corresponds to the maximum power input to the reactor. This research confirms previous work on frequency dependence of methane destruction. All future experiments on the ACPR should be conducted at the optimum frequency.

2. Methane destruction increased with increased power input and decreased with increased flow rate.

3. Methane destruction was lower in an oxygen/nitrogen atmosphere compared to an oxygen/helium atmosphere despite higher power inputs in the nitrogen case. Nitrogen, being a diatomic molecule, is believed to compete for the plasma energy.

4. Glow character can have an important impact on methane destruction. This was seen when comparing Reactors 2 and 3. Reactor 3 had better destruction levels, under fixed conditions, than Reactor 2 despite having a lower maximum power input. The silver electrode of Reactor 3 produced a much more continuous and less fragmented glow than the copper electrode in Reactor 2.

Reactor 1 was selected to test the proposed zero order kinetic model for methane decomposition. However, this model failed to accurately represent the experimental data. A new model, similar to that used by Tezuka and Miller (28) to describe anisole decomposition in a radio frequency reactor, was proposed and fit the experimental data for all destruction efficiencies greater than 14%. The final form of this expression is

$$C_a = 0.11\, C_a^{\circ} \exp[(-6.94 \times 10^{-8})(P\tau/V^t\, C_a^{\circ})] \tag{8.1}$$

Equation 8.1 is good for all power levels, flow rates and inlet methane concentrations in the ranges studied. However, this expression is valid only for an oxygen/nitrogen atmosphere in Reactor 1. Future kinetic experiments should attempt to determine a relationship between different size reactors using the constants in eq. 8.1.

Non-destructive tests can be an effective and time efficient way to study factors affecting maximum power input for scale-up of the ACPR. However, destructive studies presented here show that care must be taken so the glow is continuous and fills the entire reactor volume. Otherwise, erroneous comparisons between maximum power levels and destructive potential for different reactors could occur. This problem can be corrected by using higher voltage transformers, silver paint for the inner electrode, and higher density wire wraps for the outer electrode. These suggestions should also result in higher destruction levels than reported in this research.

Future experiments should concentrate on scale-up of the ACPR. A variety of reactors should be built to study how electrode gap width, reactor length, and electrode materials affect power input. Air should be the bulk gas used in all future experiments since it will be the bulk gas used in commercial units. Also, all future experiments should be run at the optimum frequency. As scale-up factors become better

VIMP

understood, more complex and realistic test species should be used in the ACPR.

In future studies, reaction by-products and ways to minimize toxic by-products should be investigated. Other researchers have done some work in this area. Their findings should be confirmed and expanded. To accomplish this task, better analytical equipment needs to be acquired. Specifically, a reliable thermal conductivity detector for the gas chromatograph is needed.

This author envisions a commercial ACPR set up as a three unit process. Air streams to be tested will pass first through a humidifier. Previous researchers have shown that NO_x production is minimized by humidifying the air stream. After reaction, the product gases will probably pass through a scrubber to remove any acid gases produced. The actual reactor will probably have a large L/D ratio. By having a small electrode gap width, a continuous glow can be maintained using the designed voltages. A long reactor length will maintain sufficient residence times at high flow rates. The reactor may also be packed to enhance the decomposition reactions.

VIMP

The ACPR represents an opportunity for this department to establish itself in an emerging technology. Minimal engineering research has been conducted on electrical discharge reactors for air purification. This technology has both military and industrial applications and appears at this point to be economically competitive with other air purification techniques. Further research in both kinetic and scale-up variables is certainly warranted.

BIBLIOGRAPHY

[1] Disposal of Hazardous Wastes. U. S. Environmental Protection Agency, SW-115, Report to Congress (1974).

[2] Turner, W. C. Class notes for Hazardous Waste Management, Inden 5350.9, Oklahoma State University, Stillwater, Oklahoma (Oct. 1987).

[3] Wills, R. A. "Three High Temperature Waste Disposal Methods." Unpublished paper.

[4] Boenig, H. V. Plasma Science and Technology. Chapter 1. Cornell University Press, Ithaca, New York (1982).

[5] Chen, F. F. Introduction to Plasma Physics Chapter 1. Plenum Publishing Company, New York (1974).

[6] Flinn, J. E. and W. M. Goldberger. "A Viewpoint on Electrical Discharge Devices and their Application as Chemical Reactors." Advances in Chemistry Series, 80, 441-451 (1969).

[7] Fraser, M. E. and R. S. Sheinson. "Electric Discharge Plasmas for Collective Protection." Unpublished results.

[8] Balin, L. J., M. E. Sibert, L. A. Jonas and A. T. Bell. "Microwave Decomposition of Toxic Vapor Simulants." Environmental Science and Technology, 9(3), 254-258 (1975).

[9] Balin, L. J., B. L. Hertzler and D. A. Oberacker. "Development of Microwave Plasma Detoxification Process for Hazardous Wastes." Environmental Science and Technology, 12(6), 673-678 (1978).

[10] Helfritch, D. J., P. L. Feldman and P. C. Efthimion. "High Temperature Plasma Generation by Microwave Power." In Proceedings of the International Congress on Hazardous Materials Management, Chatanooga, Tennessee (June 8-12, 1987).

[11] Sheinson, R. S. "Contaminant Destruction Chemistry in Electric Discharges." In Proceedings of the International Congress on Hazardous Materials Management, Chatanooga, Tennessee (June 8-12, 1987).

[12] Fraser, M. E., D. A. Fee and R. S. Sheinson. "Decomposition of Methane in an AC Discharge." Plasma Chemistry and Plasma Processing, 5(2), 163-173 (1985).

[13] Sheinson, R. S., N. S. Smyth, M. A. Piatt and R. A. Wills. "Plasma Induced Destruction of Hydrocarbons." In Proceedings of the International Congress on Hazardous Materials Management, Chatanooga, Tennessee (June 8-12, 1987).

[14] Fraser, M. E., H. G. Eaton and R. S. Sheinson. "Initial Decomposition Mechanisms and Products of Dimethyl Melhylphosphonate in an Alternating Current Discharge." Environmental Science and Technology, 19(10), 946-949 (1985).

[15] Clothiaux, E. J., J. A. Koropchak and R. R. Moore. "Decomposition of an Organophosphorus Material in a Silent Electric Discharge." Plasma Chemistry and Plasma Processing, 4(1), 15-20 (1984).

[16] Fraser, M. E. and R. S. Sheinson. "Electric Discharge-Induced Oxidation of Hydrogen Cyanide." Plasma Chemistry and Plasma Processing, 6(1), 27-37 (1986).

[17] Fraser, M. E. and R. S. Sheinson. "Decomposition of Ch_4, C_2N_2 and HCN is a Plasma Discharge." In Proceedings of the IUPAC 7th International Symposium on Plasma Chemistry, Eindhoven, Netherlands (July, 1985).

[18] Neely, W. C., S. R. Best and E. J. Clothiaux. "The Decomposition of Gas Phase Formaldehyde by Plasma Discharge." In Proceedings of the 1984 Scientific Conference on Chemical Defense Research, Aberdeen, Maryland (1984).

[19] Moore, R. R. and J. G. Birmingham. "The Decomposition of Toxic Chemicals in a Low Temperature Plasma Device." In Proceedings of the International Congress on Hazardous Materials Management, Chatanooga, Tennessee (June 8-12, 1987).

[20] Davis, S. R. and D. E. Tevault. "FTIR Studies of Plasma-Induced Decomposition of Diomethylsulfide in an Air-Like Environment." In Proceedings of the International Congress on Hazardous Materials Management, Chatanooga, Tennessee (June 8-12, 1987).

[21] Gilman, J. P., J. G. Birmingham and R. R. Moore." Acetonitrile as a Simulant for Cyanide Compounds for Plasma Testing." Unpublished results.

[22] Tevault, D. E., M. Chester, P. Simmons and J. G. Birmingham. "NO_x Production in a Silent Electric Discharge as a Function of Humidity, Frequency and Power." Unpublished results.

[23] Moore, R. R., J. G. Birmingham and J. A. Koropchak. "The Decomposition of Cyanide Compounds in an AC Silent Discharge Plasma Reactor." Unpublished results.

[24] Birmingham, J. G. and R. R. Moore. "Acid Gas Scrubbing in Conjunction with an Alternating Current Corona System." In Proceedings of the International Congress on Hazardous Materials Management, Chatanooga, Tennessee (June 8-12, 1987).

[25] Tevault, D. E. "Plasma Reactions of Methane in Nitrogen and Nitrogen/Oxygen Carriers by Matrix Isolation FTIR Spectroscopy." Plasma Chemistry and Plasma Processing, 5(4), 369-390 (1985).

[26] Sheinson, R. S. "Contaminant Destruction Chemistry in Electric Discharges. In Proceedings of the International Congress on Hazardous Materials Management, Chatanooga, Tennessee (June 8-12, 1987).

[27] Mach, R. and H. Drost. "Kinetics of the Methane Conversion in a Glow Discharge up to Chemical Equilibrium." Advances in Low-Temperature Plasma Chemistry, Technologies, Applications. A. V. Boenig, ed. Technomic Publishing Company, Lancaster, Pennsylvania (1984).

[28] Tezuka, M. and L. L. Miller. "Dynamics and Mechanisms of the Plasmolysis of Anisole." Journal of the American Chemical Society, 100(13), 4201-4208 (1978).

[29] Bedell, F. The Principles of the Transformer. Chapter 12. The Macmillian Company, New York (1896).

APPENDIX A

OPERATING CONDITIONS FOR THE

GAS CHROMATOGRAPH

Settings of the Gas Chromatograph:

Brand/model : Perkin Elmer/Sigma 3B

Detector : Flame Ionization Detector

Carrier Gas : Helium

Carrier Flow Rate : 42 cc/min

Helium Pressure : 40 psi

Hydrogen Pressure : 20 psi

Air Pressure : 30 psi

Injection Temperature : 25°C

Detector Temperature : 55°C

Oven Temperature : 30°C

Attenuation: 2

Column Information:

Brand/model: Alltech/CTR1

Inner Column Packing: Porapak

Outer Column Packing : Molecular Sieve

This column is a double column designed to separate methane, carbon dioxide, carbon monoxide, nitrogen and oxygen. Each column gives a separate peak for methane as seen in Figure 27. The second peak was used in concentration calculations. This peak was known to be pure methane. However, both peaks gave nearly identical results for calculating methane destructions.

Both an integrator and strip chart recorder were used to record the signal from the GC. These instruments operated independently of each other.

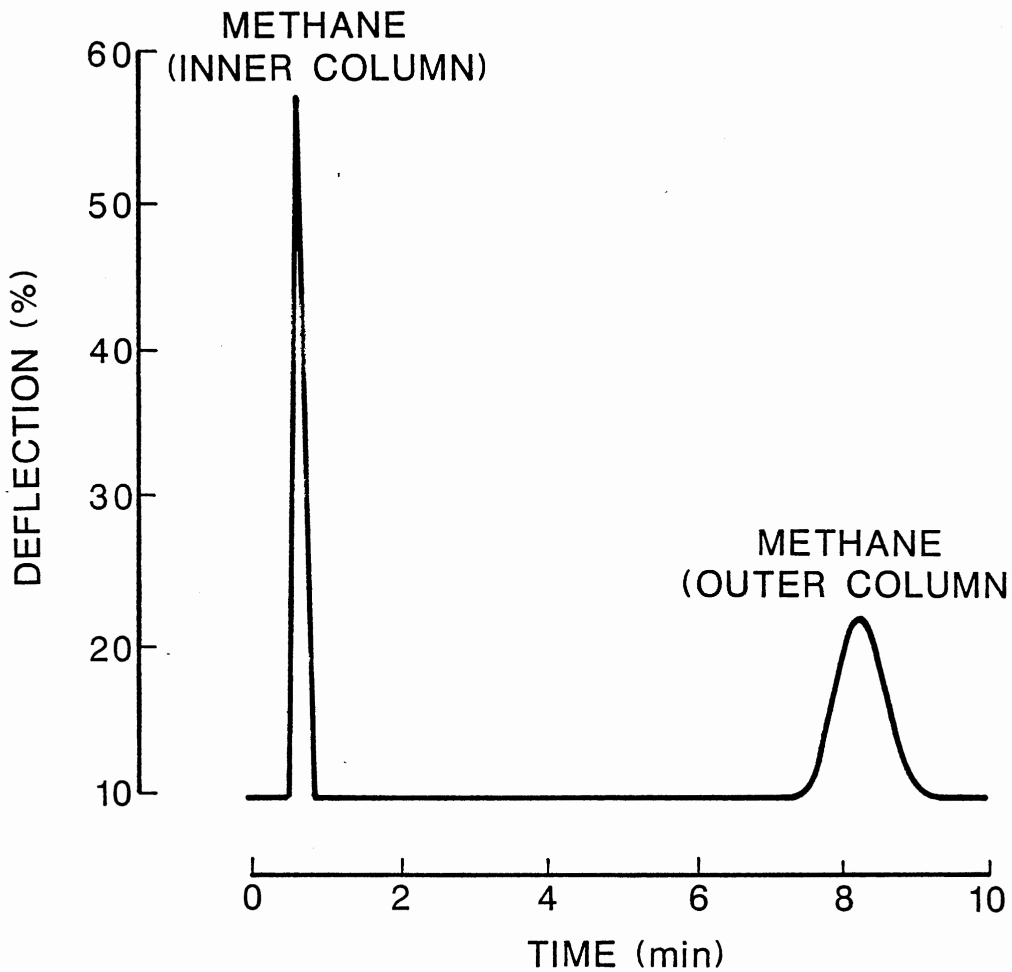

Figure 27. Sample Chromatogram

Integrator Settings:

Brand/model : Perkin Elmer/Sigma 15

Attenuation : 2

Strip Chart Settings:

Brand/Model : Alltech/Linear 1200

Deflection : 0.1 Volts

Chart Speed : 1 cm/min

Sample Calculations (for data Run 3):

1. Made standard starting with 14.2 psi of methane (atmospheric pressure checked by barometer) and filling to 120 psi with helium. Methane concentration for standard = 14.2/120 = 11.8%.

2. Flowed standard through system and took sample which gave an area of 110.4 or 9.3 GC units per 1% methane.

3. Flowed inlet sample through system (no power on) at the same regulator pressure and flow rate and took two samples which gave areas of 125.3 and 121.2. The average area was 123.3. Inlet methane concentration = 123.3/9.3 = 12.9% methane.

4. Turned on power to reactor, set desired frequency, and let come to steady state. Took two samples during destruction which gave area of 105.6 and 106.0. The average was 105.8.

5. Percent methane destruction = 1-(105.8/123.3) = 14.2%.

APPENDIX B

SAMPLE CALCULATIONS

Figure 24 Calculations

Sample calculations for Run 4 are as follows:

$$x \text{ axis} = \tau/(C_a^\circ - C_a) \tag{AB.1}$$

$$y \text{ axis} = \ln(C_a^\circ - C_a)/(C_a^\circ - C_a) \tag{AB.2}$$

and $\tau = V^t/Q$ where V^t is reactor volume and Q is the volumetric flow rate.

Assuming ideal gas law behavior

$$C_a^\circ = y_a^\circ P/RT \tag{AB.3}$$

For run 1, $V^t = 10.8$ cc, $y_a^\circ = 0.13$, $P = 0.97$ atm

$\tau = 22.5°$ C (295.5 K) and R = 82.057 atm cc/gmole K

therefore, $C_a^\circ = 5.18 \times 10^{-6}$ gmole/cc

For the various flow rates:

Q (cc/min)	τ(min)	C_a(gmole/cc)	(y axis)	(x axis)
13	0.83	4.29×10^{-6}	212,300	911,100
30	0.35	4.46×10^{-6}	207,900	486,100
60	0.18	4.65×10^{-6}	203,700	339,600
95	0.11	4.90×10^{-6}	198,500	407,100

Figure 25 Calculations

Sample calculations for Run 7 are as follows:

$$x \text{ axis} = P/n_a = P/(C_a^\circ Q) \tag{AB.4}$$

$$y \text{ axis} = -\ln (C_a/C_a^\circ) \tag{AB.5}$$

Assuming ideal gas law

$$C_a^\circ = y_a^\circ \, (P/RT)$$

where P = 1 atm, T = 23°C (296 K), R = 82.057 $\frac{\text{atm cc}}{\text{gmole K}}$

and $y_a^\circ = 0.114$

therefore, $C_a^\circ = 4.7 \times 10^{-7}$ gmole/cc

Q (cc/min)	C_a (gmole/cc)	P (watts)	(y axis)	(x axis)
13	1.18×10^{-7}	116.2	1.39	19,000,000
35	2.85×10^{-7}	87.0	0.50	5,000,000

APPENDIX C

REYNOLD'S NUMBER CALCULATIONS

In this appendix, representative Reynold's numbers are calculated for various flow rates in the reactor. All calculations show the flow regime to be laminar; however, the actual flow condition could have been well-mixed and turbulent in the plasma. One condition for a true plasma is that the motion of the particles is controlled by electromagnetic rather than hydrodynamic forces. It is not certain if this condition existed in the plasma generated by the ACPR

For calculational purposes, ideal gas is assumed. Oxygen is used as a representative (highest molecular weight) of the gases studied. Calculations are shown for the highest flow rate used in any experiment (528.2 cc/min).

For oxygen, the mass density, ρ, is

$$\rho = (P/RT)MW \tag{AC.1}$$

$$\rho = (1 \text{ atm})\ (32 \text{ gm/gmole})\ /\ [(82.057 \frac{\text{atm cc}}{\text{gmole K}})\ (298 \text{ K})\} \tag{AC.2}$$

$$\rho = 0.00123 \text{ gm/cc} \tag{AC.3}$$

For oxygen, the viscosity, $\simeq$, is 0.000205 gm/cm sec from Perry's Handbook

of Chemical Engineering.

For Reactor 1, the following calculations apply:

$$D_{in} = 0.4 \text{ cm},\ D_{out} = 1.09 \text{ cm} \tag{AC.4}$$

$$A = (\pi/4)\ [(1.09)^2 - (0.04)^2)] \tag{AC.5}$$

$$A = 0.81 \text{ cm}^2$$

For a volumetric flow rate, Q, of 528.2 cc/min:

$$Vel = (528.2\ cc/min) / (0.81\ cm^2) \tag{AC.6}$$

$$Vel = 652.7\ cm/min \text{ or } 10.9\ cm/s \tag{AC.7}$$

$$D_{eff} = D_{out} - D_{in} \tag{AC.8}$$

$$D_{eff} = 0.69\ cm \tag{AC.9}$$

To calculate a standard Reynold's number (no plasma):

$$R_e = D_{eff}\ \rho\ Vel / \mu \tag{AC.10}$$

$$R_e = (0.69)\ (0.00123)\ (10.9) / (0.000205) \tag{AC.11}$$

$$R_e = 45.0 \tag{AC.12}$$

This represents the maximum calculated Reynold's number for any flow rate in any reactor used in these experiments. In order to achieve a Reynold's number of 2100, a flow rate of 30,400 cc/min would be needed.

APPENDIX D

NON-DESTRUCTIVE TEST DATA

TABLE IX

NON-DESTRUCTIVE TEST DATA
RUN 1

Gas: Helium   Flow Rate: 13 cc/min   Temp. (C): 23.0

Regulator: 2200/20

Size: 10.8cc   Inner Elec: Cu wire   Outer Elec: 12 wraps

Primary Voltage: 20 V

Ammeter: Outer lead   Volt Probe: Inner lead

Frequency (Hz)	Secondary Current (mA)	Secondary Voltage	V*A (Watts)
70	0.0	1100	0.0
90	0.0	1100	0.0
140	0.1	1100	0.1
200	0.2	1150	0.2
250	0.4	1200	0.5
300	0.5	1200	0.6
400	0.9	1350	1.2
450	1.1	1500	1.6
500	1.5	1650	2.5
600	2.7	2300	6.2
650	3.2	2425	7.8
660	3.3	2425	8.0
680	3.4	2400	8.2
690	3.4	2375	8.1
700	3.4	2300	7.8
750	3.2	2000	6.4
800	2.9	1700	4.9
900	2.3	1200	2.8
1000	1.9	900	1.7

1st Glow: 450 HZ   Start: NA

Date: 9-30-87   End: 40 min

TABLE X

NON-DESTRUCTIVE TEST DATA
RUN 2

Gas: Helium   Flow Rate: 528 cc/min   Temp. (C): 23.0

Regulator: 2200/20

Size: 10.8cc   Inner Elec: Cu wire   Outer Elec: 12 wraps

Primary Voltage: 20 V

Ammeter: Outer lead   Volt Probe: Inner Lead

Frequency (Hz)	Secondary Current (mA)	Secondary Voltage	V*A (Watts)
70	0.0	1050	0.0
100	0.0	1050	0.0
150	0.1	1050	0.1
200	0.2	1100	0.2
250	0.4	1200	0.5
300	0.5	1200	0.6
350	0.7	1250	0.9
400	0.9	1375	1.2
450	1.2	1500	1.8
500	1.5	1700	2.6
550	2.1	2250	4.7
600	2.7	2390	6.4
650	3.2	2400	7.7
660	3.3	2400	7.9
670	3.3	2400	7.9
680	3.4	2400	8.2
690	3.4	2375	8.1
700	3.4	2300	7.8
750	3.2	2000	6.4
800	2.8	1700	4.8
850	2.5	1400	3.5
900	2.2	1200	2.6
950	2.0	1000	2.0
1000	1.8	800	1.4

1st Glow: NA   Start: NA

Date: 9-30-87   End: 15 min

TABLE XI

NON-DESTRUCTIVE TEST DATA
RUN 3

Gas: Helium   Flow Rate: 13 cc/min   Temp. (C): 22.0

Regulator: 2200/20

Size: 10.8cc   Inner Elec: Cu wire   Outer Elec: 12 wraps

Ammeter: Outer lead   Volt Probe: Inner lead

Primary Voltage: 40 V

Ammeter: Outer lead   Volt Probe: Inner Lead

Frequency (Hz)	Secondary Current (mA)	Secondary Voltage	V*A (Watts)
70	0.0	2000	0.0
100	0.1	2000	0.2
150	0.4	2025	0.8
200	0.7	2100	1.5
250	1.0	2200	2.2
300	1.3	2350	3.1
350	1.7	2500	4.3
400	2.4	2750	6.6
450	3.5	3100	10.9
500	5.1	3650	18.6
550	6.3	4450	28.0
615	7.8	4825	37.6
650	7.6	4400	33.4
700	7.1	3750	26.6
750	6.4	3150	20.2
800	5.8	2650	15.4
850	5.3	2125	11.3
900	4.8	1900	9.1
950	4.3	1650	7.1
1000	3.9	1400	5.5

1st Glow: 150 Hz   Start: NA

Date: 9-30-87   End: 30 min

TABLE XII

NON-DESTRUCTIVE TEST DATA
RUN 4

Gas: Helium Flow Rate: 528 cc/min Temp. (C): 22.0

Regulator: 2200/20

Size: 10.8cc Inner Elec: Cu wire Outer Elec: 12 wraps

Primary Voltage: 40 V

Ammeter: Outer lead Volt Probe: Inner Lead

Frequency (Hz)	Secondary Current (mA)	Secondary Voltage	V*A (Watts)
70	0.0	1950	0.0
100	0.1	2000	0.2
150	0.6	2000	1.2
200	0.9	2100	1.9
250	1.2	2200	2.6
300	1.5	2350	3.5
350	2.0	2550	5.1
400	2.6	2800	7.3
450	3.5	3200	11.2
500	4.7	3800	17.9
550	6.4	4550	29.1
580	7.1	4700	33.4
585	7.2	4750	34.2
590	7.3	4700	34.3
600	7.4	4700	34.8
610	7.5	4650	34.9
615	7.5	4625	34.7
620	7.5	4600	34.5
650	7.4	4250	31.4
700	6.9	3650	25.2
750	6.3	3050	19.2
800	5.8	2600	15.1
850	5.3	2200	11.7
900	4.7	1900	8.9
950	4.3	1600	6.9
1000	3.9	1400	5.5

1st Glow: NA Start: NA

Date: 9-30-87 End: 15 min

TABLE XIII

NON-DESTRUCTIVE TEST DATA
RUN 5

Gas: Helium　　Flow Rate: 13 cc/min　　Temp. (C): 22.0

Regulator: 2200/20

Size: 10.8cc　　Inner Elec: Cu wire　　Outer Elec: 12 wraps

Primary Voltage: 60 V

Ammeter: Outer lead　　Volt Probe: Inner Lead

Frequency (Hz)	Secondary Current (mA)	Secondary Voltage	V*A (Watts)
70	0.0	2850	0.0
100	0.2	2950	0.6
150	0.7	3000	2.1
200	1.1	3100	3.4
250	1.5	3350	5.0
300	1.9	3600	6.8
350	2.5	3950	9.9
400	3.3	4400	14.5
450	4.4	5150	22.7
500	5.9	6200	36.6
530	7.1	7050	50.1
540	7.4	7200	53.3
550	7.6	7300	55.5
555	7.7	7350	56.6
560	7.7	7350	56.6
570	7.8	7275	56.8
580	7.9	7200	56.9
590	7.9	7075	55.9
600	7.9	6900	54.5
650	7.7	6000	46.2
700	7.2	5000	36.0
750	6.5	4100	26.7
800	5.9	3400	20.1
850	5.6	2950	16.5
900	5.2	2550	13.3
950	4.9	2200	10.8
1000	4.5	1900	8.6

1st Glow: 70 Hz　　Start: NA

Date: 10-1-87　　End: 15 min

TABLE XIV

NON-DESTRUCTIVE TEST DATA
RUN 6

Gas: Helium　Flow Rate: 528 cc/min　Temp. (C): 22.5

Regulator: 2200/20

Size: 10.8cc　Inner Elec: Cu wire　Outer Elec: 12 wraps

Primary Voltage: 60 V

Ammeter: Outer lead　Volt Probe: Inner Lead

Frequency (Hz)	Secondary Current (mA)	Secondary Voltage	V*A (Watts)
70	0.0	2800	0.0
100	0.2	2900	0.6
150	0.7	3000	2.1
200	1.1	3050	3.4
250	1.5	3300	5.0
300	1.9	3550	6.7
350	2.5	3875	9.7
400	3.3	4375	14.4
450	4.5	5200	23.4
500	6.0	6300	37.8
520	6.8	6875	46.8
530	7.0	7000	49.0
540	7.3	7075	51.7
550	7.4	7125	52.7
555	7.5	7100	53.3
560	7.6	7100	54.0
570	7.7	7000	53.9
580	7.7	6850	52.7
590	7.6	6750	51.3
600	7.6	6575	50.0
650	7.4	5675	42.0
700	7.0	4800	33.6
750	6.5	4000	26.0
800	6.0	3400	20.4
850	5.5	2850	15.7
900	5.3	2550	13.5
950	4.8	2150	10.3
1000	4.5	1875	8.4

1st Glow: NA　Start: NA

Date: 9-30-87　End: 15 min

TABLE XV

NON-DESTRUCTIVE TEST DATA
RUN 7

Gas: Helium Flow Rate: 13 cc/min Temp. (C): 21.5

Regulator: 2175/20

Size: 10.8cc Inner Elec: Cu wire Outer Elec: 12 wraps

Primary Voltage: 80 V

Ammeter: Outer lead Volt Probe: Inner Lead

Frequency (Hz)	Secondary Current (mA)	Secondary Voltage	V*A (Watts)
70	0.1	3750	0.4
100	0.4	3850	1.5
150	1.0	4000	4.0
200	1.6	4100	6.6
250	2.0	4400	8.8
300	2.6	4790	12.4
350	3.4	5300	18.0
400	4.5	6000	27.0
450	6.1	7200	43.9
500	NA	NA	NA
600	NA	NA	NA
650	8.7	7125	62.0
700	8.3	5990	49.7
800	7.1	4200	29.8
900	6.2	3000	18.6
1000	5.5	2300	12.6

1st Glow: NA Start: NA

Date: 10-1-87 End: NA

TABLE XVI

NON-DESTRUCTIVE TEST DATA
RUN 8

Gas: Helium   Flow Rate: 13 cc/min   Temp. (C): 23.0

Regulator: 2175/20

Size: 64.4cc   Inner Elec: Cu mesh   Outer Elec: 17 wraps

Primary Voltage: 40 V

Ammeter: Outer lead   Volt Probe: Inner Lead

Frequency (Hz)	Secondary Current (mA)	Secondary Voltage	V*A (Watts)
70	0.0	2000	0.0
100	0.1	2000	0.1
150	0.4	2025	0.7
200	0.6	2150	1.3
250	0.9	2275	2.0
300	1.2	2425	2.9
350	1.6	2700	4.5
400	2.2	3100	7.0
450	3.1	3800	11.8
500	3.8	4250	16.4
520	4.0	4275	17.1
525	4.1	4225	17.3
530	4.1	4210	17.3
540	4.2	4190	17.4
550	4.2	4100	17.2
560	4.2	4010	16.8
570	4.3	3950	16.8
580	4.3	3850	16.4
600	4.3	3700	15.7
650	4.2	3200	13.4
700	3.9	2650	10.3
750	3.6	2200	7.9
800	3.2	1900	6.1
850	3.0	1625	4.9
900	2.8	1400	3.9
950	2.7	1275	3.4
1000	2.5	1100	2.8

1st Glow: NA   Start: 10:30 AM

Date: 10-2-87   End: 10:50 AM

TABLE XVII

NON-DESTRUCTIVE TEST DATA
RUN 9

Gas: Nitrogen   Flow Rate: 13 cc/min   Temp. (C): 23.0

Pres. (In): 30.20   Regulator: 2575/20

Size: 10.8cc   Inner Elec: Cu wire   Outer Elec: 12 wraps

Primary Voltage: 40 V

Ammeter: Outer lead   Volt Probe: Inner Lead

Frequency (Hz)	Secondary Current (mA)	Secondary Voltage	V*A (Watts)
70	0.0	1800	0.0
100	0.2	1800	0.4
150	0.7	1800	1.3
200	1.1	1850	2.0
250	1.5	1950	2.9
300	1.9	2000	3.7
350	2.4	2100	4.9
400	2.9	2200	6.4
450	3.7	2400	8.8
500	4.6	2625	12.1
550	5.9	2990	17.6
600	7.7	3410	26.1
650	10.0	4025	40.3
700	13.2	4750	62.5
710	13.5	4800	64.8
720	14.0	4875	68.0
730	14.3	4900	69.8
740	14.6	4900	71.5
750	14.8	4875	71.9
760	14.9	4800	71.5
770	14.8	4750	70.3
780	14.7	4600	67.6
800	14.2	4300	61.1
850	12.5	3550	44.4
900	10.7	2800	30.0
950	9.3	2325	21.6
1000	8.1	1900	15.4

1st Glow: NA   Start: 12.59 p.m.

Date: 10-6-87   End: 1:24 p.m.

TABLE XVIII

NON-DESTRUCTIVE TEST DATA
RUN 10

Gas: Nitrogen   Flow Rate: 528 cc/min   Temp. (C): 23.0

Pres. (In): 30.20   Regulator: 2175/21

Size: 10.8cc   Inner Elec: Cu wire   Outer Elec: 12 wraps

Primary Voltage: 40 V

Ammeter: Outer lead   Volt Probe: Inner Lead

Frequency (Hz)	Secondary Current (mA)	Secondary Voltage	V*A (Watts)
70	0.0	1800	0.0
100	0.2	1800	0.4
150	0.7	1800	1.3
200	1.1	1850	2.0
250	1.5	1950	2.9
300	1.8	2000	3.6
350	2.3	2100	4.8
400	2.9	2200	6.4
450	3.6	2350	8.3
500	4.5	2550	11.5
550	5.8	2875	16.5
600	7.5	3350	25.0
650	9.9	3990	39.5
680	11.6	4400	51.0
690	12.3	4550	55.7
700	13.0	4650	60.2
710	13.4	4775	63.7
720	13.9	4810	66.6
730	14.3	4850	69.1
740	14.6	4900	71.3
750	14.8	4875	71.9
760	14.9	4800	71.5
780	14.9	4650	69.0
800	14.5	4400	63.6
850	12.7	3600	45.7
900	11.0	2850	31.4
950	9.6	2390	22.8
1000	8.3	1950	16.2

1st Glow: NA   Start: 2:58 p.m.

Date: 10-6-87   End: 3:14 p.m.

TABLE XIX

NON-DESTRUCTIVE TEST DATA
RUN 11

Gas: Nitrogen Flow Rate: 13 cc/min Temp. (C): 22.0

Pres. (In): 30.09 Regulator: 2550/20

Size: 66.4 cc Inner Elec: Cu mesh Outer Elec: 17 wraps

Primary Voltage: 40 V

Ammeter: Outer lead Volt Probe: Inner Lead

Frequency (Hz)	Secondary Current (mA)	Secondary Voltage	V*A (Watts)
70	0.0	1800	0.0
100	0.2	1800	0.4
150	0.7	1825	1.2
200	1.1	1900	2.0
250	1.4	2000	2.7
300	1.8	2075	3.7
350	2.4	2200	5.2
400	3.1	2400	7.4
450	4.0	2700	10.8
500	5.4	3200	17.1
550	7.5	3875	29.1
570	8.7	4250	37.0
590	10.0	4650	46.5
600	10.6	4800	50.9
620	11.8	5150	60.5
640	12.6	5250	65.9
650	12.9	5250	66.4
660	12.9	5200	66.8
680	12.9	5025	64.6
700	12.6	4675	58.7
750	10.7	3650	39.1
800	9.0	2800	25.1
850	7.6	2200	16.6
900	6.6	1800	11.8
950	5.8	1500	8.7
1000	5.1	1250	6.4

1st Glow: NA Start: 1:39 p.m.

Date: 10-9-87 End: 1:55 p.m.

TABLE XX

NON-DESTRUCTIVE TEST DATA
RUN 12

Gas: Nitrogen   Flow Rate: 13 cc/min   Temp. (C): 23.0

Pres. (In): 30.00   Regulator: 2550/20

Size: 10.8 cc   Inner Elec: Cu mesh   Outer Elec: 12 wraps

Primary Voltage: 60 V

Ammeter: Outer lead   Volt Probe: Inner Lead

Frequency (Hz)	Secondary Current (mA)	Secondary Voltage	V*A (Watts)
70	0.1	2590	0.1
100	0.5	2600	1.3
150	1.2	2650	3.1
200	1.8	2700	4.7
250	2.4	2800	6.6
300	2.9	2950	8.4
350	3.6	3075	10.9
400	4.5	3250	14.6
450	5.6	3550	19.9
500	7.1	3925	27.9
550	9.2	4450	40.7
580	10.8	4990	53.6
600	12.1	5300	64.1
620	13.5	5625	75.9
640	14.6	5810	84.5
660	15.5	5910	91.3
670	15.7	5900	92.3
680	15.8	5850	92.1
700	16.0	5750	91.7
750	15.9	5210	82.6
800	15.3	4650	71.1
850	14.8	4175	61.8
900	14.4	3750	54.0
950	13.9	3350	46.4
1000	12.1	2700	32.5

1st Glow: NA   Start: 7:07 p.m.

Date: 10-15-87   End: 7:37 p.m.

TABLE XXI

NON-DESTRUCTIVE TEST DATA
RUN 13

Gas: Nitrogen   Flow Rate: 13 cc/min   Temp. (C): 24.0

Pres. (In): 30.03   Regulator: 2575/20

Size: 10.8 cc   Inner Elec: Cu   Outer Elec: 12 wraps

Primary Voltage: 20 V

Ammeter: Outer lead   Volt Probe: Inner Lead

Frequency (Hz)	Secondary Current (mA)	Secondary Voltage	V*A (Watts)
70	0.0	990	0.0
100	0.0	990	0.0
150	0.2	1000	0.2
200	0.4	1000	0.4
250	0.6	1000	0.6
300	0.8	1010	0.8
350	1.0	1025	1.0
400	1.3	1150	1.5
450	1.6	1200	1.9
500	2.0	1275	2.6
550	2.6	1400	3.6
600	3.3	1600	5.3
650	4.3	1800	7.7
700	5.6	2150	12.0
750	6.8	2350	16.0
760	7.0	2375	16.5
770	7.1	2325	16.4
780	7.1	2275	16.2
800	7.1	2200	15.6
830	6.8	2010	13.7
850	6.5	1900	12.4
900	5.7	1600	9.1
950	5.0	1350	6.8
1000	4.3	1050	4.5

1st Glow: NA   Start: 12.58 p.m.

Date: 10-16-87   End: 12:40 p.m.

TABLE XXII

NON-DESTRUCTIVE TEST DATA
RUN 14

Gas: Oxygen Flow Rate: 13 cc/min Temp. (C): 22.0

Pres. (In): 30.42 Regulator: 2225/20

Size: 10.8 cc Inner Elec: Cu Outer Elec: 12 wraps

Primary Voltage: 40 V

Ammeter: Outer lead Volt Probe: Inner Lead

Frequency (Hz)	Secondary Current (mA)	Secondary Voltage	V*A (Watts)
70	0.0	1800	0.0
100	0.2	1800	0.4
150	0.7	1800	1.3
200	1.1	1800	2.0
250	1.5	1850	2.8
300	1.8	1990	3.6
350	2.3	2025	4.7
400	2.9	2175	6.2
450	3.6	2300	8.3
500	4.5	2500	11.3
550	5.8	2800	16.1
600	7.4	3225	23.9
650	9.8	3810	37.2
670	11.0	4150	45.4
690	12.0	4375	61.3
700	12.5	4425	55.1
710	12.8	4500	57.4
720	13.1	4550	59.6
730	13.4	4575	61.3
740	13.7	4575	62.4
750	13.8	4530	62.5
760	14.0	4500	62.0
770	14.1	4410	61.8
780	14.1	4400	51.8
790	14.2	4300	60.9
800	14.1	4200	59.2
850	13.1	3600	47.0
900	11.4	2950	33.6
950	9.9	2400	23.8
1000	8.6	1950	16.7

1st Glow NA Start: 8:48 a.m.

Date: 10-21-87 End: 9:03 a.m.

TABLE XXIII

NON-DESTRUCTIVE TEST DATA
RUN 15

Gas: Oxygen Flow Rate: 13 cc/min Temp. (C): 22.0

Pres. (In): 30.42 Regulator: 2225/20

Size: 64.4 cc Inner Elec: Cu Outer Elec: 17 wraps

Primary Voltage: 20 V

Ammeter: Outer lead Volt Probe: Inner Lead

Frequency (Hz)	Secondary Current (mA)	Secondary Voltage	V*A (Watts)
70	0.0	1775	0.0
100	0.2	1800	0.4
150	0.7	1800	1.3
200	1.1	1825	2.0
250	1.4	1975	2.8
300	1.9	2025	3.7
350	2.4	2190	5.3
400	3.1	2400	7.4
450	4.1	2600	10.7
500	5.5	3025	16.5
550	7.6	3700	27.9
580	9.3	4225	39.3
600	10.6	4600	48.8
610	11.3	4800	54.2
620	11.9	4990	59.1
630	12.4	5075	62.7
640	12.8	5200	66.6
650	13.2	5200	68.6
660	13.4	5200	69.7
670	13.6	5175	70.1
680	13.6	5100	69.1
700	13.5	4800	64.6
750	11.7	3850	45.0
800	9.8	2950	28.8
850	8.2	2300	18.9
900	7.0	1850	13.0
950	6.2	1575	9.8
1000	5.5	1300	7.1

1st Glow: NA Start: 10:05 a.m.

Date: 10-21-87 End: 10:16 a.m.

TABLE XXIV

NON-DESTRUCTIVE TEST DATA
RUN 16

Gas: Oxygen Flow Rate: 13 cc/min Temp. (C): 22.0

Pres. (In): 30.25 Regulator: 2225/20

Size: 10.8 cc Inner Elec: Cu Outer Elec: 12 wraps

Primary Voltage: 40 V

Ammeter: Outer lead Volt Probe: Inner Lead

Frequency (Hz)	Secondary Current (mA)	Secondary Voltage	V*A (Watts)
500	4.3	2475	10.6
600	7.1	3200	22.7
760	13.6	4550	61.9
800	13.8	4250	58.7
900	11.1	2975	33.0
1000	8.3	1985	16.4
New Inner Electrode			
500	4.3	2450	10.5
600	7.1	3200	22.7
700	12.1	4450	53.8
760	13.5	4500	60.8
800	13.8	4250	58.7
900	11.2	2975	33.3
1000	8.4	1990	16.7

1st Glow: NA Start: 9:15 a.m.

Date: 10-28-87 End: 9:38 a.m.

TABLE XXV

NON-DESTRUCTIVE TEST DATA
RUN 17

Gas: Humid. Oxygen   Flow Rate: 13 cc/min   Temp. (C): 22.0

Pres. (In): 30.25   Regulator: 2225/20

Size: 10.8 cc   Inner Elec: Cu   Outer Elec: 12 wraps

Primary Voltage: 40 V

Ammeter: Outer lead   Volt Probe: Inner Lead

Frequency (Hz)	Secondary Current (mA)	Secondary Voltage	V*A (Watts)
70	0.0	1775	0.0
100	0.2	1800	0.4
200	1.1	1825	2.0
300	1.9	2000	3.8
400	3.0	2200	6.6
500	4.8	2650	12.6
550	6.1	3000	18.3
600	7.8	3400	26.4
630	9.0	3675	33.1
650	10.0	3900	39.0
680	11.5	4200	48.3
700	12.4	4400	54.6
720	13.0	4425	57.5
730	13.3	4410	58.4
740	13.5	4400	59.2
760	14.2	4450	63.0
770	14.1	4375	61.7
780	14.0	4225	59.1
800	13.5	4000	54.0
850	11.9	3250	38.7
900	10.4	2625	27.3
950	9.2	2200	20.1
1000	8.1	1800	14.5

1st Glow: NA   Start: 2:48 p.m.

Date: 10-28-87   End: 3:00 p.m.

TABLE XXVI

NON-DESTRUCTIVE TEST DATA
RUN 18

Gas: Humid. Oxygen Flow Rate: 13 cc/min Temp. (C): 22.0

Pres. (In): 30.25 Regulator: 2225/20

Size: 10.8 cc Inner Elec: Cu Outer Elec: 12 wraps

Primary Voltage: 40 V

Ammeter: Outer lead Volt Probe: Inner Lead

Frequency (Hz)	Secondary Current (mA)	Secondary Voltage	V*A (Watts)
200	1.1	1800	2.0
300	1.9	1990	3.7
400	3.0	2190	6.6
500	4.6	2600	12.0
550	5.9	2875	17.0
600	7.7	3300	25.2
630	9.0	3650	32.9
650	10.0	3900	39.0
680	11.6	4250	49.3
700	12.7	4475	56.8
710	13.1	4550	59.6
720	13.5	4600	61.9
730	13.8	4600	63.5
740	14.0	4600	64.4
750	14.2	4550	64.4
760	14.2	4475	63.5
780	13.9	4275	59.4
800	13.5	4000	54.0
850	12.0	3300	39.6
900	10.5	2650	27.8
950	9.2	2200	20.2
1000	8.1	1800	14.6

1st. Glow: NA Start: 3:07 p.m.

Date: 10-28-87 End: 3:16 p.m.

TABLE XXVII

NON-DESTRUCTIVE TEST DATA
RUN 19

Gas: Air Flow Rate: 13 cc/min Temp. (C): 23.0

Pres. (In): 29.99 Regulator: 2325/20

Size: 10.8 cc Inner Elec: Cu Outer Elec: 12 wraps

Primary Voltage: 40 V

Ammeter: Outer lead Volt Probe: Inner Lead

Frequency (Hz)	Secondary Current (mA)	Secondary Voltage	V*A (Watts)
70	0.0	1775	0.0
100	0.2	1800	0.4
200	1.1	1800	2.0
250	1.5	1850	2.8
300	1.8	2000	3.6
350	2.3	2025	4.6
400	2.9	2175	6.3
450	3.6	2300	8.3
500	4.6	2550	11.6
550	5.8	2800	16.2
600	7.5	3300	24.8
630	8.8	3650	32.1
650	9.8	3850	37.7
680	11.5	4275	49.2
690	12.1	4400	53.2
700	12.6	4500	56.7
720	13.4	4610	61.8
740	13.9	4625	64.3
750	14.2	4675	66.2
760	14.3	4600	65.8
770	14.4	4575	65.9
780	14.5	4500	65.2
790	14.4	4400	63.4
800	14.3	4325	61.8
850	13.1	3650	47.8
900	11.3	2950	33.3
950	9.8	2400	23.4
1000	8.5	1975	16.8

1st Glow: NA Start: 9:36 a.m.

Date: 10-29-87 End: 9:51 a.m.

TABLE XXVIII

NON-DESTRUCTIVE TEST DATA
RUN 20

Gas: Air   Flow Rate: 13 cc/min   Temp. (C): 23.5

Pres. (In): 29.99   Regulator: 2325/20

Size: 64.4 cc   Inner Elec: Cu mesh   Outer Elec: 17 wraps

Primary Voltage: 20 V

Ammeter: Outer lead   Volt Probe: Inner Lead

Frequency (Hz)	Secondary Current (mA)	Secondary Voltage	V*A (Watts)
70	0.0	1775	0.0
100	0.2	1800	0.4
200	1.1	1810	2.0
300	1.9	2000	3.8
350	2.5	2175	5.4
400	3.2	2350	7.5
450	4.1	2600	10.7
500	5.5	3000	16.5
550	7.7	3700	28.3
580	9.5	4250	40.4
600	10.8	4600	49.7
610	11.4	4800	54.7
620	12.1	4975	60.0
640	13.0	5175	67.3
650	13.4	5190	69.5
660	13.5	5150	69.5
670	13.6	5100	69.4
680	13.6	5000	68.0
700	13.4	4750	63.6
750	11.7	3800	44.3
800	9.7	2875	27.9
850	8.2	2275	18.7
900	7.0	1850	13.0
950	6.2	1550	9.6
1000	5.5	1275	7.0

1st Glow: NA   Start: 1:01 p.m.

Date: 10-29-87   End: 1:13 p.m.

TABLE XXIX

NON-DESTRUCTIVE TEST DATA
RUN 21

Gas: Air Flow Rate: 13 cc/min Temp. (C): 23.5

Pres. (In): 29.98 Regulator: 2325/20

Size: 64.4 cc Inner Elec: Silver Outer Elec: 17 wraps

Primary Voltage: 40 V

Ammeter: Inner Lead Volt Probe: Outer lead

Frequency (Hz)	Secondary Current (mA)	Secondary Voltage	V*A (Watts)
70	0.0	1775	0.0
100	0.2	1800	0.4
200	1.1	1875	2.1
300	1.9	2100	4.0
350	2.6	2250	5.9
400	3.5	2600	9.1
450	4.8	3000	14.2
500	6.8	3675	24.8
520	7.9	4075	32.2
540	9.2	4500	41.4
560	10.6	4950	52.2
580	11.7	5200	60.8
600	12.4	5200	64.2
610	12.5	5175	64.4
620	12.5	5050	62.9
640	12.3	4800	58.8
660	11.9	4400	52.4
700	10.2	3575	36.5
750	8.4	2675	22.5
800	6.9	2050	14.1
850	6.0	1650	9.9
900	5.2	1375	7.2
950	4.7	1175	5.5
1000	4.2	975	4.1

1st Glow: 500 Hz Start: 1:44 p.m.

Date: 10-30-87 End: 1:56 p.m.

TABLE XXX

NON-DESTRUCTIVE TEST DATA
RUN 22

Gas: Nitrogen   Flow Rate: 13 cc/min   Temp. (C): 23.0

Pres. (In): 14.52   Regulator: 2525/20

Size: 10.8 cc   Inner Elec: Cu wire   Outer Elec: 12 wraps

Primary Voltage: 20 V

Ammeter: Inner Lead   Volt Probe: Outer lead

Frequency (Hz)	Secondary Current (mA)	Secondary Voltage	V*A (Watts)
200	0.3	1000	0.3
300	0.7	1175	0.8
400	1.1	1200	1.3
500	1.9	1400	2.7
550	2.4	1550	3.7
600	3.2	1800	5.8
650	4.2	2050	8.6
700	5.8	2500	14.5
720	6.2	2575	16.0
740	6.5	2600	16.9
750	6.5	2625	17.1
760	6.5	2525	16.4
780	6.4	2400	15.4
800	6.2	2250	14.0
850	5.5	1875	10.3
900	4.7	1550	7.3
1000	3.5	1050	3.7

1st Glow: NA   Start: 4:00 p.m.

Date: 11-16-87   End: 4:15 p.m.

APPENDIX E

DESTRUCTIVE TEST DATA

TABLE XXXVI

DESTRUCTIVE TEST DATA
RUN 7

Temperature: 23° C   Pressure: 14.5 psi

Ammeter: Inner electrode   Reactor 1

Regulator pressure: 7 psi   Volt probe: Outer electrode

Frequency: 700 Hz   Date: 11-15-87

Inlet concentration (%): Methane 1.1
Oxygen 18.2
Helium 80.7

Flow Rate (cc/min)	Primary Voltage	Secondary current (mA)	Secondary Voltage	Power Input (watts)	Methane Destruction (%)
35	60	15.0	5800	87.0	39.3
13	70	18.3	6350	116.2	75.0

TABLE XXXII

DESTRUCTIVE TEST DATA
RUN 2

Temperature: 23.5° C

Pressure: 14.62 ps

Reactor 2

Ammeter: inner electrode

Volt probe: outer electrode

Regulator pressure: 7 psi

Date: 11-3-87

Frequency: 540

Primary Voltage: 60 V

Inlet concentration (%):			
	Methane	12.5	*12.4
	Oxygen	18.2	•
	Helium	69.3	

Flow Rate (cc/min)	Secondary current (mA)	Secondary Voltage	Power Input (watts)	Methane Destruction (%)
35	8.0	4850	38.8	26.7
*35	8.0	4850	38.8	31.2
13	8.1	4900	39.7	46.2
*13	8.1	4900	39.7	50.6
95	7.8	4800	37.4	15.5

*Denotes duplicate data run

TABLE XXXIII

DESTRUCTIVE TEST DATA
RUN 3

Temperature: 22.5° C | Pressure: 14.44 psi

Reactor 2

Ammeter: inner electrode | Volt probe: outer electrode

Regulator pressure: 7 psi | Date: 11-5-87

Frequency: 608 Hz | Primary Voltage: 60 V

Inlet concentration (%):			
	Methane	12.7	12.9*
	Oxygen	18.2	
	Helium	69.1	

Flow Rate (cc/min)	Secondary current (mA)	Secondary Voltage	Power Input (watts)	Methane Destruction (%)
13	15.4	7200	110.9	14.0
*13	15.4	7200	110.9	14.4

*Denotes duplicate data run

TABLE XXXIV

DESTRUCTIVE TEST DATA
RUN 4

Temperature: 21.0° C	Pressure: 14.28 psi
	Reactor 1
Ammeter: inner electrode	Volt probe: outer electrode
Regulator pressure: 6.5 psi	Date: 11-7-87
Frequency: 685 Hz	Primary Voltage: 60 V

Inlet concentration (%):			
	Methane	13.0	13.3*
	Oxygen	18.2	
	Helium	68.8	

Flow Rate (cc/min)	Secondary current (mA)	Secondary Voltage	Power Input (watts)	Methane Destruction (%)
30	15.0	5925	88.9	13.9
10	15.2	6000	90.9	17.9
65	14.9	5875	87.2	10.3
95	14.8	5800	85.8	5.4

*Denotes duplicate data run

NOTE: A milky white solid was visible on reactor walls after experiments. This residue dissolved in water and did not release any visible gas.

TABLE XXXV

DESTRUCTIVE TEST DATA
RUNS 5 AND 6

Temperature: 23.0° C

Pressure: 14.47 psi

Reactor 3

Ammeter: Inner electrode

Volt probe: Outer electrode

Regulator pressure: 6.5 psi

Date: 11-11-87

Flow Rate: 35 cc/min

Primary Voltage: 60 V

Run No.	Inlet Methane Concentration (%)	Frequency (Hz)	Secondary current (mA)	Secondary Voltage	Power Input (watts)	Methane Destruction (%)
5	12.7	600	13.4	6850	91.4	15.6
6	1.3	615	13.0	6400	83.2	56.5

TABLE XXXI

DESTRUCTIVE TEST DATA
RUN 1

Temperature: 23.00° C

Pressure: 30.20 in

Reactor 1

Ammeter: inner electrode

Volt probe: outer electrode

Regulator pressure: 7 psi

Date: 11-1-87

Inlet concentration (%):			
	Methane	12.7	*12.7
	Oxygen	18.2	
	Helium	69.1	

Flow Rate (cc/min)	Frequency (Hz)	Primary Voltage	Secondary current (mA)	Secondary Voltage	Power Input (watts)	Methane Destruction (%)
35	600	60	15.5	6100	94.6	16.6
*35	600	60	15.5	6100	94.6	15.5
13	600	60	15.6	6200	96.7	31.3
13	800	60	13.5	2750	37.1	19.0
13	1000	60	10.6	2125	22.5	0.0
13	400	60	4.9	3300	16.2	3.1
13	500	60	8.6	4385	37.7	10.8
13	600	40	9.3	2800	26.0	10.3
*13	600	40	9.3	2800	26.0	11.2

* Denotes duplicate runs

TABLE XXXVII

DESTRUCTIVE TEST DATA
RUN 8

Temperature: 22° C	Pressure: 14.52 psi
Ammeter: Inner Electrode	Reactor 1 Volt probe: Outer electrode
Regulator pressure: 7 psi	Date: 11-18-87
Frequency: 680 Hz	Primary Voltage: 60 V
Inlet concentration (%):	Methane 14.1 Oxygen 18.2 Helium 67.7

Flow Rate (cc/min)	Secondary current (mA)	Secondary Voltage	Power Input (watts)	Methane Destruction (%)
123	10.9	5975	65.1	2.5

TABLE XXXVIII

DESTRUCTIVE TEST DATA
RUN 9

Temperature: 22.5° C	Pressure: 14.53 psi
	Reactor 1
Ammeter: Inner electrode	Volt Probe: Outer electrode
Regulator pressure: 7 psi	Date: 11-20-87
Frequency: 685 Hz	Primary Voltage: 60 V
Inlet concentration (%):	Methane 11.4% 11.2* Oxygen 18.2 Helium 70.7

Flow Rate (cc/min)	Secondary current (mA)	Secondary Voltage	Power Input (watts)	Methane Destruction (%)
30	11.0	6200	68.2	12.8

*Denotes duplicate data points

VITA 2

Michael A. Piatt

Candidate for the Degree of

Master of Science

Thesis: METHANE DESTRUCTION IN AN ALTERNATING CURRENT PLASMA REACTOR

Major Field: Chemical Engineering

Biographical:

Personal Data: Born in Hobbs, New Mexico, February 7, 1959, the son of John R. and Elora M. Piatt.

Education: Graduated from Putnam City High School, Warr Acres, Oklahoma, in May 1977; received Bachelor of Science Degree in Chemical Engineering from Oklahoma State University, Stillwater, Oklahoma, in December 1981; completed requirements for the Master of Science degree at Oklahoma State University, Stillwater, Oklahoma, in May 1988.

Professional Experience: Research Assistant, department of Chemical Engineering, Oklahoma State University, Stillwater, Oklahoma, August, 1986 to December 1987. Reservoir Engineer, January, 1982 to May, 1986.